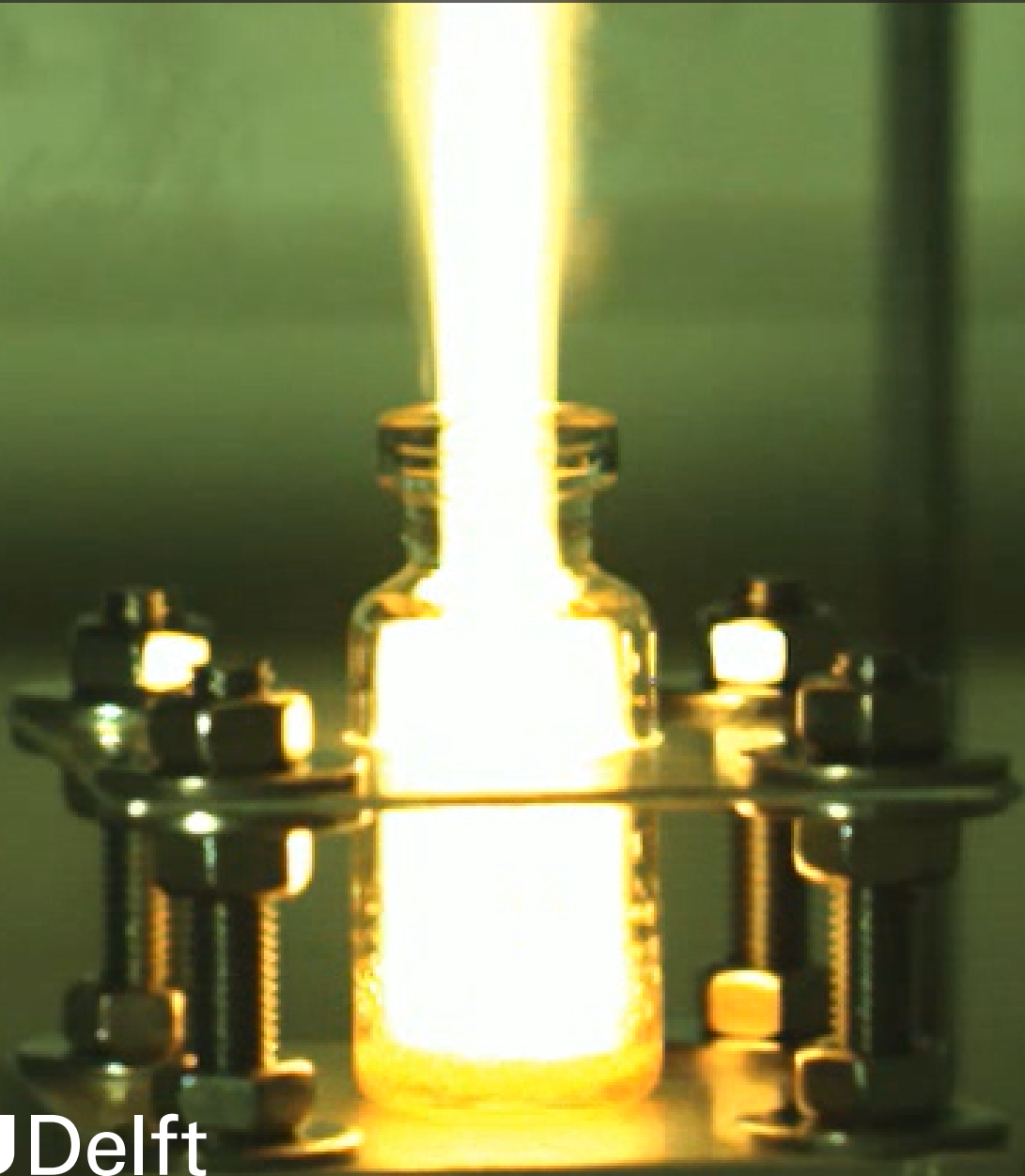# Novel Drop Test Set-Up For Hypergolic Testing

Developing a drop test set-up to characterize the performance of TNO's HTP/ethanol hypergolic propellant combination

Mateusz Glowacki

TUDelft

Novel Drop Test Set-Up For Hypergolic Testing

Developing a drop test set-up to characterize the performance of TNO's HTP/ethanol hypergolic propellant combination

by

Mateusz Glowacki

to obtain the degree of Master of Science
at the Delft University of Technology,
to be defended publicly on Monday, October 30th at 14:00.

Academic supervisor:	Dr. Botchu Jyoti
Company supervisor:	Ir. Martin Olde
Institution:	Delft University of Technology
Company:	TNO
Place:	Faculty of Aerospace Engineering, Delft
Duration:	November 2022 - October 2023

TUDelft

Preface

This report is the culmination of over a year of work dedicated to hypergolic propellant research. Although my main purpose has obviously been to obtain my Master of Science degree in Aerospace Engineering, I also wanted to contribute to the field. I wanted to first of all ensure that this report can be of great use to anyone else intending to build a drop test set-up. It is by no means a manual, but I have included all the steps which were taken to develop and successfully use the drop test set-up. I cherish the joyful expectation that it will help at least one person.

Furthermore, I wanted to build a useful scientific instrument which TNO will be able to use in the future. When reading this report, one finds that the second hermetic drop-test set up was not finished at the time of writing this report. This is because of delays encountered during the development of said set-up. Nonetheless, I will finish machining, assembling and validating it in the future even though it will have no impact on my thesis anymore. I simply want to see it used for science and the further development of novel hypergolic propellants.

I want to thank everyone who has supported me. First and foremost, I thank my academic supervisor Jyoti and my company supervisor Martin. They were always there when I needed their advice regarding both technical matters and the direction in which to take the project. Without them I would not have been able to get this far. I also thank all the great people at TNO who helped me with their extensive knowledge in machining, chemistry and testing safety. They helped me find answers whenever I was outside of my area of expertise and needed a push in the right direction. Furthermore, many thanks to the people at TU Delft's IWS and IWM workspaces for letting me machine my parts there and guiding me whenever I needed to implement machining techniques which were new for me. I also very much appreciated their taste in music which made the many machining hours more fun. Lastly, I thank my friends and family who supported me throughout this year and helped me maintain a somewhat healthy thesis-life balance. With all your support I can look back at this period in my life and be content with all that has happened. Thank you all.

Mateusz Glowacki
Delft, May 2024

Summary

The current state-of-the-art hypergolic propellants are toxic and thus efforts are being made to find alternatives. TNO's novel hypergolic propellant combination is one possible solution, consisting of HTP as the oxidizer and ethanol and two additives as the fuel. At the start of the project it was known that it was hypergolic, but a method was necessary to quantify said hypergolicity.

It was found that the research of novel hypergolic propellants starts with drop testing, continues with impinging jet testing and concludes with small engine testing. As such, it was decided that a drop test set-up was to be developed to perform the first hypergolic propellant research step. In order to reduce the project risk, first a flexible ambient set-up was developed and used to characterize the propellant combination. Based on the lessons learned, a hermetic set-up is under developed at the time of writing in order to be able to research the effects of pressure on the hypergolic performance.

The key hypergolic performance parameters were found to be the ignition chance (positively correlated with the propellant temperature and the propellant volume, negatively correlated with the impact velocity, influenced by the shape of the reaction vessel), the ignition delay time (negatively correlated with the propellant temperature), the chemical delay time (negatively correlated with the propellant temperature) and the physical delay time (negatively correlated with the propellant temperature and influenced by the propellant volume).

Table 1: Test conditions

Test series	Fuel batch	Fuel V [μL]	HTP V [μL]	Syringe type	Vial type	Top T [^{o}C]	Bottom T [^{o}C]	Drop H [mm]	Weber number
BaseA	1	110	11	1.2 taper	large	21	21	80	78
LessOx	1	110	5	0.6 taper	large	21	21	79	59
LessOF	1	50	5	0.6 taper	large	21	21	79	59
High	1	110	11	1.2 taper	large	21	21	144	138
HTPHeat	1	110	11	1.2 taper	large	24.6	21	81	79
FuelHeat	1	110	11	1.2 taper	large	21	28.3	81	79
BaseB	1	110	11	1.2 taper	large	21	21	81	79
Blunt110	2	110	11	1.5 blunt	large	21	21	80	78
BaseC110	2	110	11	1.2 taper	large	21	21	80	78
BaseC150	2	150	11	1.2 taper	large	21	21	80	78
BaseC200	2	200	11	1.2 taper	large	21	21	80	78
BaseC250	2	250	11	1.2 taper	large	21	21	80	78
BaseC350	2	350	11	1.2 taper	large	21	21	80	78
Vial110	2	110	11	1.2 taper	small	21	21	80	78
Vial150	2	150	11	1.2 taper	small	21	21	80	78
Vial200	2	200	11	1.2 taper	small	21	21	80	78

Table 2: Ambient Results

Series	Tests	Ignitions	PDT	CDT	IDT	Comment
BaseA	5	80%	22	38	60	-
LessOx	5	0%	24	-	-	One not recorded
LessOF	5	0%	27	-	-	Weak decomposition, one not recorded
High	8	38%	21	46	66	Characterized by variability
HTPHeat	6	50%	22	31	53	One not recorded
FuelHeat	3	100%	15	28	43	Temperature determined afterwards
BaseB	5	80%	20	43	63	Ensuring propellants did not deteriorate
BaseA+BaseB	10	80%	21	41	62	Summation of two test series
Blunt110	5	40%	25	31	57	One not recorded
BaseC110	5	0%	21	-	-	One not recorded, two drops via side of vial
BaseC150	5	60%	21	30	51	-
BaseC200	5	100%	24	28	53	-
BaseC250	5	100%	23	24	46	-
BaseC350	3	100%	25	26	51	-
Vial110	5	40%	23	26	49	-
Vial150	5	40%	23	26	49	-
Vial200	5	40%	24	33	58	Two drops via side of vial

The test conditions and the results of the tests can be found in tables 1 and 2 respectively. TNO's novel hypergolic propellant was found to have an ignition chance of 100% when the oxidizer and fuel volumes were at least 11 µL and 200 µL respectively. The ignition delay time was found to be 50 ms on average which is generally deemed acceptable, although not ideal. However, the mixture of ethanol and the two additives has not yet been optimized for a minimal ignition delay time thus it is likely that this value can be decreased by doing so.

Contents

List of Figures

List of Tables

Nomenclature

Abbreviations

Abbreviation	Definition
ADCS	Attitude Determination and Control Systems
CCAT	copper chloride hydrous
CDT	Chemical Delay Time
CEA	Chemical Equilibrium Applications
COTS	Commercial Of The Shelf
DLR	Deutsches Zentrum für Luft- und Raumfahrt
FEM	Finite Element Method
HTP	High Test Peroxide
IDT	Ignition Delay Time
LED	Light Emitting Diode
MCAT	manganese (III) acetylacetonate
MMH	MonoMethyl Hydrazine
N2	Nitrogen
NASA	National Aeronautics and Space Administration
NPS	National Pipe Straight
NPT	National Pipe Tapered
NTO	diNitrogen TetrOxide
O/F ratio	Oxygen to Fuel ratio
PDF	Probability Density Function
PDT	Physical Delay Time
RSS	Reactive Stream Separation
RSS	Residual Sum of Squares method
SAE	Society of Automotive Engineers
TNO	Nederlandse Organisatie voor Toegepast Natuurwetenschappelijk Onderzoek
UNF	UNified Fine thread

Symbols

Symbol	Definition	Unit
d	Diameter	$[m]$
g_0	Standard gravity	$[\frac{m}{s^2}]$
H	Height	$[m]$
Hz	Frequency	$[\frac{1}{s}]$
I_{sp}	Specific impulse	$[s]$
I_{ssp}	System specific impulse	$[\frac{Ns}{kg}]$
l	Length	$[m]$
P	Pressure	$[Pa]$
T	Temperaure	$[^oC]$
t	Thickness	$[m]$
v	Velocity	$[\frac{m}{s}]$
V	Volume	$[L]$

Symbol	Definition	Unit
We	Weber number	[-]

Symbol	Definition	Unit
ρ	Density	$[\frac{kg}{m^3}]$
σ	Strength	[Pa]
σ	Surface tension	$[\frac{N}{m}]$

1

Introduction

Space exploration is currently at a very interesting point in time. For decades, it has progressed in a steady albeit slow pace, especially compared to the space race which culminated in humans taking their first steps on the moon during the Apollo program. Now, it seems that this progress has sped up again. SpaceX has made the price of launching payloads into space cheaper than ever, project Artemis makes the prospect of returning to the moon in the near future very real and overall innovation seems to be increasing with an unprecedented amount of start-ups being created in the space sector.

However, one area which has not yet seen much innovation is that of hypergolic propellants. These are liquid rocket propellant combinations that ignite on contact with each other, which has the great benefit of making igniters unnecessary. This results in these propellants being very reliable and allowing for very small impulse burns at high efficiency. The problem is that the current state-of-the-art hypergolic propellants are extremely toxic. As such, a need exists for a novel hypergolic propellant combination which does not have such a problem.

One institution which is developing such an alternative is TNO. Its propellant combination is based on hydrogen peroxide as the oxidizer and ethanol with two additives as the fuel. This combination has been proven to be hypergolic in previous tests done by TNO. However, it is necessary to quantify this hypergolicity in order to ascertain whether the propellant combination can be used in actual thrusters. This thesis report aims to provide an answer to that. It should be noted that the proprietary nature of this fuel does not allow for the names of these two additives to be included in this report.

It should furthermore be noted that this thesis report builds on a previous literature study report, which was also written by the author. As such, large parts of said literature study report can be found in this report [32]. One consequence of this is that some of the research questions as found at the end of the introduction chapter have already been answered in the chapter itself. However, they have been included nonetheless as the answers to said questions are an integral part of the overall report.

1.1. Literature Study

Propulsion systems in spacecraft provide the means to change the direction and velocity of travel of said spacecraft. This allows for the launch of objects into space and the maneuvering of objects once they are in space. Conventionally, this is attained by expelling mass at a high velocity, which generates thrust. Integrated over time and divided by the mass of the spacecraft one gets the delta-v, which is the maximum velocity vector change which a propulsion system can provide. Ensuring this value is as high as possible while using as few resources as possible (especially minimizing the mass of the propulsion system) is the goal of propulsion systems engineering.

1.1.1. System parameters

There are some parameters which denote the performance of a propulsion system. These are useful when comparing different such systems and are as follows.

Specific impulse
Probably the most important parameter for any propellant is the specific impulse or I_{sp}. It denotes how much velocity can be obtained from a unit mass of a propellant. It is equivalent to the exhaust velocity which indicates the velocity with which a given unit mass of propellant is expelled from an engine [29][67].

System specific impulse
A related parameter is the system specific impulse or I_{ssp}. This is equal to the total impulse divided by the propulsion system mass. This value makes comparing different propulsion subsytems easier as both the fuel efficiency and the hardware specific to this propellant and acceleration method are included [29].

Density
Density has a direct influence on the volume requirement of the propellant. Although some propellants may have a relatively high I_{sp}, if they have a low density the resulting volume requirement may make them unsuitable for a given use case anyway. The product of I_{sp} and density is called the density specific impulse [29][67].

Electrical power
Electrical power is generally used for the actuation of the propulsion system, although it can also be used for the acceleration of the propellant itself. A need for more electrical power necessitates a power system with more mass and volume, both of which should be minimized, thus electrical power usage should be minimized [29].

Thrust
Thrust is the force which is generated by the propulsion system. A higher thrust can enable spacecraft to perform maneuvers to attain mission goals while requiring less delta-v and/or time, which in general is beneficial. An example of this is the launch of objects into orbit [29].

1.1.2. Types of propulsion systems
There are many types of propulsion systems which can be divided into different categories. Each such system has its pros and cons making it more optimal for some missions and less optimal for others. The highest division describes how mass expelled by a rocket is accelerated, which can be divided into thermal acceleration (propellant temperature is converted into propellant velocity), electro-static acceleration (positively charged ions are accelerated by an electric field) and electro-dynamic acceleration (plasma accelerated by an electromagnetic field).

The main distinction is in terms of efficiency and thrust acceleration. Thermal propulsion has a lower exhaust velocity (1-20 km/s), a higher thrust acceleration (0.1-10 g_0) and is simpler compared to both electro-static and electro-dynamic propulsion (both of which have an exhaust velocity of 5-100 km/s and a thrust acceleration of $10^{-3} - 10^{-5}g_0$) [68]. The higher acceleration makes thermal propulsion the only viable option for launching payloads into orbit and is preferred for human exploration as it shortens mission duration compared to lower-thrust alternatives. It also has the benefit of not using electrical power for the acceleration of the exhaust mass, which directly translates into a lower power subsystem mass. Furthermore, its relative simplicity increases its reliability which is also critical for human exploration. On the other hand, the higher exhaust velocity (and thus fuel efficiency) makes electo-static and electro-dynamic propulsion preferred for deep-space missions where both mission duration is less critical and high-thrust maneuvers are not necessary.

Thermal (acceleration) propulsion can be divided into two further categories, chemical propulsion and non-chemical propulsion. The former utilizes chemical reactions of the propellant to heat the reaction products of the propellant. The latter uses other methods to do so, which include electrical power and nuclear power (internal power sources), the sun and lasers (external power sources) [68]. Currently, chemical propulsion sees widespread use while non-chemical propulsion is still mostly experimental.

Chemical propulsion can be further divided into utilizing solid propellants, hybrid propellants (utilizing one solid and one liquid part), liquid monopropellants and liquid bipropellants. A comparison can be

seen in table 1.1 [68]. As can be seen, liquid bipropellants are the preferred option when problems with complexity are overcome, especially if a high specific impulse (efficiency) is needed.

Table 1.1: Comparison of different chemical propellants

Propulsion type	Typical specific impulse range [s]	Small and accurate minimum impulse bit	Reignitable	Relative thrust	Relative complexity
Solid	170-250	no	no	high	low
Hybrid	230-270	no	yes	medium	medium
Liquid monopropellant	160-230	yes	yes	low	low
Liquid bipropellant	200-385	yes	yes	high	high

A typical liquid bipropellant system can be found in figure 1.1. It consists of two tanks where the fuel and oxidizer are stored separately. These propellants are then transported to the combustion chamber, either by a pump or another method. The two propellants are then ignited in said combustion chamber, which produces heat. This energy is used to exhaust the reaction products from the nozzle which provides thrust.
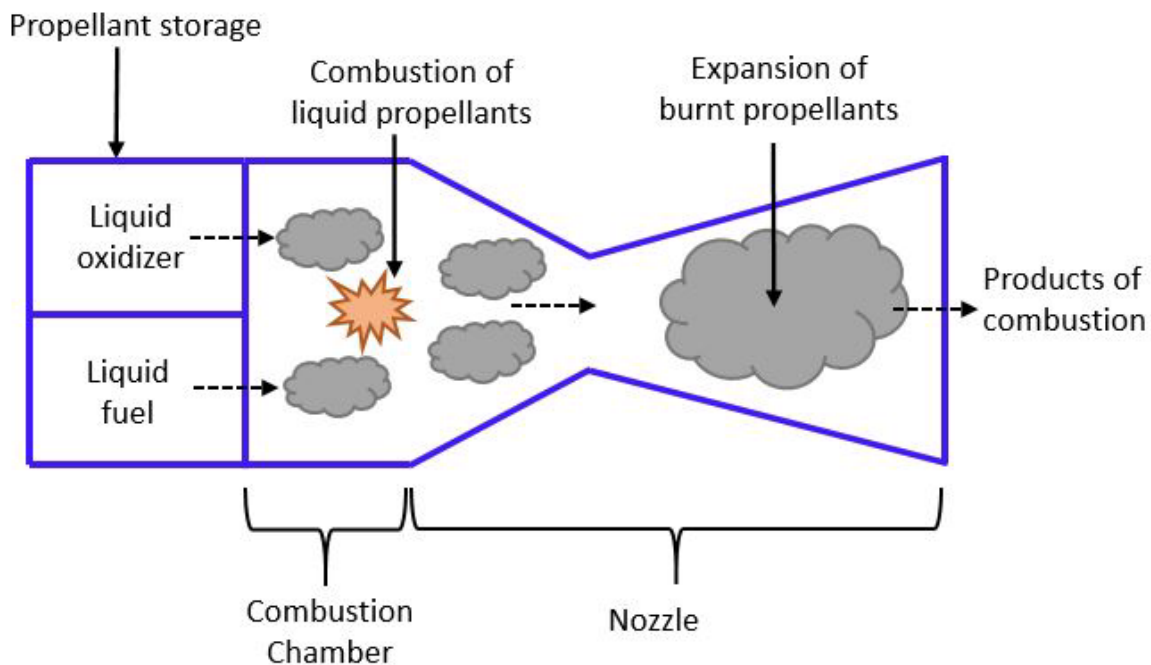
Figure 1.1: Typical liquid bipropellant system[1]

1.1.3. Liquid bipropellant system parameters

There are many parameters which are relevant when designing a liquid bipropellant system, aside from the parameters relevant for all propulsion systems which have been mentioned. These are as follows.

Viscosity

The viscosity of a propellant has an impact on its behavior both in the feed system and the engine. A lower viscosity means a lower pressure drop over a feed system which results in lower pressure head requirements. This can for example result in lower blow-down pressurization sub-system mass and volume requirements, as less pressurant is required for the same injection pressure. A lower viscosity also promotes better atomization of the propellant resulting in a better mixing efficiency and thus less demanding design requirements. It is an especially important parameter for gelled propellants [29][22].

Adiabatic flame temperature

The adiabatic flame temperature is the maximum theoretical temperature which can be reached during a combustion reaction. It is important to know this value in order to predict the temperature in the combustion chamber. This temperature in turn has an effect on the choice of materials used for the combustion chamber, its geometry, possible cooling methods, etc. Furthermore, higher adiabatic flame temperatures correlate with higher I_{sp} given that all other conditions are equal [29][67].

Molecular mass

The molecular mass is the mass of a single molecule of a given compound. Its importance lies in the fact that, given that all other conditions are equal, a lower molecular mass results in a higher specific impulse. This is due to the fact that less mass needs to be accelerated using the same amount of energy. This makes it generally desirable to minimize this value [29].

Atomization

Atomization describes the propellant droplet size distribution, which relates to injector design and the fluid properties. A smaller mean droplet size results in better mixing efficiency which in turn shortens the required characteristic length. This means a smaller engine which in turn directly translates into mass and volume savings. An example of different degrees of atomization can be found in figure 1.2 [43][48].
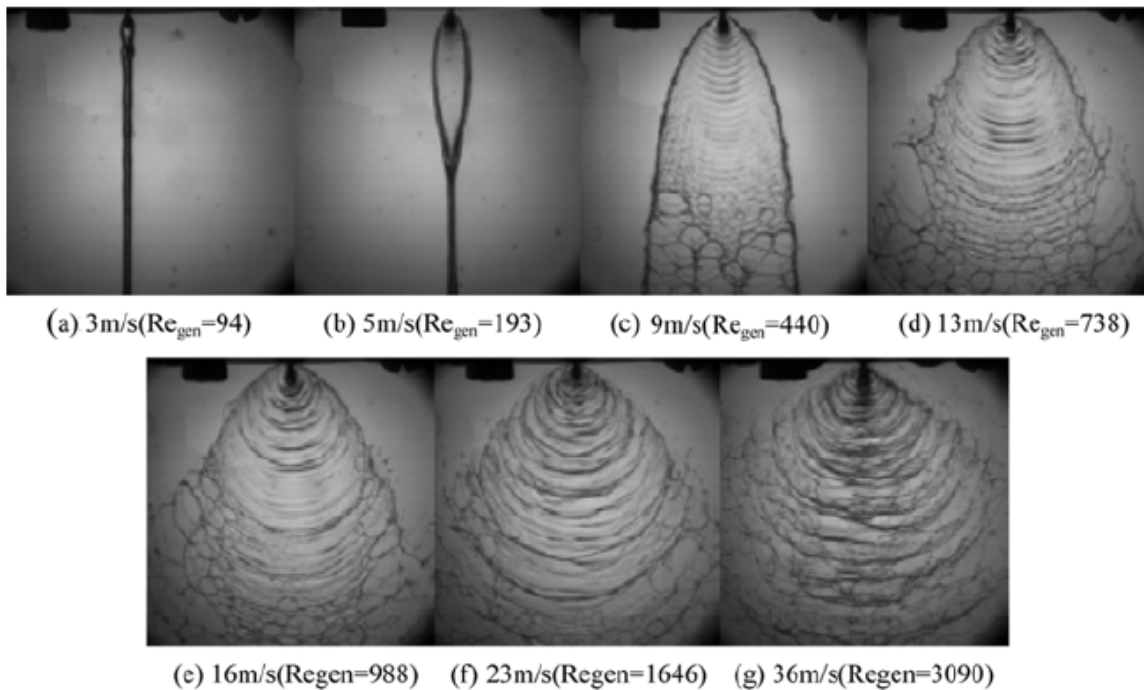
Figure 1.2: Different degrees of atomization [9]

Combustion stability

Good combustion stability means that there are no fluctuations in the combustion process (e.g. pressure, temperature, etc.) if there are no fluctuations in the input parameters (e.g. propellant massflow, propellant temperature, etc.). This is important as severe combustion instability can decrease the combustion efficiency and even lead to a catastrophic failure of the engine. Examples of combustion instabilities are low-frequency chugging and high-frequency screaming for all bipropellant combinations [29], as well as reactive stream separation and popping for hypergolic bipropellant combinations specifically.

Cavitation

Cavitation is the formation of vapor bubbles in a liquid stream due to the liquid pressure locally dropping below the vaporization pressure. This decreases the combustion efficiency. Reasons for this are the improper design of the injector or the feed system [58][24].

Characteristic length
The characteristic length is the volume of a combustion chamber divided by the nozzle sonic throat area theoretically necessary for complete mixing and combustion of the propellants. As the throat diameter for de Lavale nozzles is always smaller than the combustion chamber diameter, this value is only theoretical and actual combustion chamber lengths are shorter. It is nonetheless a useful concept and is analogous and proportional to the residence time, which denotes the average time of stay of a given propellant mass in the combustion chamber [29].

Operating temperature range
The operating temperature range is the temperature range of the propellants over which they are usable for rocket propulsion. For liquid bipropellant engines this means that the propellants are above their freezing point and below their vaporization temperature (i.e. they are liquid). For hypergolic propellants specifically this depends on the desired ignition delay time and ignition behavior. Furthermore, the operating temperature range can be influenced by the requirements like viscosity, combustion stability or cooling capabilities, all of which depend on the temperature of the propellants [29][67].

Material compatibility
Material compatibility entails that the propellants do not react with materials used in the design, like for example the feed system pipes or the combustion chamber itself. Oxidizers in particular require special attention regarding this, as for example liquid oxygen has been known to explode in feed systems if these have not been designed and cleaned properly [29].

Thermal characteristics
Thermal characteristics entail the thermal conductivity and thermal capacity of a propellant. These are particularly important when using a given propellant to cool the engine, as is the case when using regenerative cooling where a propellant is fed through the wall of an engine during operation which cools said wall preventing structural failure [29].

Storability
Storability denotes the behavior of propellants over time when stored, mainly the change in their composition [67]. Storability can especially be a concern during long-term missions where propellants are sometimes stored for years before being used. However, it is also important in the lab, as a compound can degrade over time into something which becomes unusable for a given experiment. Although HTP is known to decompose over time, this rate can be as low as 0.4% per year given proper storage. It can thus be considered stable over a period of a few months [63].

Toxicity
Toxicity is possibly the most important parameter on this list, as it is the very reason this project exists. It entails both health and environmental hazards, with some chemicals necessitating handling precautions and the use of personal protective equipment leading to higher costs. There are many ways to qualify and quantify toxicity [46], but for the intents and purposes of this project it can be summarized that the state-of-the-art hypergolic propellants Monomethyl hydrazine (MMH) and Nitrogen Tetroxide (NTO) are toxic. As such, this project seeks to find an alternative in the form of a combination of HTP and ethanol + additives. Legally speaking, the European REACH regulation designates substances of concern, with for example hydrazine being a substance of very high concern [47].

Cost and availability
Cost and availability are two parameters which, while not inherent to a given propellant, nonetheless can and often do have a decisive impact on the propellant choice. A given propellant might have the best characteristics of any propellant, but if it is unavailable or it costs more than a given project allows for it becomes unviable nonetheless. Often there is a trade-off between performance on the one hand and cost and availability on the other [29].

1.1.4. Hypergolicity

A specific type of liquid bipropellants are hypergolic propellants. These are bipropellants which ignite when the fuel and oxidizer come into contact with each other. This is due to an exothermic reaction occurring resulting in a rise in temperature to the point of ignition of the mixture. Hypergolicity is a useful characteristic as it removes the need for an ignition source, which in turn simplifies the system thus decreasing its mass and volume and increasing its reliability. This is very beneficial when said reliability is paramount, as for example was the case for the Apollo missions where ignition failure was unacceptable as it would directly lead to a loss of the crew.

Hypergolicity has another benefit in the form of being able to provide a very low impulse bit at high efficiency. This is due to the fact that very small propellant amounts can be brought together without the need of precisely timing the activation of an ignition source. Using an ignition source would make this process unnecessarily complex and unreliable compared to using hypergolic propellants instead. This is especially useful for the Attitude Determination and Control System (ADCS), which needs to be able to perform very small burns to dump any rotation it may have acquired when in orbit.

While liquid monopropellants could also provide such a minimum impulse bit with high reliability, they are less efficient than liquid bipropellants and thus less preferred, especially for longer missions. This is due to the fact that the propellant amount in ADCS systems often proves to be the limiting factor for the overall mission duration. This means that having a more efficient propellant combination results in a longer mission given the same amount of propellant, which is why hypergolic propellants are often the preferred choice.

1.1.5. Types of hypergolic propellants

Representative for the current state-of-the-art hypergolic propellant combinations are monomethyl hydrazine (MMH) as the fuel and dintrogen tetroxide (NTO) as the oxidizer. They are reliable and provide very good performance. However, a large downside of these propellants is their toxic nature, even requiring a hazmat suit to handle. As such, they are classified as dangerous under the REACH regulation of the European Chemical Agency [55][54]. This means that finding a viable green alternative to the current hypergolic propellants would be of great benefit to the space industry.

Research is ongoing, but promising alternatives include combinations of either ionic liquid-based fuels or ethanol-based fuels with HTP (high-test peroxide, or concentrated hydrogen peroxide) as the oxidizer. There are multiple institutes in Europe which are researching possible novel green hypergolic propellants. One of these institutes is TNO, which is developing an alternative based on hydrogen peroxide and ethanol with additives.

This combination was chosen based on an earlier study performed within TNO, which performed a trade-off based on multiple measures of effectiveness as defined in said study. Ethanol was chosen for the fuel as it has a low health risk index, an acceptable performance and the development risks are low. HTP was chosen for the oxidizer as it satisfied all requirements defined in said study and had the best theoretical performance characteristics among the remaining candidates [66]. However, HTP/ethanol propellants are not hypergolic by themselves and thus additives are necessary to be added to the ethanol in order to induce said hypergolicity.

TNO distinguishes two types of additives: catalysts and propagators. Catalysts decompose HTP resulting in oxygen and water with a temperature of over 1000K. Propagators (as currently understood) exothermically react with oxygen at said temperature, which increases the temperature even further leading to ignition. However, more research on the latter is needed to better understand this process [59].

This propellant combination is still experimental and needs to be further researched to ensure it is viable for commercial spaceflight. At the start of this Thesis the development of this propellant combination was at a stage where the mixture ratio with the highest ignition probability was determined. This mixture ratio also showed good theoretical specific impulse. Using NASA-CEA with a combustion chamber pressure of 10 bar and a nozzle expansion ratio of 100 (which are typical for hypergolic bipropellant

thrusters in operation [42]), an I_{sp} of 308 s was found for 97% HTP as the oxidizer and an O/F ratio of 2.3. Comparing this to an I_{sp} of 331 s for MMH/NTO (a difference of 7%) shows the potential of TNO's propellant combination as a safer alternative. The next step was quantifying its hypergolic performance.

1.1.6. Hypergolic propellant system parameters

The nature of hypergolic propellants introduces new considerations and system complexities which are not present in non-hypergolic systems. These are new performance parameters (aside from "normal" performance parameters, like thrust, specific impulse, etc.) and testing methods dedicated to testing hypergolic behavior. These are presented in this section.

Ignition probability

Under some conditions propellant combinations can be hypergolic only some of the time, which is denoted by the ignition probability parameter. It denotes the probability of a given fuel/oxidizer propellant combination to hypergolically ignite upon contact for a given set of conditions. A probability of less than 100% is seen as undesirable. One could argue that if for example the probability is 90% during drop testing, when used in an engine this probability would eventually become 100% as enough fuel and oxidizer are brought together. However, the result of this could be an ignition delay of such magnitude as to result in a hard start. Thus, the ignition probability should be 100%.

It has been found that multiple factors influence this parameter, which thus need to be considered during design. Propellant composition is the most important one, as propellant combinations with additives added to the fuel and/or oxidizer to induce hypergolicity need enough of said additives to reach the 100% ignition probability. One could consider propellant storage part of this, as improper storage could result in changes of the propellant composition, for example due to a decrease in concentration of HTP or the increase in moisture in a fuel [14].

Contact parameters are relevant as well. For example, the Weber number and thus the contact velocity in a drop test [11] or the impact angle between droplets (i.e. if the drops are off-center compared to each other) in a drop test have an influence on this. A bounce can occur when the impact angle is too large (>7°) [34] and a splash can occur when the Weber number is too high (>250) [11][34], which negatively influence the ignition probability.

Finally, the atmospheric composition can play a role. For example, while ignition probability can be 100% for argon-filled and oxygen-filled atmospheres it can be 0% for a helium-filled atmosphere. This shows that the thermal properties of the atmospheric composition have an impact on the ignition probability [14]. Whether oxygen in the atmosphere can have an impact on the ignition probability as a chemical reactant is unclear.

Ignition delay time

One of the most important parameters for any hypergolic propellant combination is the ignition delay time. This is due to the fact that if the ignition delay time is too long an instability phenomenon known as a hard start can occur which can result in damage to the engine [37]. Furthermore, a shorter ignition delay time allows for a shorter minimum impulse bit, which allows for finer attitude control [40]. The combination of these two factors suggests that the ignition delay time should be as short as possible.

However, decreasing ignition delay time increases the chance of reactive stream separation and popping occurring, which are combustion instabilities which negatively impact engine efficiency [43]. There is thus a desirable ignition delay time range which depends on the application in question. Nonetheless, in general a lower ignition delay time is preferred, with an IDT below 50 ms being deemed acceptable and an IDT below 10 ms being deemed preferable for most applications [45][35].

Parameters which influence the ignition delay time are as follows. A shorter ignition delay time is a result of higher pressure up to a point (6 bar was noted in the case of 93% HTP as the oxidizer, high-density Polyethylene as the fuel and sodium borohydride as the additive) [14], a smaller droplet size (by as much as 25%) [14] and a higher HTP content [14]. A higher Weber number also shortens the

ignition delay time [11], although there are both an upper [34] and lower [11] limit beyond which ignition probability suffers.

The IDT is also influenced by the atmospheric composition, with argon reducing it by as much as 48% compared to nitrogen and air, likely due to the differing thermal properties [14]. The oxygen content of the atmosphere can also have an impact on the IDT due to its chemical reactivity, although whether this effect is present depends on the propellant combination in question [2]. Lastly, the choice for a propellant lead has also been found to have an effect on IDT, with the preferred lead time and the preference for fuel or oxidizer as the lead depending on the propellant combination in question. This is related to vapor formation of the lead propellant before the arrival of the droplet [62].

Ignition delay time itself can be divided parts, which is useful as it furthers our understanding of this process. There is one division which is uniform in literature, which is the pre-chemical delay time and the chemical delay time, as the former depends on the set-up while the latter is relatively constant given identical conditions, independent of the set-up. However, the period before the chemical delay time is broken up differently depending on the source, with some sources having one pre-chemical delay time (vaporization time) and others dividing it into two further times (droplet entry time and mixing time). The ones presented here are relevant to drop tests. It can also be noted that this division is the same for both gelled and non-gelled propellants [62][14].
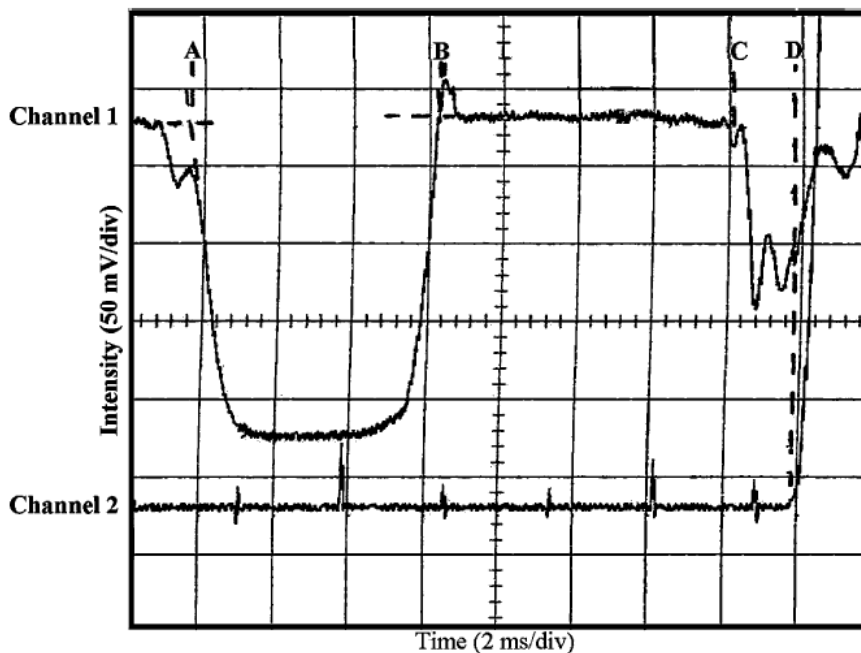
Figure 1.3: Ignition delay time division example [12]

An example of such a division of the ignition delay time as seen in a drop test can be found in figure 1.3. Channel 1 denotes a laser and sensor pair which intersects with the path of the falling drop, while being right above the liquid into which said drop will fall. Channel 2 is a photoreceptor which is used to detect ignition. One can find the droplet entering the liquid between A and B. Mixing occurs between B and C, after which vapor forms between C and D. Finally, ignition occurs at D.

Chemical delay time
The chemical delay time is the time between the start of chemical reactions leading to ignition and ignition itself. The former is usually defined by the first observed appearance of mixed propellant vapor while the latter is defined by the first appearance of a flash [62][36].

Vaporization time

Vaporization time is the time between the fuel and oxidizer droplets first coming into contact and the first observed appearance of mixed propellant vapor. This can either be taken as the total pre-chemical delay time or further divided into the droplet entry time and mixing time [62]. The example found in figure 1.3 shows a typical drop test for UDMH/RFNA and was found to be representative for hypergolic propellants in general.

Droplet entry time

Droplet entry time is the time between the fuel and oxidizer droplets first coming into contact with each other and the two separate drops becoming one larger droplet [36].

Mixing time

Mixing time is the time between the end of the droplet entry time and the first observed appearance of mixed propellant vapor [36].

Flame propagation velocity

The next hypergolic propellant parameter is the flame propagation velocity. This is the velocity with which the flame travels from the initial ignition point outwards. A higher velocity is positively correlated with a lower pressurization time, which denotes the time from ignition to full pressurization in an engine. According to a study by Slocum-Wang et al. a lower pressurization time increases the chance of a hard start, thus making a lower flame propagation velocity desirable [62].

Important parameters relating to this are as follows. If the droplet velocity is high enough to result in a splash, flame propagation velocity starts increasing compared to no splash, with a larger splash resulting in a higher velocity. Secondly, a higher chamber pressure results in a higher velocity as well. Finally, argon seems to result in a higher velocity compared to air [14].

Reactive stream separation

Reactive Stream Separation or RSS for short is the incomplete mixing of the fuel and oxidizer in unlike impinging jets which results in the blowing apart of the propellant streams. This is mainly caused when the propellant reactivity is relatively high and mixing does not occur fast enough, which results in the vaporization of propellants which blows them apart [43]. An ignition delay time lower than the mixing time promotes RSS [26], although it does not guarantee it [43]. A visualization of this can be found in figure 1.4. This results in a decrease of the combustion efficiency and thus the I_{sp}. RSS is promoted by a higher chamber pressure, a higher average fuel temperature, a higher propellant injection velocity and a larger injection orifice diameter [43].
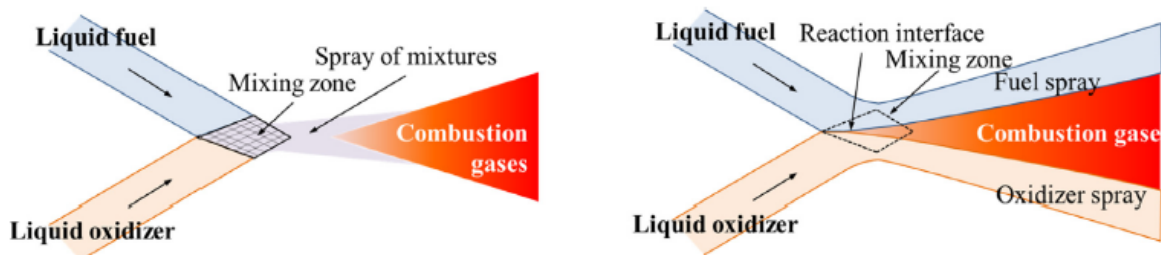
Figure 1.4: Normal operation (left) vs. RSS (right) [48]

Popping

Popping is the occurrence of random explosions (from which popping gets its name) which result in a temporary increase in both the pressure and burning rate. These occur downstream of the impingement point but before complete atomization. This is defined as the ligament zone, which is the thin sheet of liquid created by impingement as can be seen in figure 1.5. An ignition time lower than the the time until atomization promotes popping, although it does not guarantee it. Nonetheless, solutions based on this assumption are effective at eliminating popping [43]. Similarly to RSS, it decreases the combustion

efficiency and thus the I_{sp}. The occurance of popping is dependent on the chamber pressure, the propellant temperature, the mixing efficiency, the injection orifice diameter, the injection velocity and the distance between unlike injectors [65][43][44].
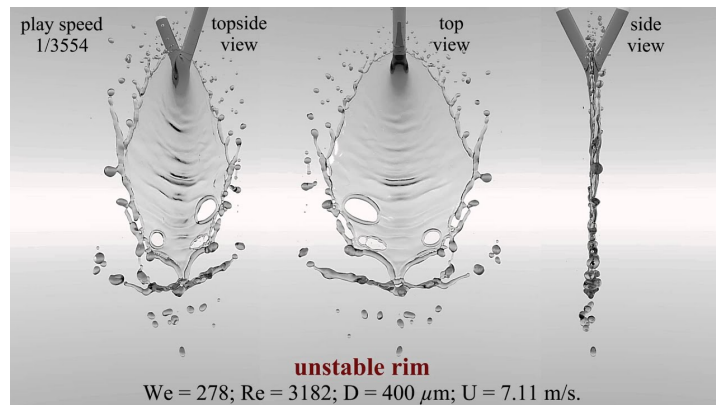
Figure 1.5: Ligament zone [60]

1.1.7. Design parameters

Aside from parameters inherent to the propellant combination, when designing an engine or any other such system it is important to keep the design parameters in mind as well. These are the engineering choices which together with the propellant parameters determine the resulting performance of the system. Furthermore, as most propellant characteristics are a function of these parameters, they are also important for any propellant characterization. Not included are parameters like for example the throat diameter, as these do not directly influence propellant performance, but rather influence parameters (like the chamber pressure) which themselves directly influence propellant performance. Only the latter are presented.

Propellant composition

The propellant composition is the basic question of what the propellant combination consists of. It is the most basic and direct input for the resulting propellant parameters.

O/F ratio

The oxidizer-to-fuel ratio is the ratio of the oxidizer mass to the fuel mass. It is key in determining the chemistry of the reaction and the associated parameters like the adiabatic flame temperature, I_{sp}, products, stability or hypergolicity. Theoretically, the optimal ratio is the stoichiometric ratio where all the fuel reacts with all the oxidizer. This also results in the highest adiabatic flame temperature. In practice however, the mixture is run slightly richer (relatively more fuel). This is due to the fact that this tends to result in a lower molecular weight at a comparatively less significant loss of temperature resulting in a higher specific impulse. There are other reasons due to which one might deviate from the stoichiometrically optimal or I_{sp} optimal as well, which directly relate to the parameters dependent on the O/F ratio stated before [29].

Chamber pressure

The chamber pressure is the pressure which is found in the combustion chamber during operation. As stated, it has an impact on multiple parameters like the specific impulse, the ignition delay time and combustion stability, among others. Of particular interest are vacuum conditions, as these are experienced during space-flight missions and thus during in-flight ignition [43][14].

Propellant back-pressure

The propellant back-pressure is the pressure which is used to inject the propellants into the combustion chamber. This pressure not only must be proportionally higher than the combustion chamber in order to inject the propellants at the desired velocity, but also as to overcome the pressure drop over the feed system and the injector. This desired pressure can be achieved in multiple ways, which includes using a separate pressurization gas, turbopumps or even a self-pressurizing propellant [29].

Propellant temperature
The propellant temperature has an impact on combustion stability, mixing efficiency [43], cooling properties as well as general performance [29]. For hypergolic propellants specifically, a higher propellant temperature correlates with lower ignition delay times [8].

Propellant contact geometry
The propellant contact geometry denotes the way in which the fuel and oxidizer come into contact with each other. This includes the massflow, the angle, the velocity, etc, which is most relevant for the ignition delay time, combustion stability and atomization [65][21].

Weber number
The Weber number is a dimensionless number which relates the inertial force to the surface tension force. It has been found to be negatively correlated with IDT, with a Weber number above 250 resulting in a discontinuity in this correlation, which should thus be avoided during testing. In general, a larger droplet diameter and a higher drop height result in a higher Weber number. The exact formula is as follows: [64]

$$We = \rho v^2 l / \sigma \tag{1.1}$$

Where "We" is the dimensionless Weber number, ρ is the density in kg/m^3, v is the (droplet impact) velocity in m/s, l is the characteristic length or droplet diameter in m and σ is the surface tension in N/m.

1.1.8. Testing methods
There are multiple testing methods available for the hypergolic characterization of propellants. The most notable ones are drop tests, impinging jet tests and small engine tests. However, there are other less frequently used methods as well. All of these are described in this subsection.

Drop test
A drop test is the most basic way of hypergolic propellant testing. In essence, it comes down to dropping a drop of a fuel or oxidizer into a certain amount of the other propellant and measuring whether ignition occurs. This set-up can become relatively complex depending on what input variables are controlled for and what measurement techniques are used. An example of a drop test set-up can be found in figure 1.6.
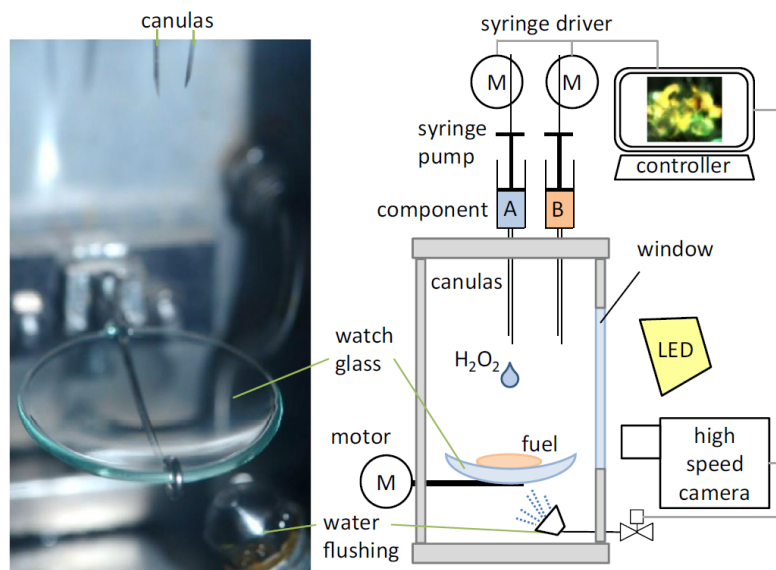
Figure 1.6: Example of a drop test set-up [6]

Small engine test

The idea of the small engine test is to test hypergolic propellants in an environment in which they will actually be used, namely an engine. However, as building a full-scale engine is expensive, a smaller engine can be built which provides almost the same amount of data using less resources. The oxidizer and fuel are injected into the combustion chamber of the engine where they hypergolically ignite. The resulting combustion can be studied in order to better understand characteristics like ignition delay time, combustion efficiency, combustion stability or atomization [62].

Impinging jet test

In an impinging jet test hypergolic propellants are mixed using two or more jets, similarly to what can be found in an injector in a rocket engine. Just as in a small engine test, the ignition delay time, combustion efficiency, combustion stability or atomization can be studied. It is often used as a step between a drop test and a small engine test, as it is much simpler than the latter yet provides critical data for further development which cannot be gained from a drop test, like RSS or atomization behavior. An example of a combustion chamber used in such a test can be found in figure 1.7 [49][57].
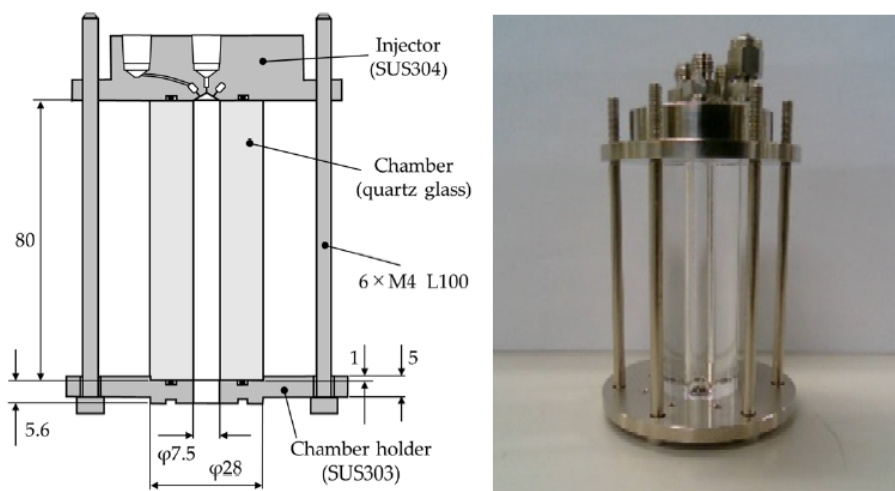
Figure 1.7: Example of a combustion chamber used in an impinging jet test [49]

Forced mixing test

The forced mixing test entails the initiation of sudden contact between the fuel and oxidizer, for example by breaking a glass ampule containing one when submerged in the other. The results of this test are generally less clear and useful than the results of a drop test, with the ignition delay time results having been found to be unreliable [57][28].

Bomb test

The bomb test is a test where a given amount of fuel and oxidizer reacts with each other in a closed chamber. This results in a final pressure, temperature and mixture composition which can be analyzed to give a good insight into the chemical processes which took place. It can be similar to a drop test with a spectrometer where the mixture composition is analyzed as well, although in a bomb test the hypergolic behavior itself is less important than the final state of the system [61][28].

Microreactor test

The microreactor test is a test where the fuel and oxidizer are brought together in a microscale set-up. Often observed real-time under a microscope, it gives a unique view into the chemical processes taking place at this scale. Especially the analysis of the fluid dynamics and the changes in temperature can give a good insight into the processes taking place [57][39].

1.1.9. **Most relevant studies**

The following list includes studies which were deemed to be of the greatest relevance to the project, along with their most relevant findings. Some of these findings have already been mentioned in this chapter, while others have not. The goal of this list is to organize said information into a sort of "summary" and to ensure the most relevant findings are highlighted.

- DLR has created a drop test set-up with a hermetically sealed chamber which can vary the pressure and atmosphere. It can clean the combustion vessel (on which the droplets combust) by rotating it and using a water spray to remove any residue, as it can not be cleaned manually without opening the set-up [23].

- Purdue University has created a drop test set-up which is unique in using an impact sensor for the detection of the droplet impact and a microphone for the detection of ignition [50].

- The Center of Space Technologies in Warsaw has created a drop test set-up which had a hermetically sealed test chamber, which could vary temperature pressure (up to 30 bar) and the atmospheric composition. Furthermore, the combustion vessel was heated and fluctuations in pressure could be use to detect ignition [53].

- DLR has looked into the question of how to properly define and characterize a "green" propellant. This included toxicity, exposure danger, handling and safety requirements. There was not one optimal propellant choice, but rather the right choice depends on the needs to be fulfilled [46].

- A study by P.A.W. van Dommelen showed the following ignition delay times for liquid ethanol, MCAT (Manganese (III) acetylacetonate) as the catalyst and 97% HTP. 52.3±1 ms of which 35.5±4.4 ms was the chemical delay time for 10% MCAT, 50.6±13.1 ms of which 35.7±17.7 ms was the chemical delay time for 5% MCAT. The drop height was 23 cm at atmospheric conditions [30].

- The Center of Space Technologies in Warsaw showed that an average ignition delay time of 63.2 ms could be achieved using ethanol using 15% 2-ethylohexanoate cobalt (II) as the catalyst and 98% HTP. The tests were done in a hermetically sealed test chamber with the temperature and pressure constant at 20^oC and 1 atmosphere respectively [53].

- The ignition delay time can be divided into two parts: the chemical delay time and the pre-chemical delay time. The former is characterized by the fact that chemical reactions are measurably taking place, while the latter is the period before that, but after droplets come into contact with each other during a drop test. The start of the chemical delay time can either be defined as the start of formation of a vapor cloud above the mixture as can be seen in a study from the University of Alabama in Huntsville [12], or as the start of the rise in temperature of the mixture measured in the IR-spectrum as can be seen in a study from the Xi'an Jiaotong University (which measures the drop test using three different cameras) [19].

- The minimum ignition delay time for a propellant combination using HTP found in literature was 1.33 ms, as found in an article by B.V.S. Jyoti, M.S. Naseem and S.W. Baek [22]. The HTP concentration was 90%, the fuel was ethanol with 4$ Boron, 1% Manganese (II) acetylacetonate and 4% propyl cellulose as the gelling agent. It was a multi-drop test, with its single-drop test yielding an ignition delay time of 37.0 ms. The lowest single drop test ignition delay time was 4.15 ms, using an HTP concentration of 90%, ethanol with 4$ Aluminium, 1% Copper chloride hydrous and 4% propyl cellulose as the gelling agent. In the same study an interesting alternative was found to using infrared cameras, namely using thermal probes.

- One negative effect of minimizing the ignition delay time is the increase in chance of rapid stream separation (RSS) and popping occurring. These are combustion instabilities which lead to a decrease in performance [43].

- A study by A. Mayer and W. Wieling shows the reasoning behind TNO's choice for using ethanol as the fuel. The reason is that while no fuel is best in all trade-off aspects, ethanol was chosen as it has a low health risk index, an acceptable performance and the development risks are low, with HTP being chosen as it is a "green" oxidizer with good handling characteristics. Although it is not hypergolic with HTP at atmospheric conditions, it can be made so using additives [66].

- Two important parameters often disregarded in drop tests are the drop height and the drop impact angle (whether the droplets contact each other off-center). It was found in a study at Purdue University that splashes occur above a Weber number of 250. Below that number bounces can also

occur if the impact angle is greater than 7 degrees. Both of these impact the ignition delay time and thus should be avoided [34]. Furthermore, in a study Northwestern Polytechnical University in Xi'an, it was shown that the Weber number is negatively correlated with the ignition delay time, meaning that the impact parameters between the two droplets are of great importance [11].

- HTP/ethanol combinations without additives auto-ignite from 85% HTP and 473K. The ignition delay time decreases with increasing temperature, with an ignition delay time of less than 100 ms at 543K [33].

1.2. Research direction

The initial goal of this project was to ascertain whether TNO's novel propellant combination has satisfactory hypergolicity characteristics to be used in thrusters. During the literature study it was found that the main characteristic which quantifies hypergolicity is the ignition delay time. This ignition delay time is dependent on many parameters which need to be taken into account when doing any research on it. Furthermore, the ignition delay time can be subdivided into a chemical delay time and a physical delay time, both of which are also relevant for properly understanding the hypergolic behavior of a propellant combination. Thus, the goal of this project should be to ascertain the respective delay times of TNO's propellant combination while controlling for the parameters which influence said delay times.

In order to meet this goal, a testing methodology had to be set up, of which the first step was choosing the testing method (or in other words a testing set-up). As TNO did not have a set-up already, a novel set-up needed to be chosen, designed, built and validated. After the choice for the set-up would be known, the research objective and the research questions could be determined.

1.2.1. Testing method trade-off

The choice for the testing method was made based on a trade-off. This trade-off looked at what is typically characterized using a certain method and the expected complexity of designing, building and validating the testing set-up in question. It can be found in table 1.2.

Table 1.2: Trade-off of different methods of characterizing hypergolic performance

Method	Typically used to characterize	Expected complexity
Drop test	Ignition delay time Pre-ignition thermal behavior	Low
Small engine test	Ignition delay time General non-hypergolic performance	High
Impinging jet test	Ignition delay time General hypergolic performance General non-hypergolic performance	Medium
Forced mixing test	Ignition delay time (unreliable)	Low
Bomb test	Ignition delay time Final combustion products	Medium
Microreactor test	Pre-ignition fluid behavior Pre-ignition thermal behavior	High

As mentioned, at this stage of development of TNO's propellant combination ignition delay time should be characterized. This excludes the microreactor test. Looking at the remaining options, the drop test and forced mixing test are the only ones with a low expected complexity. However, the forced mixing test is known to give unreliable ignition delay times. As such, the drop test method emerges as a clear winner. This was actually expected, as the development of hypergolic propellants typically follows the path of first performing drop tests to characterize the ignition delay time, then performing impinging jet tests to predict various aspects of the behavior of the propellant combination in an engine and finally performing small engine tests to determine the actual behavior of the propellant combination.

It was thus decided to create a drop test set-up which could measure the ignition delay time accurately, with the added benefit of it being a simple and the most widely used testing method for the characterization of novel hypergolic propellants. Furthermore, it gives good insight into the hypergolic pre-ignition (thermal) behavior of the propellant combinations in question. After this trade-off a clear research objective emerges:

To design, build and calibrate a drop test set-up to be used to characterize the hypergolic performance of TNO's HTP/ethanol hypergolic propellant combinations.

1.2.2. Research questions

In order to meet the research objective it is necessary to pose research questions which help direct the project. They are based on the research objective itself as well as the literature study. It should be noted that some of these research questions have already been answered during this literature study. However, they are still included, as the literature study is seen as an integral part of the larger project and its conclusions are included in this thesis. The research questions are as follows:

- What are the most important parameters for the characterization of hypergolicity of HTP/ethanol based bipropellants for space propulsion systems?

  - What are the most important performance parameters which determine the hypergolicity?
  - What are the most important variable input parameters which influence the important performance parameters?
  - Which variable input parameters influence which performance parameters and how?
  - What are the preferred and acceptable ranges of these parameters?

- What test methods can be used to characterize the hypergolic performance of HTP/ethanol based bipropellants?

  - What test methods exist to perform characterization of hypergolic performance and which one is the most suitable?
  - What is a viable test set-up design to measure the hypergolic performance as a function of the variable input parameters?
  - What are the testing procedures necessary for safe and efficient calibration and use of this test set-up?

- What is the hypergolic performance of TNO's HTP/ethanol propellant combinations?

  - How does the hypergolic performance change as a function of the variable input parameters?
  - How does the hypergolic performance change as a function of the propellant composition?
  - Into what stages can the ignition delay time be divided?

1.2.3. Ignition delay time in drop test set-ups

A significant question when performing drop tests is what a good result is. Reiterating, the ignition delay time is the most important parameter for answering this. Ignition delay times of 10 ms or less are considered to have good hypergolic performance, while ignition delay times of 50 ms or less can be deemed acceptable [45].

Not a lot of research has been done on the hypergolic behavior of ethanol while in liquid form when combined with HTP [52]. One study seen in figure 1.8 found an average ignition delay time of 63.2 ms using 15% 2-ethylhexanoate cobalt (II) as the catalyst and 98% HTP. In another study seen in figure 1.9 ethanol with 10% MCAT (Manganese (III) acetylacetonate) and 97% HTP showed a total ignition delay time of 52.3±1 ms of which 35.5±4.4 ms was the chemical delay time, while 5% MCAT and 97% HTP showed a total ignition delay time of 50.6±13.1 ms of which 35.7±17.7 ms was the chemical delay time. 3% MCAT showed no ignition and had the highest physical delay time of the three. In this test campaign the drop height was 23 cm.

Table 3. Results of IDT for catalytically promoted fuels at highest content of additives with 98% HTP.

Fuel	Additive/ Content	Lowest IDT, [ms]	Averaged IDT, [ms]	Highest IDT, [ms]
Benzaldehyde	20% FeCl$_3$·6H$_2$O	47	50,1	53,7
Ethanolamine (MEA)	4% CuCl$_2$·2H$_2$O	32,1	37	44
Ethanol	15% 2-ethylohexanoate cobalt (II)	53,1	63,2	82,7
Izoamyl Alcohol	20% 2-ethylohexanoate cobalt (II)	38,8	48,5	54,7
Jet-A/TMPDA (80/20)	20% (II) cobalt neodecanoate	21,2	22,5	24,6
TMPDA	20% 2-ethylohexanoate cobalt (II)]	5,4	6,6	7,8

Figure 1.8: Ignition delay times using 98% HTP [53]

Table 6.5: Average physical, chemical, and total ignition delay times measured using PDs and HSC for all samples presented in Table 6.4. All values are given in ms.

#	Variant	Physical delay		Chemical delay		Total ignition delay	
		PD	HSC	PD	HSC	PD	HSC
1	5% MCAT	43±12.3	51.6±9.8	45.5±9.8	23.8±4.2	89.5±3	75.4±5.6
2	3% MCAT	65.3±8.4	68.8±8.9	57.2±3.3	27.2±12.9	122.4±9.6	96.1±17.6
3	2% MCAT	82.1±2.4	84.6±4.1	62.7±27.7	46±17.3	144.8±26.4	130.6±13.5
4	1% MCAT	155.2±5.7	158.9±18.6	228.7±9.9	224.7±13.6	383.9±14.4	383.5±13.2
5	0.5% MCAT	430±41.8	445±26.3	627.2*	567*	1086.7*	1038.3*
6	95% HTP	74±1.8	78.3±4.7	77.3±4.7	45.2±6.7	151.4±4.7	123.4±3.9
7	90% HTP	86±9.7	87.9±12.2	83.1±12.3	67.6±7.5	169.1±3.6	155.5±5
8	87.5% HTP	112±8.1	118.5±4.7	**	**	**	**
9	Liq. 10% MCAT	13.9±3.6	16.8±3.9	40.3±5.3	35.5±4.4	54.2±21	52.3±1
10	Liq. 5% MCAT	14.7±4.1	14.9±4.6	46.2±20.6	35.7±17.7	60.9±16.6	50.6±13.1
11	Liq. 3% MCAT	22.2±1.3	23.6±1	**	**	**	**
12	But. 5% MCAT	42.4±4.1	43.3±3.5	38.9±7	20±1.7	81.4±9.7	63.3±5
13	But. 3% MCAT	61.5±4.9	62.8±4.1	77.6±23	29.5±2.7	141.9±19.4	94.8±0.2
14	5% FCAT	2161.2±970.8	1513.2±90.8	145±65.7	115±32.4	2306.2±91.4	1628.4±58.4
15	3% FCAT	3341.2±158.3	3374.1±163.3	153.4±19.5	92.8±38.6	3494.6±140.9	3466.9±137.3
16	0.3 ml fuel	48.2±17.5	53.7±15.2	84.3±18.8	36.4±4.8	132.6±2.4	90.1±10.7
17	0.2 ml fuel	50.7±8.8	55.6±7.9	58.5±9.3	29.4±3.8	109.2±2.7	85±9.6
18	0.05 ml fuel	65.3±5.5	68.6±6.5	53.5±6.2	19.7±3.4	118.8±3	88.2±4.1
19	4 weeks old	202.3±16.9	219.9±15.2	271.2±17.7	230.3±28.1	473.5±33.5	450.2±40.3
20	18 cm drop height	65.8±4.7	67±7	53.4±6.4	22.6±7	119.2±11	89.6±13.8
21	28 cm drop height	52.7±0.4	55.6±2.4	48.5±3.6	33.1±2.2	101.1±3.7	88.7±3.6

*Ignition was achieved only one out of three times. Therefore no standard deviation could be calculated.

**Ignition was not achieved in any case.

Figure 1.9: Ignition delay times using 97% HTP [30]

It is notable that a higher catalyst mass fraction did not yield significantly lower ignition delay times in the second study, implying that there is a sweet-spot or at least a plateau for the amount of catalyst to use. It should also be noted that in all three cases only one additive was used as opposed to the intended two to be used by TNO. This extra additive could result in lower ignition delay times compared to fuels using only one additive, resulting in an ignition delay time of <50 ms which has been deemed as acceptable in literature, but it may not reach a <10 ms ignition delay time deemed as desirable in literature [45].

However, 90% HTP and gelled ethanol characterization tests have been found to yield ignition delay times of 1-30ms. The lowest was 1.33 ms using Manganese (II) acetylacetonate as a catalyst with an addition of boron in a multi drop test, but it yielded a result of 37.0 ms for a single drop test (which is the standard amount of drops in a drop test used for hypergolic performance comparison). The lowest single drop test was 4.15 ms using copper chloride hydrous aluminum as a catalyst with an addition of aluminum, which can be seen in figure 1.10. As the use of liquid ethanol results in higher Weber numbers (which is the ratio of the drag forces to the cohesion forces, which in practice translates to being positively correlated with the drop height) compared to gelled ethanol and higher Weber numbers are correlated with lower ignition delay times [11] it can be assumed that HTP and liquid ethanol characterization tests would yield such lower ignition delay times. This implies that an ignition delay time of <10 ms is possible for an HTP/liquid ethanol hypergolic propellant combination.

Table 2
Ignition delay of pure and metalized gelled ethanol fuel with hydrogen peroxide.

Gelled fuel	Oxidizer quantity	Ignition delay (ms)
S_P CCAT	Single drop	Rapid decomposition, No ignition
S_P CCAT	Multi drop	50
S_P MCAT	Single drop	13.46
S_P MCAT	Multi drop	19.8
S_{Al} CCAT	Single drop	4.15
S_{Al} CCAT	Multi drop	28.7
S_{Al} MCAT	Single drop	47.7
S_{Al} MCAT	Multi drop	7.0
S_B CCAT	Single drop	115.0
S_B CCAT	Multi drop	90.0
S_B MCAT	Single drop	37.0
S_B MCAT	Multi drop	1.33
S_C CCAT	Single drop	24
S_C CCAT	Multi drop	14.35
S_C MCAT	Single drop	19.2
S_C MCAT	Multi drop	18.6

Figure 1.10: Ignition delay times using 90% HTP [22]

An expansive list of typical ignition delay times for hypergolic combinations with HTP can be found in appendix B, with times as low as 1.88 ms which was achieved by 90% HTP and a gelled ethanolamine propellant mixture [3].

1.2.4. Existing drop test set-ups

Although the principle of drop testing is simple, there are many variations possible to the set-up itself depending on the requirements and the resources available. The most significant variation is whether the pressure can be varied, and if so, in what range. There are three main possibilities which are represented by the following drop test set-ups. The Purdue Hypertester as seen in figure 1.11 is an ambient (1 bar) set-up not using a high-speed camera for data acquisition, necessitating many different instruments to compensate. The Warsaw set-up as seen in figure 1.12 is a 0-30 bar set-up which allows drop testing at all operational pressures. The DLR set-up as seen in figure 1.13 is a 0-1 bar set-up which combines relative simplicity with the ability to test at ignition pressures.

The set-ups in question demonstrate the main aspects of a drop test set-up well. The Purdue Hypertester shows the syringe and push rod combination which produces a droplet and a crucible which holds the other propellant and into which said droplet falls. This produces a hypergolic reaction. In the DLR set-up the crucible is a watch glass which can be rotated and cleaned with a jet of water between tests. Furthermore, two syringes are placed above it: one which dispenses the "falling droplet" (which initiates the ignition) and another which dispenses the "resting propellant" (which is the propellant at rest). The former is centered above the watch glass, while the other can be slightly off-center as the resting propellant can be expected to pool in the middle of the watch glass.
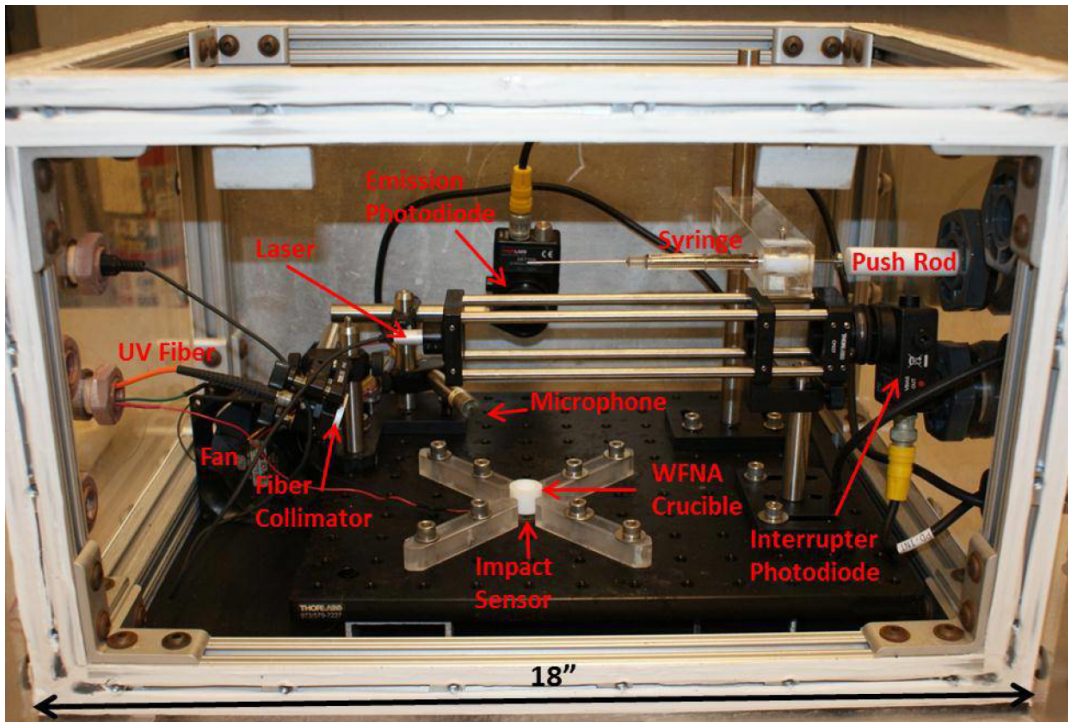
Figure 1.11: Purdue Hypertester
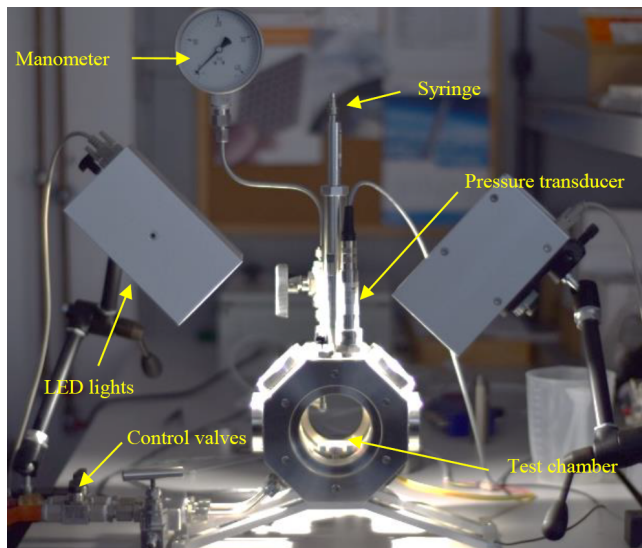
Figure 1.12: Warsaw 30 bar set-up
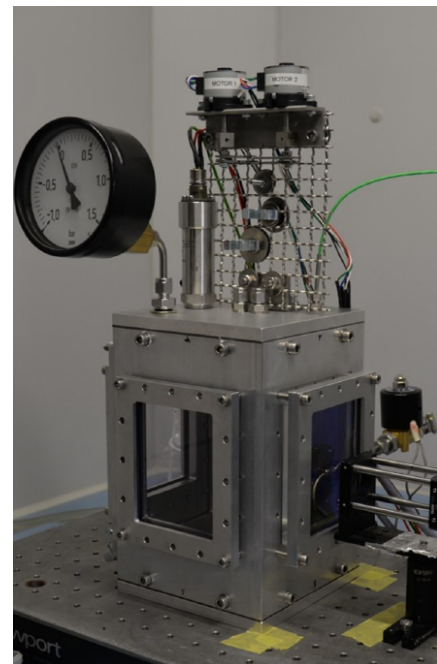
Figure 1.13: DLR 0-1 bar set-up

Nowadays, the hypergolic reaction and the ignition delay time are measured using a high-speed camera, as is the case in the Warsaw and DLR set-ups. This technique necessitates a sufficient amount of light, as seen in the Warsaw set-up where LED lights are used. However, if a high-speed camera is unavailable, other instruments can be used. For example the Hypertester used a combination of an interrupter photodiode, an impact sensor and a microphone to measure the IDT. The DLR set-up also includes a spectrometer which allows for the determination of the reaction products. However, to allow this windows which are transparent at the relevant wavelenghts of lights are necessary.

If a hermetic chamber is chosen, the structure must be adequately strong, it must be leak-tight and the atmosphere needs to be controllable using control valves as seen in the Warsaw and DLR set-ups. A high-pressure set-up introduces significantly harder engineering challenges and safety concerns compared to a sub-ambient set-up. As such, a sub-ambient set-up is preferable if resources are limited. However, a sub-ambient set-up can only be used to simulate in-space (vacuum) conditions which are relevant only during ignition, while a high-pressure set-up also allows for the simulation of operational (~10 bar) conditions. The former allows for the predictions of engine behavior during ignition, while the latter allows for predictions of engine behavior during both start and operation. The ambient set-up cannot be used for either. Instead, its strength lies in its reduced complexity and the fact that most ignition delay times in literature have been found under ambient conditions. As can be seen, drop test set-ups differ greatly and are the result of the requirements chosen and the resources available.

1.2.5. Testing parameters

There are many variations possible in a drop test set-up, which can broadly be divided into three categories. These are: the measurement techniques which are used for data acquisition, the variable input parameters which ensure the testing conditions are as desired and the other variations which are not directly related to either of the other two. They are presented and discussed in the following paragraphs. From these possible variations a selection was made to be implemented in the actual design of the set-up.

Measurement techniques

There are multiple measurement techniques which can be implemented in a drop test set-up. The one currently used the most is a high-speed camera, mainly due the amount of information that can obtained using it. First and foremost, the ignition delay time can be determined by looking at the time between droplet contact and ignition. The result of the droplet impact can also be studied, along with the flame propagation velocity after ignition and, in favorable conditions, vapor formation.

Other optical methods exist as well, chief among them being the infrared camera, which can measure the change in temperature. The added benefit that it can not only measure this after ignition, but also before, which is very useful data in order to better understand the ignition process. A similar method is the use of thermal probes, which are placed in predetermined locations. It can provide data of similar usefulness as an infrared camera if employed correctly.

Another light-based method is the employment of a laser and optical sensor pair, which can measure discontinuities for a given light spectrum and critical path. This can detect a droplet passing by or the formation of a vapor cloud [36]. An even simpler technique is the use of a light sensor which can detect the flash of an ignition [36].

Two final optical methods are schlieren photography [13] and shadowgraph photography [4]. Both of these allow for the detection of non-uniformities in density of a gas, which in turn allows for the measurement of a vapor cloud that can form during a drop test. Broadly speaking, the difference between these two techniques is that schlieren photography provides more useful and accurate data at the cost of being much harder to implement in a set-up than shadowgraph photography [25].

Two other measurement techniques are the use of an oscilloscope or a spectrometer. The former can detect when a droplet impact occurs by detecting the vibrations resulting from such an impact. The latter can be used to analyze the combustion products of the propellant combination which can help understand the combustion process. One needs the test chamber to be hermetically sealed for this technique [36].

Variable input parameters

There are a few key input parameters which have been found to be important during literature research. Most importantly, the propellant composition and O/F ratio are important as these constitute the propellant combination one is measuring. The O/F ratio can be controlled by using oxidizer and fuel droplets of a predefined and exact volume. The drop height and how centered the droplets are is also important. The former is related directly to the Weber number and thus determines whether the drops merge or

splash, while the latter (related to the impact angle) determines the chance for a drop to bounce off.

The chamber pressure and atmospheric composition can be controlled using a vacuum pump and a gas inlet valve, with the set-up itself being hermetically sealed. A higher pressure increases the chance of ignition, shortens the ignition delay time and increases the flame propagation velocity, while the effects of the atmospheric composition depend on the propellant combination and atmospheric composition in question. Lastly, the propellant temperature increases the reactivity of the hypergolic propellants which decreases the ignition delay time, but at the cost of an increased risk of RSS during actual engine operation. This can be controlled using heating elements, for example installed around the syringe of the falling droplet or under the vessel in which the resting droplet is located.

Other variations
There are many drop test set-up variations not related to the measurement techniques and the input parameters. Some of these are as follows. The structure of the set-up (i.e. the geometry and materials used) is relevant for the ease of manufacturing, cost, sturdiness and ergonomics. This is particularly relevant for ensuring the drop height and alignment can be calibrated and centered. The layout of the measurement instruments and accompanying hardware (e.g. light sources) must be properly set up. The degree of automation must be decided upon and the procedure of changing one propellant combination to another must take an acceptable amount of time and effort.

Chosen parameters
Ideally, all of the measuring techniques would be implemented and all variable input parameters would be controlled. However, due to resource constraints, only some of these options can be selected. A first selection can made be by discarding the most complex of any two redundant options, which results in the following selection.

- The set-up is a hermetically sealed structure with a vacuum pump and a gas inlet. This allows for the pressure and atmospheric composition to be controlled. It has windows which are transparent for both the visible light spectrum and the light spectrum used for spectroscopy. A door allows access to the inside space.
- A syringe-like device is used to drop propellant droplets into a non-reactive vessel with resting propellant, which is directly below it ensuring a droplet impact angle of less than 7 degrees. Both the syringe-like device and the vessel with resting propellant have heating elements and temperature sensors allowing for the propellant temperature to be controlled. The syringe-like device is height adjustable for the drop height and thus impact velocity to be controlled and the device itself is adjustable allowing for the droplet diameter to be controlled. If the droplet-dispensing part of the device is chosen to be a needle, the needle diameter is to be adjustable. By controlling both the impact velocity and droplet diameter, the Weber number can also be controlled. The resting propellant volume needs to be controlled, which together with controlling the droplet diameter allows for the O/F ratio to be controlled.
- The non-reactive resting propellant vessel is to either be able to be cleaned or changed between two tests, in order to remove any residue and remaining propellants. This allows the propellant composition to be controlled and thus adjustable.
- A high-speed camera is used to measure the ignition delay time, chemical delay time and physical delay time, observe the pre-ignition behavior of the propellant combination and be able to measure the flame propagation velocity. This makes the use of a laser and optical sensor pair, a light sensor and an oscilloscope redundant, as all of these are used to measure the ignition delay time but in a more complex way.
- Either an infrared camera (preferably high-speed) or thermal probes are used to measure the temperature at the most relevant locations of an experiment. This includes the resting propellant itself, the volume into which the mixed propellant vapor travels and ignites as well as the volume occupied by the resulting flame.
- Schlieren photography is used to visualize the mixed propellant vapor formation before ignition more accurately than when using just a high-speed camera.
- A spectrometer is used to characterize the resulting combustion products after a successful ignition.

Based on the literature study, initial preferred variable input parameter ranges can be determined which can be found in the list below. It should be noted that some variable input parameters (e.g. the droplet diameter) did not have a clear preferred range and are thus absent. The viability of the ranges is partially discussed here and partially in chapter 2, where the actual design is presented and the design choices are explained.

- Propellant temperature: From ambient temperature at ~293K until the auto-ignition temperature of an 85%+ HTP/ethanol mixture at ~473K [33] to cover the entire sub-auto-ignition temperature range. Tests at lower temperature would be useful, for example to ascertain whether the propellants could be stored and used in space at temperatures lower than ambient. However, no cooling systems were found in any drop test set-up and thus introducing such an element into the set-up was determined to pose an unacceptable design risk.
- Weber number: Below 250 to prevent splashes, as these splashes make the observation of thermal processes harder and produce discontinuous results compared to results with a Weber numbers below 250 [34].
- Droplet impact angle: Below 7 degrees to prevent bounces, as these bounces produce discontinuous results compared to results with droplet impact angles below 7 degrees [34].
- Chamber pressure: From 0 bar (conditions found in space during ignition) to at least 10 bar [42] and preferably 20 bar [68] (the former being typical for hypergolic thruster and the latter being typical for non-launcher engines).
- Chamber atmospheric composition: Fully adjustable, as it could have an effect on the ignition probability and the ignition delay time and is easily achieved when using a hermetic set-up with a vacuum pump and gas inlet [14][2].

This combination of performance parameters and variable input parameters allows for the answering of all of the research questions. Furthermore, it allows for the research of the effect of specific additives, in particular the role of the propagator as it is currently not fully understood. Especially the analysis of the thermal and vaporization processes would be of interest. As such, a hypothesis relating to the last research sub-question is proposed to be tested alongside the characterization of the propellants in question. This hypothesis is as follows:

"The ignition delay time can be divided into a mixing phase, an HTP decomposition phase and a propagator reaction phase."

This hypothesis basically states that when the fuel and oxidizer come into contact with each other, first they mix, then the HTP decomposes, then the propagator reacts with the oxygen, which finally results in ignition. If time and resources allow, this hypothesis will be tested more rigorously by also performing drop tests without the propagator added to the ethanol. Comparing the results of these tests with results of tests which do include a propagator will give a clearer idea of the role of the propagator in the process. The details of what tests will be performed and their exact testing parameters will be decided upon during the project itself, as they depend on the systems engineering and the design phases which are part of the project.

2

Methodology

To meet the research objective and answer the research questions a drop test set-up needs to be designed, built, validated and used. A decision was made to divide the development process into two steps. Firstly, an ambient set-up would be developed and used to validate engineering solutions by performing drop tests at ambient pressure. The lessons learned from this ambient set-up would then be used to propose a design for a hermetic set-up. The tests performed using the ambient set-up would also be used for determining the hypergolic performance of TNO's hypergolic propellant combination.

The reasoning for this approach is as follows. An ambient drop test set-up can be designed to be far easier to modify than a hermetic set-up. A hermetic set-up needs to be air-tight which means that any modifications are constrained by this, which can be a major engineering challenge if significant changes are to be made. Furthermore, if pressurization is desired, additional safety concerns need to be addressed and possibly re-addressed after every modification. Thus, as many design challenges as possible would be solved during the development the ambient drop test set-up in order to prevent facing much harder design challenges during the development of the hermetic set-up.

This approach also allowed for testing the significance of the effect of certain factors like drop height, fuel temperature, etc. on the ignition delay time. This would allow for deciding whether these factors needed to be controlled or at least measured in the hermetic set-up. If their effects were found to be insignificant, they could be left out of the hermetic set-up thus simplifying its design.

In this section the design of the ambient set-up is shown along with the reasoning behind it, including its upgrade after the first test campaign. Afterwards, the tests to be performed using the ambient set-up are shown. This includes both drop tests and validation tests of the set-up.

2.1. Ambient set-up
The first step of designing the ambient drop test set-up consisted of setting up a list of requirements. Afterwards, the design considerations were determined from which finally the design of the set-up emerged.

2.1.1. Requirements
Many requirements follow naturally from the goals of the ambient study, while others follow from other considerations. The list of requirements along with their respective justification is as follows:

Req.1 **The ignition delay time shall be measured with a resolution of 1 ms or better:** Fundamental for determining the hypergolic performance of the propellant mixture in question, with 1 ms being the standard minimum resolution as found across literature

Req.2 **The chemical delay time shall be measured with a resolution of 1 ms or better:** Fundamental for determining the hypergolic performance of the propellant mixture in question, with 1 ms being the standard minimum resolution as found across literature

Req.3 **The Weber number shall be no more than 250:** In order to prevent splashing which impacts the ignition delay time and chemical delay time, which would make direct comparison between tests which exhibit such splashing and those which don't impossible

Req.4 **The drop height shall be controllable:** The drop height impacts the Weber number

Req.5 **The falling droplet diameter shall be controllable:** The droplet diameter impacts the Weber number and the O/F ratio

Req.6 **The falling droplet temperature shall be controllable:** The falling droplet temperature is negatively correlated with the ignition delay time and chemical delay time

Req.7 **The resting propellant temperature shall be controllable:** The resting propellant temperature is negatively correlated with the ignition delay time and chemical delay time

Req.8 **The set-up shall retain its structural integrity at all times:** Normal handling, testing and storage should not result in the set-up getting damaged

Req.9 **The set-up shall not corrode:** All materials shall be chemically compatible with materials and possibly propellants they are in contact with

Req.10 **The set-up shall allow for a minimum of six tests with different fuels per hour:** Ensures a sufficient amount of tests can be performed in the time available

Req.11 **There shall be no risk of personal injury:** Basic safety requirement

2.1.2. Design

Based on these requirements design choices could be made, which were made with performance, cost, ease of acquisition and manufacturability in mind. Flexibility of the design was a priority. Complex designs are rarely final, and it was (correctly) assumed the the first prototype would need changes to work as intended. The list of design choices along with their justifications is as follows.

General
- The design was aimed to be simple and relatively modular, in order to be able to easily redesign one part of the set-up without needing to redesign other parts as well.
- The set-up was placed in a fume hood for the sake of safety.
- The structural elements of the set-up was mainly made of aluminium, as it is easy to machine and chemically compatible with HTP.
- The main two structural elements were the bottom structural plate and the top structural plate. These were parallel relative to each other, with their distance being controlled by threaded rods with nuts and washers. By adjusting the location of the nuts and washers along the threaded rods, the distance between the two plates (and thus the drop height) could be adjusted and any errors in orientation could be corrected. The holes through which the threaded rods went were accurately machined (precision of <0.1 mm) to ensure the middle of the top structural plate was exactly above the middle of the bottom structural plate.
- In general, M5 nuts, bolts, washers and threaded rods were used for intra-system standardization. This ensured that any changes to the fastening configuration could use readily available elements.
- Adjustable feet were placed at all four corners of the bottom structural plate in order to be able to adjust its orientation. This ensured that the gravity vector would be perpendicular to both structural plates, thus ensuring that the HTP droplet would fall into the center of the vial.

Propellant system
- A drop of HTP was dropped into a small pool of fuel (as opposed to a drop of fuel into a pool of HTP), as that is the preferred order for HTP-based hypergolic propellants. Furthermore, it somewhat mimics the fact that in a hypothetical engine fuel would be injected before HTP.
- The small pool of fuel was held in a borosilicate vial. Borosilicate glass can withstand the expected high temperature gradients resulting from a rapid heating of the inside by the flame of the hypergolic reaction, as opposed to normal glass.
- The vial was placed on an aluminium heating plate, which is heated using a 12V heating strip. This was chosen due to its simplicity and expected effectiveness.

- The vial was accurately positioned using a stabilizing plate, which was a 1 mm aluminium plate with hole with a diameter of the vial, itself held in place by nuts and bolts connecting it to the aluminium heating plate and in turn to the main body. The vial could then be placed in said stabilizing plate ensuring it would be accurately lined up with the center of the bottom structural plate and thus the top structural plate. As it is symmetrically placed, the impact angle is 0 degrees thus being less than 7 degrees.
- The droplet of HTP was first to be dropped from a custom-made replaceable tip in order to be able to accurately adjust the droplet diameter. This was later changed to a needle as all custom-made tips would eventually form a big droplet of HTP around the tip, which would only grow when a droplet was dispensed until a droplet of varying size would fall, repeating the process. The needle was attached to a custom-made replaceable Luer Slip adapter.
- The custom-made replaceable adapter was connected to a "buffer", which was a round metal element in the middle of the top structural plate, thus aligning the needle with the vial.
- The buffer was heated using a heating strip, which was chosen due to its simplicity and expected effectiveness.
- A syringe actuated by a syringe pump was used to dispense the droplets of HTP in accurate amounts automatically, meaning that after activation of the syringe pump timer there was enough time to close the fume hood and be ready to automatically trigger the high-speed camera.
- The Luer (Lock) syringe connection system was used due to it being one of the industry standards for syringes, being easy to use and having a pressure rating of 14 bar.
- A flexible tube connected the syringe with the buffer in order to be able to place the syringe pump in a natural position. An adapter was used to be able to connect the Luer Lock tube end with a threaded opening of the buffer.
- A second syringe pump was used for accurately filling the vials with a certain amount of fuel. This was done with the needle attached directly to the horizontal syringe, with the vial being placed under the needle tip when dispensing the fuel.

Data acquisition
- A K-type thermocouple was used to measure the temperature of the buffer. An assumption was made that the temperature of the buffer (with HTP in direct contact with its inner walls) would equal the temperature of the fuel droplet. However, this was not validated and is a possible source of errors.
- A Pt1000 RTD was used to measure the temperature of the heating plate. At a later time, a test was to be performed in order to determine the relation between the the heating plate temperature and the fuel temperature.
- The respective choice for the K-type thermocouple and the Pt1000 RTD was due to them being available in the lab. Their placement choice was due to the fact that the RTD was very easily attachable to the heating plate and moderately easily attachable to the buffer, while the thermocouple was moderately easily attachable to both the heating plate and the buffer. Thus the easiest configuration was attaching the RTD to the heating plate and the thermocouple to the buffer.
- The data from the temperature sensors was collected using a National Instruments CompactDAQ system connected to a computer with the appropriate software. The connected relais were also used to turn the two heating strips on or off. The electrical power was provided by a 12V power supply.
- A high-speed camera was used to capture the phenomena occurring. It was set to 3000 Hz to fulfill the >1000 Hz requirement and provide even more data.

Excluded design choices
- A heating element capable of heating the heating plate beyond what the 12V heating strip was able to was deemed unnecessary for this stage of the drop test set-up. This is due to the fact that determining a rough relation between the fuel temperature and IDT was determined to be sufficient.
- An infrared camera or thermal probes to measure the temperatures of the fuel directly or the space around the fuel directly before and after ignition were not possible to include. This was due

resource constraints and the choice of focusing on the determination of the IDT of the fuel and determining what the relation is between the IDT and the input parameters.

- Schlieren photography was not included due to resource constraints and the choice of focusing on the determination of the IDT of the fuel and determining what the relation is between the IDT and the input parameters. Furthermore, vapor formation could be somewhat observed using the high-speed camera.
- A spectrometer was not included due to resource constraints and the choice of focusing on the determination of the IDT of the fuel and determining what the relation is between the IDT and the input parameters.

Resulting set-up

The resulting set-up of these design choices can be seen in the CAD drawings as seen in figures 2.1, 2.2 and 2.3. The photo's of the actual set-up as can be seen in figures 2.4 and 2.5. This was the set-up used for the first test campaign.
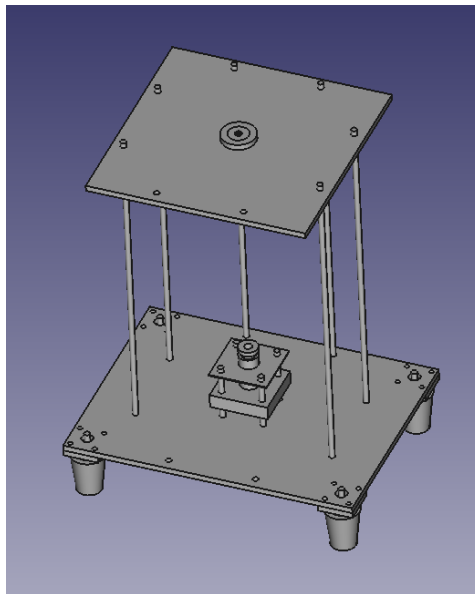

Figure 2.1: Full view of ambient set-up

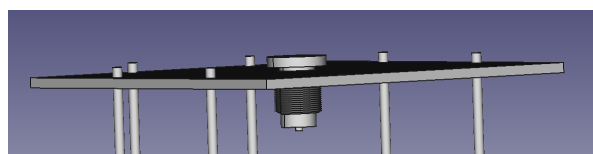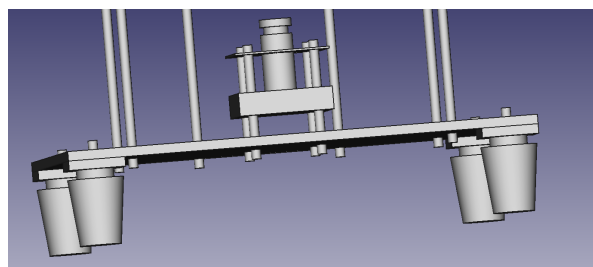

Figure 2.2: High view of ambient set-up

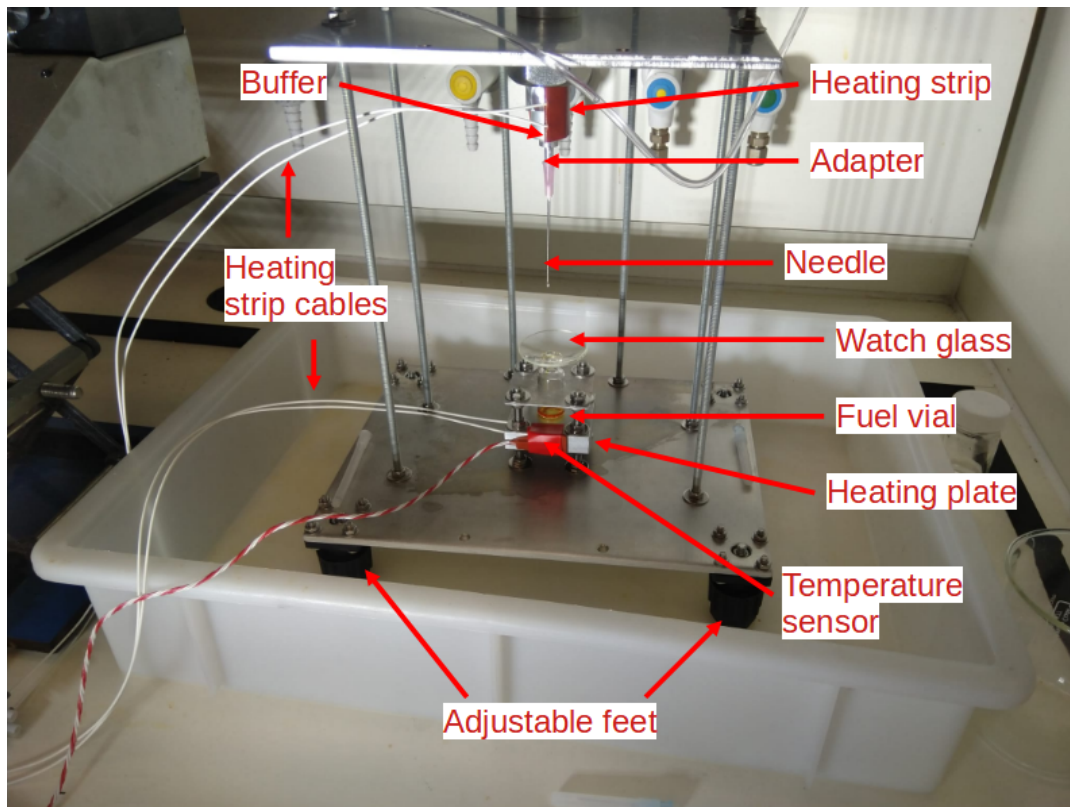**Figure 2.3:** Low view of ambient set-up

Figure 2.4: View of the ambient set-up during the first test campaign
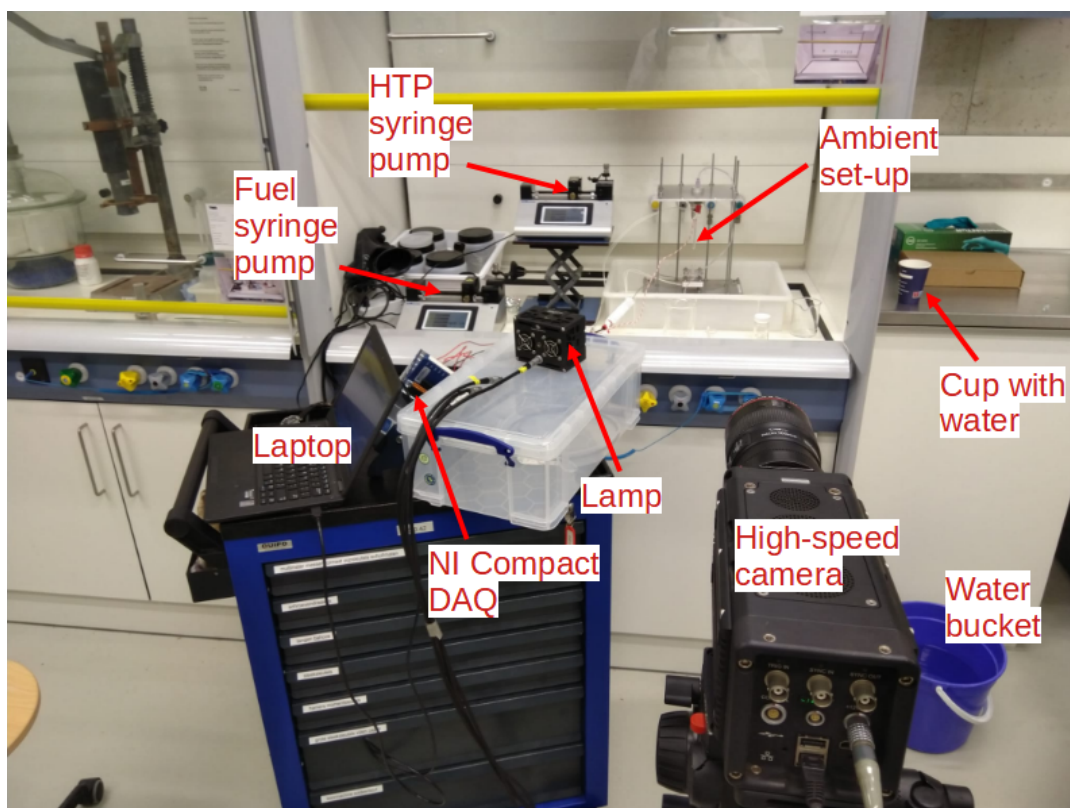
Figure 2.5: View of the ambient set-up including DAQ and control elements

It should be noted that another issue was encountered during the first test campaign aside from the issue of the replaceable tip. This was the result of the inside diameter of the buffer where the HTP was heated being too large. This resulted in some air being trapped in said volume, as it would not be completely forced out by the liquid as was the case for the syringe, the flexible tube and the needle.

The result was that while in most cases a normal droplet formed, sometimes it did not. This always resulted in the need to pause the drop test at hand, remove the vial and actuate the syringe pump a few times until a few droplets of HTP would fall at once into an empty vial. After this, normal testing could resume with the vial with fuel.

A second result was that sometimes an HTP droplet could start forming before the actuation of the syringe pump. This necessitated covering the fuel vial with a watch glass to prevent accidental ignition while work was being done in the fume hood. However, this forming droplet could be removed directly before testing ensuring it had no impact on the results themselves.

The solution to this proved to be a little complex and can be seen in figure 2.6. As one can see, the shape of the buffer was changed in order to more easily attach the heating strip and temperature sensor. This buffer was connected to the top structural plate with two screws without touching it directly, which decreased heat loss to the structural plate during heating. The flexible tube was connected in the same way as the old buffer, via an adapter. The syringe was connected to the buffer via a COTS NPT-to-Luer Lock adapter, with the thread in the buffer being a female NPS thread (compatible with male NPT threads).
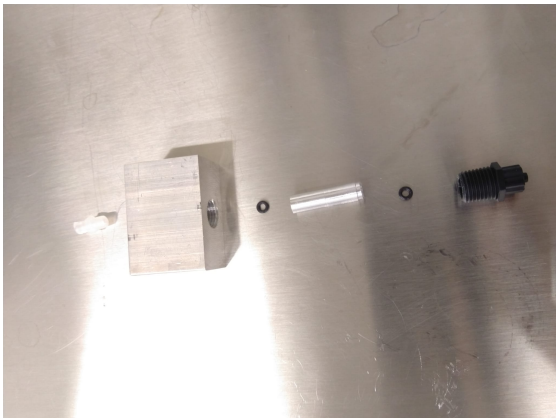
Figure 2.6: Buffer assembly
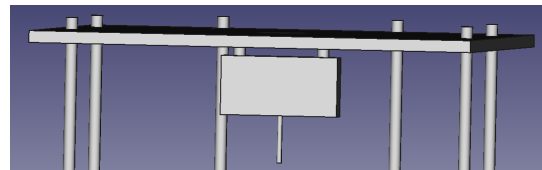
Figure 2.7: View of mounted buffer assembly

Now, a "narrower" piece was used to decrease the effective diameter of the buffer to match it with the diameter of the flexible tube and both adapters, which was 3 mm. This would prevent air from being trapped in the space through which HTP would flow. This was accomplished by machining a cylinder with an outside diameter equal to the large inner diameter of the adapter to the syringe which would hold it in place, while also having a hole through the centerline with a diameter of 3 mm. The ends of the narrower would be machined in such a way as to house one Viton o-ring each ensuring no leak between this piece and the two adapters, maintaining a constant 3 mm outer diameter. The shape can be seen in figures 2.8 and 2.9. It should be noted that in order to ensure the o-ring sealed on the side of the flexible tube adapter, the threaded part of the buffer was made shorter than the threaded part of the flexible tube adapter. This solution proved to work as intended.

Figure 2.9: Top view of narrower
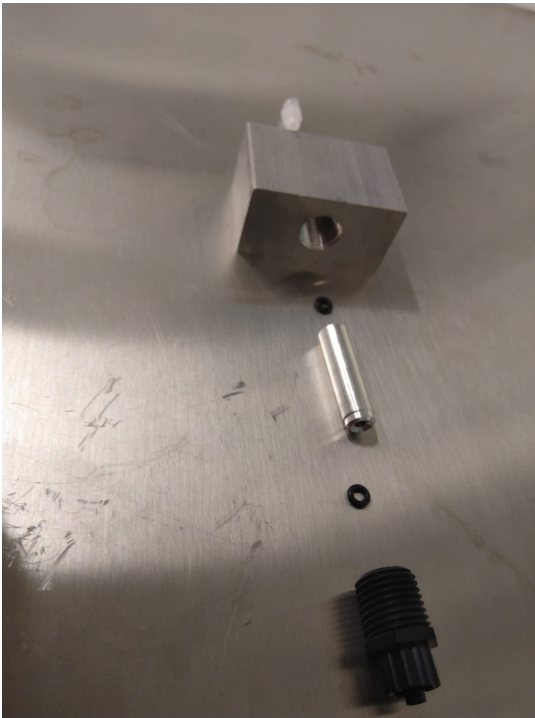
Figure 2.8: Bottom view of narrower

However, this solution creates a new problem, namely the fact that there is no direct thermal interface between the buffer and the narrower. This means that heat cannot easily travel from the heating strip to the HTP, which makes the assumption that the temperature of the buffer is equal to the temperature of the HTP invalid. For this, a solution was found by assembling this assembly under water, resulting in a thermal interface in between the buffer and the narrower in the form of water. While less efficient than a direct interface, if given time to reach steady state it can once again be assumed that the temperature of the outside of the buffer matches the temperature of the HTP inside the narrower, although this has not been validated.

2.2. Testing

Using this set-up drop testing could be performed. This was split into two test campaigns, with the first test campaign focused on the effects of input parameters on the ignition delay time and the second test campaign focused on the hypergolic performance of TNO's hypergolic fuel. The most recent test procedures can be found in appendix C which are to be used for the hermetic set-up, but if one ignores the steps relating to pressure it results in the the ambient test procedures. Furthermore, validation tests were performed to ensure the drop test set-up worked correctly and the results were accurate.

2.2.1. First test campaign

Ideally, the influence of every input parameters on the ignition delay time would be determined by performing multiple tests across a wide range of values, even varying multiple input parameters simultaneously. However, due to limitation in time and resources, choices needed to be made with regards to which parameters to test and how many tests to perform. The main consideration was whether a parameter was an inherent characteristic of the set-up.

HTP concentration

The concentration of the HTP could be varied by adding distilled water to the nominal 97.1% HTP available for testing. Lowering the HTP concentration would result in a lower ignition probability. The concentration was determined by using a refractometer and repeating the measurement 10 times. It can thus be considered accurate to the significant digit presented (0.1%). Since this parameter is independent of the set-up, it was not varied.

HTP amount

The amount of HTP could be varied by changing the syringe type, as it was found that each syringe produced droplets of constant volume. Changing the amount of HTP should theoretically have no impact on the ignition delay time, but it was deemed important to confirm this, thus it was included in the first test campaign. The nominal volume was set at 11 µL (the larger needle available), with a varied value of 5 µL (the smaller needle available). These volumes were validated by having the syringe pump dispense 10 times the nominal volume (respectively 110 µL and 50 µL) and ensuring 10 droplets would fall. This was indeed the case thus demonstrating an maximum deviation of 10%. It was furthermore confirmed that the syringe pump dispensed the correct volume by looking at the volume indicators on the syringe itself. The HTP amount was varied in test series: "LessOx" and "LessOF".

Drop height

The drop height could be varied by changing the distance between the top and bottom stabilizing plates thus changing the distance between the needle tip and the vial bottom. It was defined as the distance between the needle tip and the bottom of the inside of the vial which was measured using a ruler with 0.5 mm indicators. The accuracy of this measurement was +-1 mm, as the 0.5 mm indicators were too close to confidently state which was situated at the needle tip, while the 1 mm indicators were far enough. Increasing the drop height was expected to decrease the ignition delay time and was thus included in the first test campaign. The nominal value was 80 mm, with a varied value of 144 mm. This was varied in test series: "High".

HTP temperature

The HTP temperature was assumed to be equal to the buffer temperature, thus heating the buffer would heat the HTP. This should not be done beyond ~30°C due to thermal decomposition. The maximum steady-state temperature which could be reached by the buffer when heated by the heating strip in the first ambient set-up was ~24.6°C, which was acceptable and used as the varied value. This was measured using a K-type thermocouple which showed at least two digits after the comma, thus the first digit after the comma was assumed to be accurate. The nominal temperature was ~21°C, which was the room temperature. The accuracy of the latter was +-~0.5°C, as that was the increment of the digital thermometer in the room. The HTP temperature was varied in test series: "HTPHeat".

Fuel mixture

The fuel mixture could be varied by changing the ratio of ethanol, the catalyst and the propagator. Changing this would impact the ignition probability as demonstrated during earlier tests within TNO. However, since this parameter is independent of the set-up, it was not tested in this test campaign. The exact fuel mixture was determined by weighing the individual mixture components before combining them (including measuring the residue). This was done using a 1 mg accurate weighing scale. As the smallest amounts were on the scale of 100 mg, the maximum deviation can be assumed to be 1%.

Fuel amount

The amount of fuel could be varied by changing the amount of fuel dispensed by the syringe pump into the vial. Changing the amount of fuel should theoretically have no impact on the ignition delay time, but it was deemed important to confirm this, thus it was included in the first test campaign. The nominal volume was set at 110 µL, as it seemingly gave the highest ignition probability as seen in the preparatory tests (Test ID: "Prep#") as seen in Appendix A. Furthermore, it is a fuel-to-oxidizer ratio of 10 which was found quite frequently in literature. The varied value was set to be 5 µL and combined with an HTP varied value of 50 µL, as this maintained the fuel-to-oxidizer ratio of 10. These volumes were dispensed using a syringe pump which formed individual drops. The last drop would be shaken off of the syringe into the vial. The droplets were unfortunately not counted for validation, but the leftover fuel on the syringe after shaking off the last droplet was certainly never more than 10% of the total dispensed volume, thus that can be assumed to be the maximum deviation. The fuel amount was varied in test series: "LessOF".

Vial type

The vial type (more precisely: its shape) could influence the geometry of the fuel, the mixing process and the ignition location. However, as it is not dependent on the overall set-up and is relatively easy to swap (necessitating only a change in the stabilizing plate), it was not included in the first test campaign.

Fuel temperature

The fuel temperature was assumed to be dependent on the heating plate, with the relation between the two being determined during a later validation test. The nominal value was ~21°C, which was the room temperature. The varied value had a final heating plate temperature of ~28.3°C, which was roughly the maximum temperature which could be reached by the heating plate. The determination and validation of the fuel itself is discussed later in this chapter. This was varied in test series: "FuelHeat".

Weber number

The Weber number is included in the analysis, as increasing it decreases the ignition delay time. Furthermore, it should not be higher than 250, as this changes the impact mode to a splash, which was found to have an impact on the ignition delay time beyond the increase of the Weber number itself. The Weber number is influenced by the drop height and the HTP droplet diameter, which itself is computed from the HTP droplet volume. It can thus be assumed to be as accurate as the the drop height and droplet diameter. This was varied in test series: "LessOx", "LessOF" and "High".

This gives the following test conditions to be performed. It was decided to perform 5 tests per test series, with a baseline test at the beginning ("BaseA") and end ("BaseB"), in order to both determine the ignition delay time at nominal conditions and to ensure that the test results did not vary in time (as the test campaign lasted four days).

Table 2.1: Test conditions

Test series	Fuel batch	Fuel V [µL]	HTP V [µL]	Syringe type	Vial type	Top T [°C]	Bottom T [°C]	Drop H [mm]	Weber number
BaseA	1	110	11	1.2 taper	large	21	21	80	78
LessOx	1	110	5	0.6 taper	large	21	21	79	59
LessOF	1	50	5	0.6 taper	large	21	21	79	59
High	1	110	11	1.2 taper	large	21	21	144	138
HTPHeat	1	110	11	1.2 taper	large	24.6	21	81	79
FuelHeat	1	110	11	1.2 taper	large	21	28.3	81	79
BaseB	1	110	11	1.2 taper	large	21	21	81	79

2.2.2. Second test campaign

The second test campaign would focus on the hypergolic performance of TNO's hypergolic propellant mixture itself, performing all drop tests in nominal conditions ("BaseA" and "BaseB" conditions) using the ambient set-up with the improved buffer. The hypothesis to be tested is whether the ignition delay time of TNO's novel propellant combination is 50 ms or less, as that is seen as a maximum value for an acceptable hypergolic performance. The main test goal will thus be to determine whether the average ignition delay time at nominal conditions is 50 ms or less.

In order to increase the scientific value of this test campaign, variations were added in areas which theoretically should have no influence on the results. This allows the research of whether these variations indeed have no influence on the results, and if they do, what influence it is. This is a secondary test goal. The variations are as follows.

- The test series: "BaseC110" had identical conditions as those in the test series: "BaseA" and "BaseB".
- Needle tip type: using a blunt needle tip type as opposed to a tapered type. The diameter chosen (1.5 mm blunt needle) was the one which was thought to dispense 11 µL HTP droplets (the same as the 1.2 mm tapered needle), as HTP droplet volume was found to have a significant effect on the ignition probability during the first test campaign. This was varied in the test series: "Blunt 110".
- Fuel amount: changing the fuel amount while keeping the HTP amount constant. This was done in order to confirm the assumption made during the preparatory phase of the first test campaign that 110 µL of fuel was roughly the optimal amount for the highest ignition probability. This was varied in the test series: "BaseC150" (150 µL), "BaseC200" (200 µL), "BaseC250" (250 µL) and "BaseC350" (350 µL).

- Vial type: changing the vial type along with the amount of fuel. Other studies do not explicitly mention the effects of the vial geometry on the ignition delay time, thus this is a novel experiment in terms of drop test set-up design analysis. This was varied in the test series: "Vial100", "Vial150" and "Vial250", with the fuel amounts being varied in the same way as in the "Re" test series and the vial type being constant across the "Vial" test series.

Table 2.2: Test conditions

Test series	Fuel batch	Fuel V [µL]	HTP V [µL]	Syringe type	Vial type	Top T [°C]	Bottom T [°C]	Drop H [mm]	Weber number
Blunt110	2	110	11	1.5 blunt	large	21	21	80	78
BaseC110	2	110	11	1.2 taper	large	21	21	80	78
BaseC150	2	150	11	1.2 taper	large	21	21	80	78
BaseC200	2	200	11	1.2 taper	large	21	21	80	78
BaseC250	2	250	11	1.2 taper	large	21	21	80	78
BaseC350	2	350	11	1.2 taper	large	21	21	80	78
Vial110	2	110	11	1.2 taper	small	21	21	80	78
Vial150	2	150	11	1.2 taper	small	21	21	80	78
Vial200	2	200	11	1.2 taper	small	21	21	80	78

2.2.3. Validation tests

In order to ensure the ambient set-up performed as intended and gave accurate results it was necessary to perform validation to ensure the requirements were met. The validation tests differed per requirement and have been summarized in a compliance table. Some further tests were also performed to ensure the ambient set-up performed as intended. Only the major tests have been described in detail, while the minor tests are described in the validation summary.

Ensuring the correct alignment of the dispensing unit and the vial

In order to ensure that the HTP droplet would drop into the vial, the correct alignment of the dispensing unit and the vial was necessary. This would be achieved by using a level on the bottom structural plate and adjusting the adjustable feet until the bottom structural plate was perpendicular to the gravity vector. This process would be repeated with the top structural plate while adjusting the nuts along the threaded rods connecting both structural plates. Finally, the proper alignment would be validated by dispensing a droplet from the dispensing unit and ensuring it falls in the vial. This was successfully performed.

Ensuring the temperature sensors were properly calibrated

As the temperature sensors were used and calibrated during other tests at TNO, a quick test where their calibration would be roughly checked was deemed to be sufficient. The test would consist of both sensors measuring the ambient temperature. Their results would be compared to each other, and if they would differ by less than 0.1°C and show roughly the same temperature as the digital thermometer present in the room, the test would be considered a success. The reasoning was that if one sensor would be faulty, the two sensors would show a discrepancy in temperature. If both sensors would be faulty, it would be highly unlikely for the sensors to both show the same value (meaning they would have the same error) as well as a temperature similar to the digital temperature. Although a more rigorous test would be preferable, this test was deemed sufficient as these sensors were in regular use. It was performed successfully with the difference indeed being less than 0.1°C and the value itself being roughly the same as the digital thermometer present in the room, although the exact measurements were not written down.

Ensuring no leaks in the buffer assembly used for the second test campaign

In order to ensure the buffer assembly would not leak thus introducing air into the volume occupied by HTP, a leak test was to be performed. Firstly, it would be ensured that the buffer assembly was dry, after which it would be assembled. Then, a syringe filled with water would be attached and actuated manually with as much force as possible, producing a pressure higher than could be expected during operation. Then, the assembly would be carefully disassembled and the space between the narrower

and the buffer would be checked for water. If none would be present, the buffer assembly would be assumed to be leak-tight for HTP as well. This was performed successfully with no water present between the narrower and the buffer after disassembly.

Determining the relationship between the heating plate temperature and the fuel temperature
While the temperature of HTP was assumed to be equal to that of the buffer, the same was not done for the fuel. This was for the following reasons. Firstly, the vial and fuel are not inside of the heating plate but rather outside and merely in contact with it, which introduces significant thermal losses. Secondly, the vial bottom was not perfectly flat decreasing the contact interface between the vial and the heating plate. These two factors necessitated finding a relationship between the heating plate and the fuel using experimental methods. In order to determine this relationship the heating conditions encountered in the experiments would be recreated using a vial partially filled with water. The temperature of this water would then be measured when the desired conditions were met. This validation test was performed after the first test campaign.

Table 2.3: Water temperature after heating by heating plate

Heating plate start temperature	Heating plate end temperature	Heating time	Final water temperature
27.73°C	27.68°C	11:30 minutes	26.54°C
28.06°C	27.68°C	16:30 minutes	26.61°C

The results of the heating plate relationship test can be seen in table 2.3. The starting temperature was ambient at 21°C. Firstly, it can be seen that a temperature above 28.06°C could not be reached by the heating plate, which is less than the final temperature of all the FuelHeat tests. The reason for this is unclear.

This makes the estimation of the fuel temperature in all three FuelHeat tests difficult, as they all ended at a higher temperature as seen in table 3.1. What can be seen is that the final temperature of the water in the vial seems to largely depend on the final temperature of the heating plate, with heating time and starting temperature having a very small influence. This implies that the fuel temperature in all three FuelHeat tests was roughly equal with a maximum difference of no more than roughly 0.28°C, as that is the difference between the lowest and highest final heating plate temperature (28.12°C for FuelHeat1 and 28.40°C for FuelHeat3).

As can also be seen, the final water temperature was on average 1.10°C lower than the final heating plate temperature. If this relationship is roughly constant, then one can expect that the fuel temperatures were roughly 27.02°C for FuelHeat1, 27.24°C for FuelHeat2 and 27.30°C for FuelHeat3. Said temperatures would certainly not be higher than their respective final heating plate temperatures, or lower than 26.54°C, which is the lowest final water temperature in the relationship tests where both final heating plate temperatures were below those of all the FuelHeat tests. The maximum deviation is thus +17% and -16%.

Compliance table
The summary of the validation tests can be found below along with the compliance table (table 2.4). As can be seen, the set-up is compliant with most requirements but only partially compliant with the rest. However, the latter cases have been found acceptable. This was firstly due to the fact that they provided sufficient accuracy to be able to determine if a certain parameter had an influence on the IDT which was the goal of the first test campaign. Secondly, although the measurements were not very accurate, they were precise enough to ensure constant enough input conditions to measure the effect of the varied parameter on the IDT. It can thus be considered that the set-up performs as intended and gives accurate results.

Req.1 **The ignition delay time shall be measured with a resolution of 1 ms or better:** The high-speed camera was set to record with a frame rate of at least 1000 Hz (specifically: 3000 Hz), which was assumed to give a resolution of 1 ms or better.

Req.2 **The chemical delay time shall be measured with a resolution of 1 ms or better:** The high-speed camera was set to record with a frame rate of at least 1000 Hz (specifically: 3000 Hz), which was assumed to give a resolution of 1 ms or better.

Req.3 **The Weber number shall be no more than 250:** This was ensured by calculating the Weber number for all testing conditions, as seen in tables 2.1 and 2.2. Its accuracy is related to the drop height and droplet diameter, giving a maximum deviation of ~10% relating to the droplet diameter uncertainty.

Req.4 **The drop height shall be controllable:** This was ensured by having the top structural plate be adjustable through changing the location of the bolts and washers it rested on along the threaded rod connecting it with the bottom structural plate. The accuracy is +-1 mm, which gives a maximum deviation of ~1%.

Req.5 **The falling droplet diameter shall be controllable:** This was ensured by using a syringe pump and different needles to produce different droplet diameters. As stated, the maximum deviation was determined to be 10% by dispensing 10 times the nominal volume and confirming 10 droplets formed.

Req.6 **The falling droplet temperature shall be controllable:** This was ensured by using a combination of a heating strip and a temperature sensor to maintain the correct temperature of the buffer. It was assumed that the temperature of the HTP drop is equal to that of the buffer, as the HTP in the buffer is practically completely surrounded by the buffer itself.

Req.7 **The resting propellant temperature shall be controllable:** This was ensured by using a combination of a heating strip and a temperature sensor to maintain the correct temperature of the heating plate. A relation was found between the heating plate temperature and fuel temperature giving a range of +-17%.

Req.8 **The set-up shall retain its structural integrity at all times:** This would be validated during operation if the set-up did not fall apart, which indeed was not the case.

Req.9 **The set-up shall not corrode:** This would be validated during use and storage if the set-up did not corrode, which indeed was not the case.

Req.10 **The set-up shall allow for a minimum of six tests with different fuels per hour:** This would be validated by performing more than six tests per hour, which was indeed the case. Specifically, one test per three minutes could be performed as can be seen in appendix A which translates to twenty tests per hour. Although this was done with vials with a constant fuel mixture, vials with different fuel mixtures in them can be swapped equally quickly.

Req.11 **There shall be no risk of personal injury:** This would be validated during use if no personal injury would be sustained, which indeed was not the case. This was furthermore ensured by setting up and following testing procedures as found in appendix C which included both preventative safety measures and a contingency checklist.

Table 2.4: Compliance table

Requirement	Validation	Compliance
1: The ignition delay time shall be measured with a resolution of 1 ms or better	The camera is set to 3000 Hz giving a resolution of 0.33 ms	Compliant
2: The chemical delay time shall be measured with a resolution of 1 ms or better	The camera is set to 3000 Hz giving a resolution of 0.33 ms	Compliant
3: The Weber number shall be no more than 250	The Weber number was at most 138 +-10% which is well below 250	Compliant
4: The drop height shall be controllable	The drop height is controllable using nuts on a threaded rod to within ~1% deviation	Compliant
5: The falling droplet diameter shall be controllable	The droplet diameter is non-continuously controllable using different needles with a deviation of at most 10%	Partially compliant
6: The falling droplet temperature shall be controllable	The buffer temperature was controlled and is assumed to be equal to the falling droplet temperature	Partially compliant
7: The resting propellant temperature shall be controllable	The heating plate temperatue was controlled which gave a fuel temperature control with a maximum deviation of 17%	Partially compliant
8: The set-up shall retain its structural integrity at all times	The set-up retained its structural integrity at all times	Compliant
9: The set-up shall not corrode	The set-up did not corrode before, during or after testing	Compliant
10: The set-up shall allow for a minimum of six tests with different fuels per hour	The set-up allowed for up to twenty tests per hour	Compliant
11: There shall be no risk of personal injury	No injury was sustained and safety was incorporated in the procedures	Compliant

<div align="right">3</div>

Results and Discussion

The two test campaigns were performed successfully and the results are presented and discussed in this chapter. However, in order to illustrate what the results mean first an example of a test resulting in ignition is shown and the test result tables are explained.

3.1. Results introduction

A nominal drop test can be seen in figures 3.1, 3.2, 3.3, 3.4, 3.5, and 3.6, with the time of occurrence in the bottom right corner. The sequence of events during a nominal drop test is as follows. Firstly, the syringe pump is activated and a droplet is formed and starts falling, as seen in figure 3.1. Afterwards, the HTP droplet enters the fuel as seen in figure 3.2. The exact moment of entry is defined as the frame the two fluids come into contact with each other. After mixing, the presence of the catalyst leads to HTP dissociation which increases the temperature of the mixture. This in turn increases the dissociation rate thus creating a positive feedback loop known as a thermal runaway [51]. The propagator aids this process. This results in a "rise" of liquid and generation of gas as seen in figure 3.3.

The time from the moment of entry to the first frame where the "rise" of liquid can be seen has been defined as PDT (Physical Delay Time). The CDT (Chemical Delay Time) is then defined as the time from this frame to the first frame in which the ignition kernel resulting in ignition is seen as seen in figure 3.4. The IDT (Ignition Delay Time) is defined as the sum of the PDT and CDT. The fire kernel generally results in a flame as seen in figure 3.5. After the flame finishes burning slight smoke can be observed as seen in figure 3.6.

The individual test results can be found in tables 3.1 and 3.2. The accuracy of these results is 0.33 ms, as the high-speed camera was set to a frame rate of 3000 Hz. In the comments one can find if an ignition occurred and whether the test was recorded (a test without a recording was the result of the recording being started too late thus not capturing the test itself). A summary of the test results can be found in table 3.3. The average IDT, PDT and CDT values were computed using only nominal tests (explained later in this chapter), as it was found that non-nominal tests gave different results compared to nominal tests.

<div align="center">35</div>

Figure 3.1: Start of droplet fall

Figure 3.2: After droplet impact
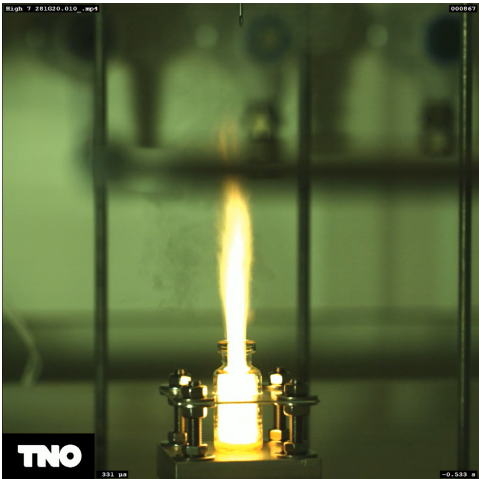

Figure 3.3: Chemical reaction

Figure 3.4: Ignition kernel

Figure 3.5: Fire

Figure 3.6: After fire

Table 3.1: Summarized test results of first test campaign

Test ID	PDT	CDT	IDT	Comment
Prep1	-	-	-	100 µL, no ignition, no recording
Prep2	-	-	-	150 µL, ignition, no recording
Prep3	-	-	-	150 µL, no ignition, no recording
Prep4	-	-	-	150 µL, no ignition, no recording
Prep5	25	26	51	150 µL
Prep6	22	39	61	50 µL
Prep7	26	46	72	200 µL
Prep8	22	-	-	25 µL, no ignition
Prep9	24	22	46	100 µL
BaseA1	22	33	55	
BaseA2	23	30	53	
BaseA3	23	-	-	Ignition kernel at IDT: 63, CDT: 40
BaseA4	21	21	42	
BaseA5	21	67	91	
LessOx1	25	-	-	Ignition kernel without ignition at IDT: 38, CDT: 12
LessOx2	22	-	-	Ignition kernel without ignition at IDT: 35, CDT: 13
LessOx3	25	-	-	No ignition
LessOx4	-	-	-	No ignition, no recording
LessOx5	23	-	-	No ignition
LessOF1	26	-	-	No ignition, weak decomposition
LessOF2	30	-	-	No ignition, weak decomposition
LessOF3	26	-	-	No ignition, weak decomposition
LessOF4	-	-	-	No ignition, no recording
LessOF5	24	-	-	No ignition, weak decomposition
High1	22	-	-	No ignition
High2	19	-	-	No ignition
High3	22	43	65	
High4	20	-	-	Ignition kernel at IDT: 46, CDT: 26
High5	20	22	42	
High6	23	-	-	No ignition
High7	20	72	92	First ignition kernel in liquid at IDT: 32, CDT: 12
High8	23	-	-	No ignition
HTPHeat1	22	25	47	
HTPHeat2	21	35	56	
HTPHeat3	22	-	-	No ignition
HTPHeat4	21	-	-	No ignition
HTPHeat5	-	-	-	No ignition, no recording
HTPHeat6	22	33	55	
FuelHeat1	16	24	40	T=0:00 27.73C, T=11:30 28.12C
FuelHeat2	15	32	47	T=0:00 28.12C, T=16:30 28.34C
FuelHeat3	14	27	41	T=0:00 28.34C, T=12:00 28.40C
BaseB1	20	33	53	
BaseB2	21	-	-	No ignition
BaseB3	20	33	53	
BaseB4	21	28	49	
BaseB5	20	76	96	

Table 3.2: Summarized test results of second test campaign

Test ID	PDT	CDT	IDT	Comment
Blunt110_1	26	41	67	
Blunt110_2	-	-	-	No ignition, recording started late
Blunt110_3	25	-	-	No ignition
Blunt110_4	23	-	-	No ignition
Blunt110_5	25	22	46	
BaseC110_1	30	-	-	No ignition, HTP drop went in via vial side
BaseC110_2	-	-	-	No ignition, HTP drop went in via vial side, recording started late
BaseC110_3	21	-	-	No ignition
BaseC110_4	21	-	-	No ignition
BaseC110_5	22	-	-	No ignition
BaseC150_1	22	26	48	
BaseC150_2	21	-	-	No ignition
BaseC150_3	23	-	-	No ignition
BaseC150_4	21	31	53	
BaseC150_5	18	33	51	
BaseC200_1	23	31	55	
BaseC200_2	21	24	45	
BaseC200_3	24	22	47	
BaseC200_4	27	17	44	
BaseC200_5	25	47	72	
BaseC250_1	25	31	55	
BaseC250_2	23	20	43	
BaseC250_3	20	21	41	
BaseC250_4	24	24	48	
BaseC250_5	23	21	44	
BaseC350_1	27	19	45	
BaseC350_2	25	19	44	
BaseC350_3	25	39	64	
Vial110_1	22	26	47	
Vial110_2	24	26	50	
Vial110_3	22	-	-	No ignition
Vial110_4	24	-	-	No ignition
Vial110_5	23	-	-	No ignition
Vial150_1	24	29	53	
Vial150_2	22	-	-	No ignition
Vial150_3	21	23	45	
Vial150_4	24	-	-	No ignition
Vial150_5	24	-	-	No ignition
Vial200_1	29	27	56	HTP drop went in via vial side
Vial200_2	25	-	-	No ignition
Vial200_3	28	-	-	No ignition, HTP drop went in via vial side
Vial200_4	23	-	-	No ignition
Vial200_5	25	33	58	

Table 3.3: Ambient Results

Series	Tests	Ignitions	PDT	CDT	IDT	Comment
BaseA	5	80%	22	38	60	-
LessOx	5	0%	24	-	-	One not recorded
LessOF	5	0%	27	-	-	Weak decomposition, one not recorded
High	8	38%	21	46	66	Characterized by variability
HTPHeat	6	50%	22	31	53	One not recorded
FuelHeat	3	100%	15	28	43	Temperature determined afterwards
BaseB	5	80%	20	43	63	Ensuring propellants did not deteriorate
BaseA+BaseB	10	80%	21	41	62	Summation of two test series
Blunt110	5	40%	25	31	57	One not recorded
BaseC110	5	0%	21	-	-	One not recorded, two drops via side of vial
BaseC150	5	60%	21	30	51	-
BaseC200	5	100%	24	28	53	-
BaseC250	5	100%	23	24	46	-
BaseC350	3	100%	25	26	51	-
Vial110	5	40%	23	26	49	-
Vial150	5	40%	23	26	49	-
Vial200	5	40%	24	33	58	Two HTP drops via side of vial

3.2. First test campaign

The first test campaign was aimed to look at the influence of input parameters on the hypergolic performance parameters.

Prep & BaseA

At the start of the first test campaign, preparatory tests were performed with them having Test ID's: "Prep#" and "BaseA#". The former tests were used to determine what fuel amount was to be used as the baseline, while the latter was used to confirm that value and was also included in the summarized test results. The reasoning behind this was that testing time was limited, otherwise more preparatory tests would be performed.

As can be seen, initial tests were performed around the fuel volume of 110 µL, which is the fuel-to-HTP ratio of 10 as often seen in literature. Based on the results, a decision was taken to perform tests with a fuel volume of exactly 110 µL ("BaseA#"). This yielded promising results with an ignition probability of 80%, or even 100% if the ignition kernel present in the BaseA3 is included. As the four tests at 150 µL yielded an ignition probability of 50% and the 200 µL test yielded the longest IDT, it was assumed that increasing the fuel amount beyond 110 µL was likely to decrease the ignition probability while possibly increasing the IDT. Thus, testing with a fuel volume of 110 µL was deemed to be the most optimal choice.

The average IDT of the the BaseA test series was 60 ms, which is above the maximum value of 50 ms. However, as this mixture had not yet been optimized for IDT, this result was actually considered promising. Also, one can observe the that the PDT has a lower variability than the CDT. This would prove to be a rule throughout all the test series.

BaseB

The BaseB test series was performed during the last day of the first test campaign and was intended to ensure that the results were time independent. If that were to be the case, the same results would be expected for both BaseA and BaseB. The ignition probability was found to be the same and the average PDT and average CDT were similar, with the average PDT being slightly lower and the average CDT being slightly higher in the BaseB test series. These minor differences can be explained by the low amount of tests performed per test series. It is thus concluded that the quality of the fuel did not significantly deteriorate and the test results were time independent. As these two test series were identical, they will be referred to jointly henceforth.

LessOx & LessOF

For the test series LessOx (HTP volume of 5 µL instead of 11 µL) and LessOF (HTP volume of 5 µL and fuel volume of 50 µL) one can see that the ignition probability was 0%. Furthermore, the average PDT of LessOx (24 ms) was higher than that of BaseA+BaseB (21 ms), while that of LessOF was even higher (27 ms) with the decomposition being relatively weak (as can be seen when comparing figures 3.7 and 3.8). This means that decreasing the HTP amount decreases the ignition probability and increases the average PDT and that this was not due to a change in the fuel-to-HTP ratio, with a proportional decrease in the fuel amount increasing the PDT even further. A possible explanation is that part of the heat generated by HTP dissociation is taken up by the vial, and since the amount of propellant decreases while the vial remains the same relatively speaking more heat is taken up by the vial. This decreases the heating rate of the propellant mixture thus increasing the PDT.
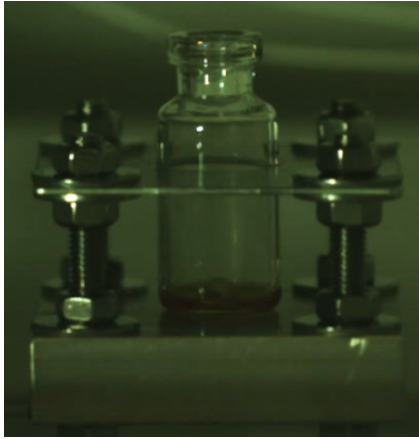

Figure 3.7: Weak decomposition of test "LessOF1"
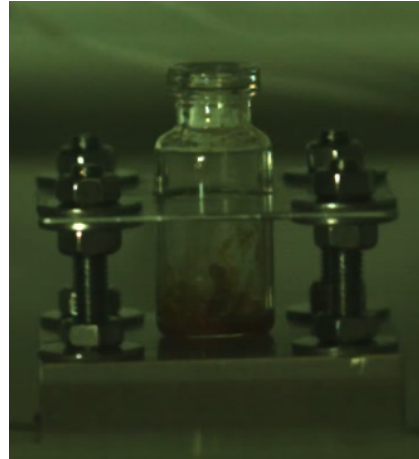
Figure 3.8: Normal decomposition of test "Deca1"

It should be noted that although there were no ignitions, two ignition kernels were observed with both a very low IDT (LessOx1: 38 ms, LessOx2: 35 ms). However, these ignition kernels were observed in the liquid (as seen in figure 3.9) as opposed to the location for nominal ignition kernels (as seen in figure 3.10). This was also the case for the ignition kernel of test High7 which would have resulted in the lowest IDT of any test. As such, these can be considered a unique type of ignition kernel with a low IDT but not leading to ignition.

Figure 3.9: Ignition kernel in liquid of test "LessOx1"

Figure 3.10: Nominal ignition kernel of test "Deca3"

High

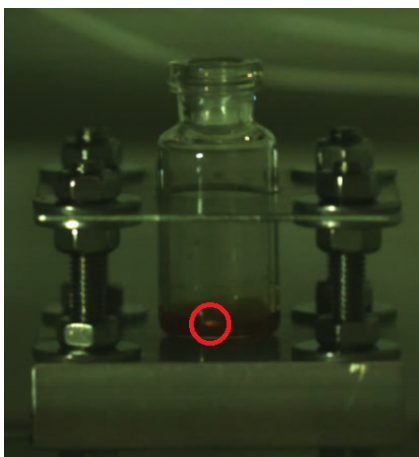This test series was expanded after the initial planned 5 tests to 8 tests in order to decrease the influence of chance on the results, as the results were unexpected. According to literature, the average IDT should decrease with an increase in the Weber number, but this turned out not to be the case with the average IDT increasing compared to BaseA+BaseB. Furthermore, the ignition probability significantly decreased.

However, two ignition kernels not resulting in a fire were observed in this test series, including the earliest ignition kernel of all tests with an IDT of just 32 ms as seen in figure 3.11. This shows a possibility of a higher drop height leading to more random results, as furthermore both a very short (42 ms) and very long (92 ms) IDT were observed in this one test series with three results. This randomness is also reflected in the standard deviation of the test series, which is 20.4 ms when excluding ignition kernels and 20.7 ms when including ignition kernels, while for BaseA+BaseB it is 18.9 ms and 17.8 ms respectively. The reason for a possible relation between drop height and increased variability of results in not clear.
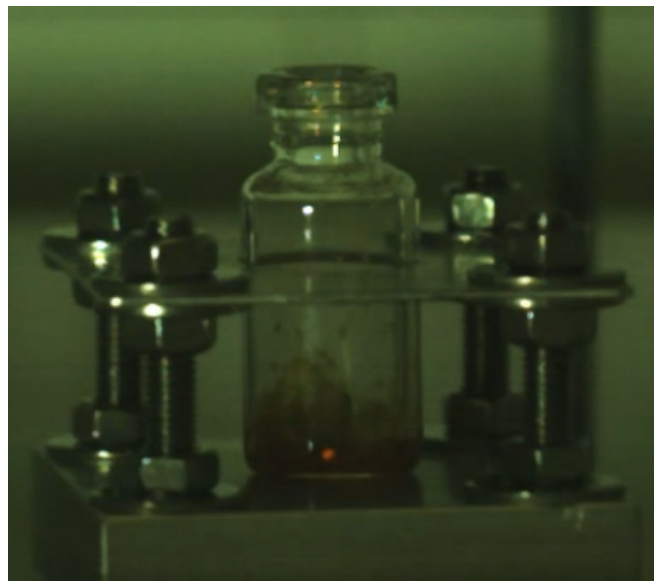

Figure 3.11: Early ignition kernel in test "High7"

It should be noted that changing the drop height changes the distance between the flame and the needle. This could theoretically have an effect on the results, for example by heating the needle more when the drop height is lower as the flame is closer to the needle. However, no clear relation was observed and thus the distance between the flame and the needle in the drop height range which has been tested can be assumed to have no impact on the results.

HTPHeat & FuelHeat

According the literature, heating either of the propellants leads to a lower IDT. This was indeed observed, although a lower ignition probability for HTPHeat (the heating of the HTP) was observed as well which was unexpected.

For the HTPHeat test series six tests were performed as one test was not recorded, and 5 quantitative data points were desired for the unexpected results of a relatively low ignition probability. One explanation could be that the increased temperature of HTP leads to a slight decomposition of the HTP thus lowering its concentration which leads to a decrease in the ignition probability according to literature. Aside from that, a decrease was seen in average CDT while the average PDT remained constant compared to BaseA+BaseB, resulting in an overall decrease of the average IDT as well. The slope of this decrease was found to be -2.45 ms/K, as seen in figure 3.12.
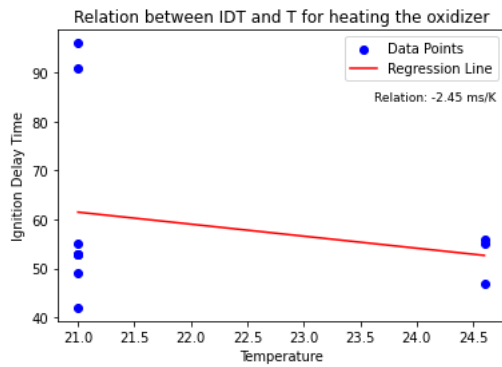
Figure 3.12: Relation between the ignition delay time and the temperature of the oxidizer
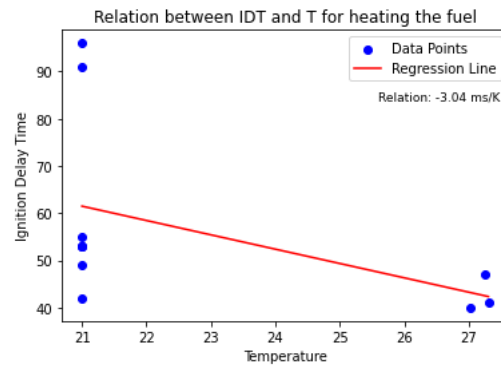
Figure 3.13: Relation between the ignition delay time and the temperature of the fuel

For the FuelHeat test series (heating of the fuel) 3 tests were deemed as enough, as the results clearly show a decrease in both the average PDT and average CDT and thus the average IDT. An ignition probability of 100% was noted as well. Taking the average FuelHeat fuel temperature of 27.24^{o}C (assuming the 1.10^{o}C relation as determined in the validation test in chapter 2) and comparing the FuelHeat average IDT of 43 ms to the BaseA+BaseB (21°C) average IDT of 62 ms, gives an IDT/T slope of -3.0ms/^{o}C, which can also be seen in figure 3.13. Taking the highest and lowest possible fuel temperatures (as also described in the validation test in chapter 2), slopes of -3.4ms/^{o}C and -2.6ms/^{o}C respectively are found, which establishes the possible range of the IDT/T slope for based on the 3 FuelHeat drop tests.

3.3. Second test campaign

The second test campaign was focused on quantitatively assessing the hypergolic performance of TNO's propellant mixture. This was done while varying values which theoretically should have no influence on IDT and the ignition probability, namely the syringe tip shape, the vial geometry and the fuel amount in order to challenge these assumptions. It was also done to challenge the assumption of the first test campaign that 110 μL was the optimum fuel amount for drop testing.

BaseC

The test series which had the exact same test configuration as the BaseA+BaseB test series (aside from the changed buffer, which theoretically should have no influence on the results) was BaseC110. However, one can see a clear difference with an ignition probability of 0% as opposed to 80%. Assuming the actual ignition probability is indeed 80%, the likelihood of having an ignition probability of 0% is $(20\%)^5 = 0.032\%$, which is a statistically significant change in ignition probability.

This discrepancy could be explained by a difference in the ratios of the ethanol, catalyst and propagator of the respective mixtures used in the two test campaigns. It is unlikely that the difference in results was because of the natural slight variation in mass when preparing a mixture by hand, as a microgram scale was used to measure the weight of the cups used to add the ingredients to the mixing cup before, and after adding the ingredients, which gives the mass added. Comparing these values showed a variation of 0.5% for the ethanol, 0.06% for the catalyst and 1.8% for the propagator, which seems to low for such a drastic difference in the ignition probability. However, in order to disprove such sensitivity drop tests with varying fuel mixture ratios would need to be performed.

A more likely explanation is a mistake on the part of the experimenter preparing the fuel batches, as the first and second fuel batch were respectively the first and second mixtures prepared by the experimenter using such a precise scale and while the scale was in a fume hood as well. This theory would be supported if the drop test experiment in the BaseA+BaseB+BaseC110 configuration was repeated with a third fuel batch, whose results would then show agreement with one of the two fuel batches. The fuel batch it would disagree with would be the one where the mistake would have been made.

The BaseC test series also disproved the assumption that 110 µL was the optimal fuel volume for drop testing, as increasing the fuel amount increased the ignition probability reaching a consistent 100% from a volume of 200 µL. It should also be noted that test BaseC110_1 had the HTP drop enter the fuel via the vial side, resulting in a longer PDT time (30 ms vs. an average of 21 ms for the other three BaseC110 tests).

Aside from that, PDT showed a slight positive correlation with fuel amount while CDT showed a slight negative correlation instead, resulting in no clear correlation of the IDT. As the number of tests per test series was relatively limited, it cannot be said that said slight correlations are not the result of stochastic error. However, the PDT relation could possibly be explained by the fact that the same amount of HTP is being dissociated while heating a larger total propellant volume. This could result in a longer heating time thus resulting in a longer PDT time.

Vial

The Vial test series used a vial which had a LessOF inner diameter, meaning there was less internal volume an the a given fuel volume would result in a higher fuel level from the bottom of the vial compared to the other test series. This proved to be more difficult to align resulting in the HTP drop hitting the side and entering the fuel via said side and in two Vial200 tests(Vial200_1 and Vial200_3), compared to one BaseC110 test. This also resulted in longer PDT times in said two tests (average of 29 ms vs. average of 24 ms for the other three Vial200 tests).

The results of the Vial test series were unexpected, as not only did they not follow the trend of an increasing ignition probability with an increasing fuel volume, they had a constant ignition probability of 40%. The reason for these two phenomena is likely the different geometry of the vial. Tests with a third type of vial could help further the understanding of this phenomenon.

Finally, a slight positive correlation between the fuel volume and both the PDT and CDT was observed. However, as in the case of the BaseC test series, this could very well be the result of stochastic error. Furthermore, the CDT correlation is opposite to the one seen in the BaseC test series, further supporting this theory.

Blunt110

The first test series of the test campaign was performed using a new blunt needle tip which was expected to dispense droplets with the same volume as the tapered needle tip while being shorter, which could be useful in future designs with limited height. The intention was to use it for the entire test campaign except for a single test series using the old needle type, the purpose of which would be to ensure that the results from both needles are identical. However, as can be seen the results were neither identical to BaseC110 nor to BaseA+BaseB. Thus it was decided to not use this needle type for the rest of the test campaign and use the needle type used in the previous test campaign.

The HTP volume dispensed by the needle tip was assumed to be equal to the option selected in the syringe pump, which seemed to work as a droplet would fall every time when 11 µL was set to be dispensed. However, in the recordings of the drop tests the droplets of the 1.5 mm blunt tip seemed larger in size compared to 1.2 mm tapered tip.

Although the recordings did not have a high enough resolution to conclusively determine the droplet sizes, a crude version of the syringe pump validation test was performed by manually dispensing 1 mL of water through either needle and counting the number of droplets. The 1.2 mm tapered needle yielded 54 droplets and the 1.5 mm blunt needle yielded 35 droplets, for respective volumes of 19 µL and 29 µL. As this test was performed using water and not 97.1% HTP, the former result does not disprove that the HTP drops used during testing had a volume of 11 µL. Although not conclusive, this test indicates that the selected syringe pump volume does not necessarily equal the droplet volume. This relation should thus be validated before any test campaign.

It would also explain the higher ignition chance compared to BaseC110, as the HTP drop volume was found to correlate positively with ignition probability in the LessOx and LessOF test series. One can

also observe that the average PDT, CDT and IDT are relatively high compared to the BaseC and Vial series, implying that a larger HTP volume results in higher PDT, CDT and IDT. This PDT relation was also suggested by the BaseC and Vial series, which supports the theory that an increase in overall propellant volume increases the PDT, although an inverse relation was found in the LessOx and LessOF test series suggesting that this relation is dependent on the total propellant volume. The CDT and IDT relations are the result of only two observations and thus necessitate further testing to confirm this relation with more certainty.

It should be noted that droplets form differently at the end of different types of needles, as tapered tip droplets form off-center on the "shorter side" of the needle while blunt tip droplets form centrally under the needle. This makes it impossible to directly compare the droplet size of blunt and tapered needles based on their orifice diameters.

3.4. Hypergolic performance of the fuel

The IDT of nominal tests in the second test campaign (thus excluding the results of the Blunt110 test series and the Vial200_1 and Vial200_3 tests) where ignition was observed can be said to be relatively constant. No clear trend could be observed. As such, the initial assumption of the fuel volume and vial shape having no influence on the IDT is valid. The hypergolic performance of the fuel at ambient conditions can thus be ascertained.

For this, the PDT, CDT and IDT of all the tests except for the Blunt test series, Vial200_1 test, Vial200_3 test and the two tests with no data were excluded. While a correlation between fuel volume on the one hand and PDT and CDT respectively on the other hand was found to be possible, the limited amount of tests means this could also very well have been the result of stochastic error. This can be researched by analyzing and comparing both the IDT and the CDT, the latter being the IDT without the PDT and thus correcting for any possible correlation. It should furthermore be noted that no clear relation between the ignition probability and PDT, CDT and IDT respectively can be seen. As such, another assumption for further analysis is made that there indeed is no such relation.

For the data in question, the average IDT is 50 ms and the average CDT is 27 ms. This IDT is at the limit of what is deemed an acceptable IDT, which is 50 ms. However, two things should be noted. Firstly, the fuel mixture was optimized for ignition probability, not IDT. This means that it is likely that the IDT could be brought down further by optimizing the mixture, as the IDT and ignition probability were found to be independent.

Secondly, it should be noted that data from different drop test set-ups in general cannot be compared directly, due to differences in drop height, droplet diameter, reaction vessel geometry, etc. [27]. If a comparison is to be made between fuels, it should be done using either the same drop test set-up, or two set-ups which have been made identical in terms of all input parameters. As drop test set-ups found in literature are not standardized (and such a standard does not exist) thus differing in these parameters, 50 ms should be taken as a rough estimate of an acceptable IDT. This also means that even though the IDT is 50 ms, it could actually be too high for practical application.

It is important to acknowledge the fact the the value of 50 ms is an average, meaning that one can expect the IDT to be longer than this in some tests thus exceeding this value. Although it could be possible that ignition delay times in engines are much more constant than those observed during drop testing, it is nonetheless useful to have an understanding of the delay time probability distribution. The data was thus analyzed in order to determine the shape of the probability density functions (PDF) of the IDT and the CDT. This was done using Python and a statistical analysis module called "distfit". It allowed for determining what probability density function best fit the data. This was done as follows.

Firstly, different types of PDF's were fitted to the data. They were then all analyzed using the Residual Sum of Squares method (RSS) to determine the quality of this fit. This method basically looks at how far individual data points are from the PDF curve in question. A lower score indicated a better fit thus allowing for the PDF's to be compared. However, it is necessary to ensure this result is robust and thus

that the PDF's are not overfitting (i.e. correlating well with the sample data set itself but not correlating well with the underlying distribution). This can be accomplished using a combination of Bootstrapping and the Kolmogorov-Smirnov test.

Bootstrapping is the process of taking the available data set and randomly selecting data points of this list with replacement, to create a data set with equal length to the original one. New PDF's are then fitted to this data set. The Kolmogorov–Smirnov test can then analyze how well these new PDF's fit the original data set. This is repeated, in this case 999 more times for a total of 1000. Based on this, a score can be given. The higher this score, the more robust the data. Combining this method with the RSS analysis shows well which PDF best fits the data.

Using the distfit Python module it was found that the best PDF for both the IDT and CDT data sets was the Gamma distribution. The Gamma distributions themselves can be seen in figures 3.16 and 3.17. The X-axis shows the delay time in ms and the Y-axis shows the probability of a certain delay time occurring in a test. This is a logical result due to the right skew of the data, meaning that measuring forwards in time, there is first a very sharp rise in probability before the respective modes at 44.27 ms for IDT and 21.40 ms for CDT, which then decreases at a much slower rate. These are the most robust distributions as can be seen in figures 3.14 and 3.15, as they have the highest bootstrap score in both cases.

It should be noted that for CDT the best fitting distribution was actually the Log-normal distribution followed by the Generalized extreme value distribution (RSS of 2.75175e-05 and 4.98081e-05 respectively), with the Gamma being the third best (RSS of 9.63253e-05). However, as they were not the most robust the Gamma function was selected instead. Comparing the three distributions in figures 3.17, 3.18 and 3.19 shows their similarity, making the discussion concerning which PDF to select more of a mathematical matter rather than a practical one.

The general shape of these distributions also makes sense from the physical perspective. For ignition, both the mixture and the temperature of the gasses as seen in figure 3.3 need to reach a certain point. The precise mechanisms of this are not clearly understood, but for the sake of discussion one can assume a single variable I which is a rough combination of the two. In order to reach ignition, this value needs to pass a certain threshold, let's call it the ignition threshold, above which ignition is possible. Below this threshold the ignition probability is 0. Looking purely at the temperature, we expect to see a sudden rise as the HTP decomposes in a thermal runaway process and a further increase as oxygen reacts with the propagator. Afterwards, the temperature should decrease but at a lower rate compared to the rise. This is exactly what we see in the Gamma Probability Density Function.
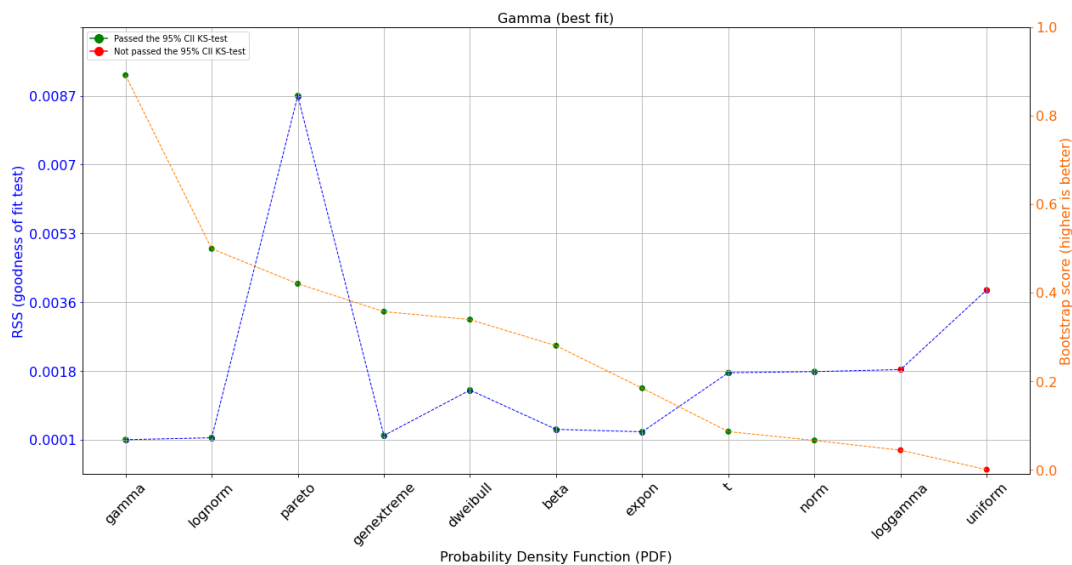
Figure 3.14: IDT of nominal tests of the second test campaign: Comparison of different Probability Density Functions
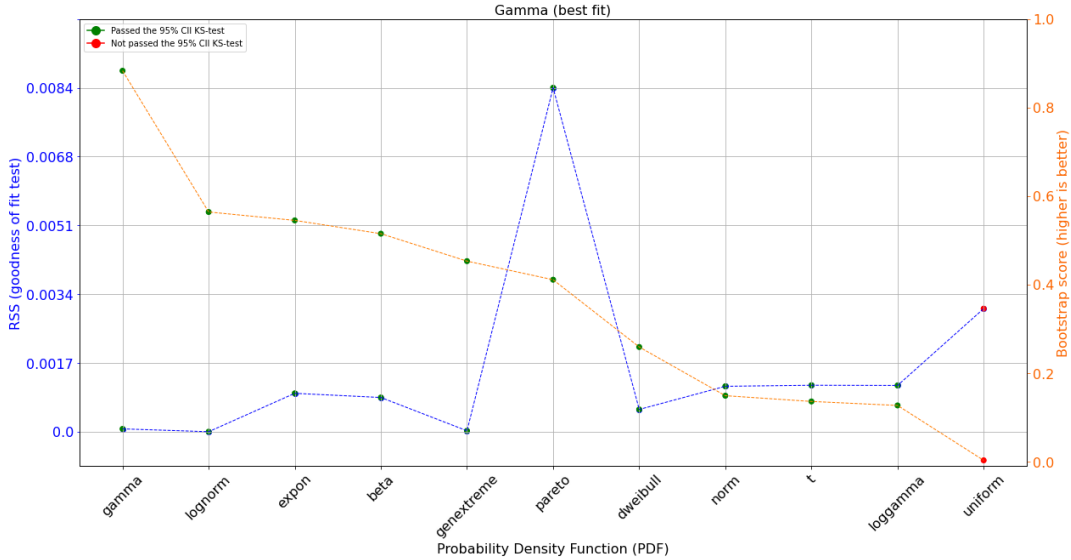
Figure 3.15: CDT of nominal tests of the second test campaign: Comparison of different Probability Density Functions

Figure 3.16: IDT of nominal tests of the second test campaign: Gamma distribution fitted to the data

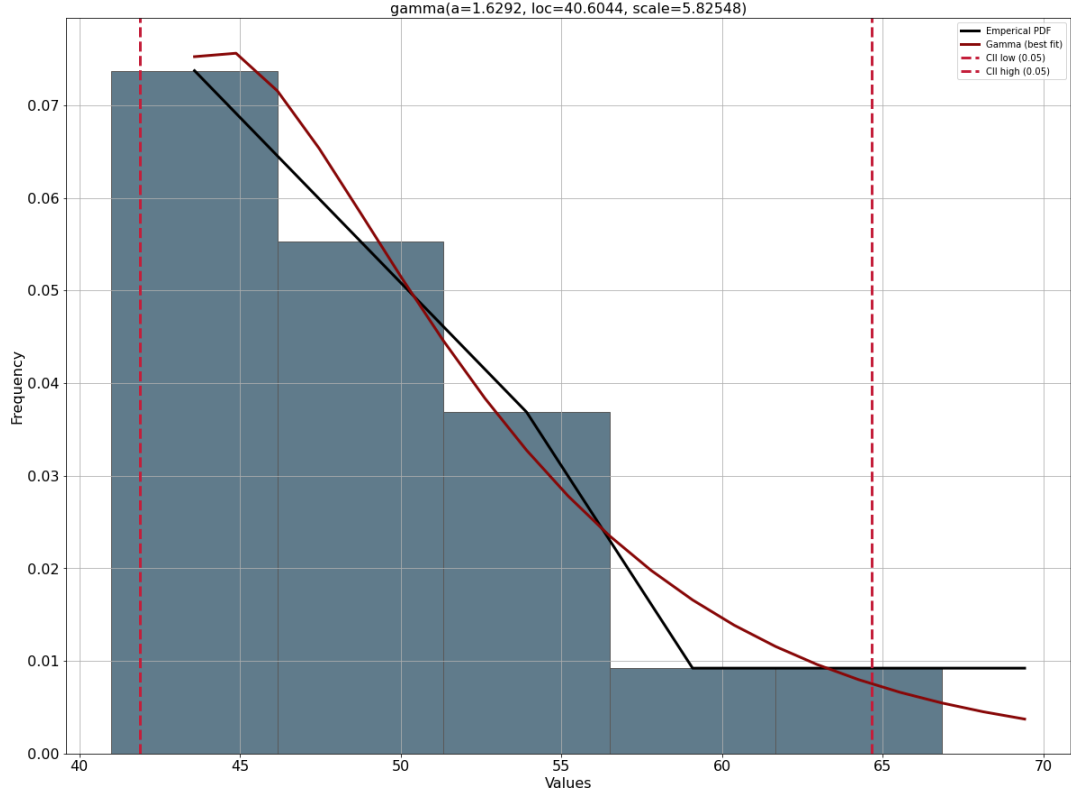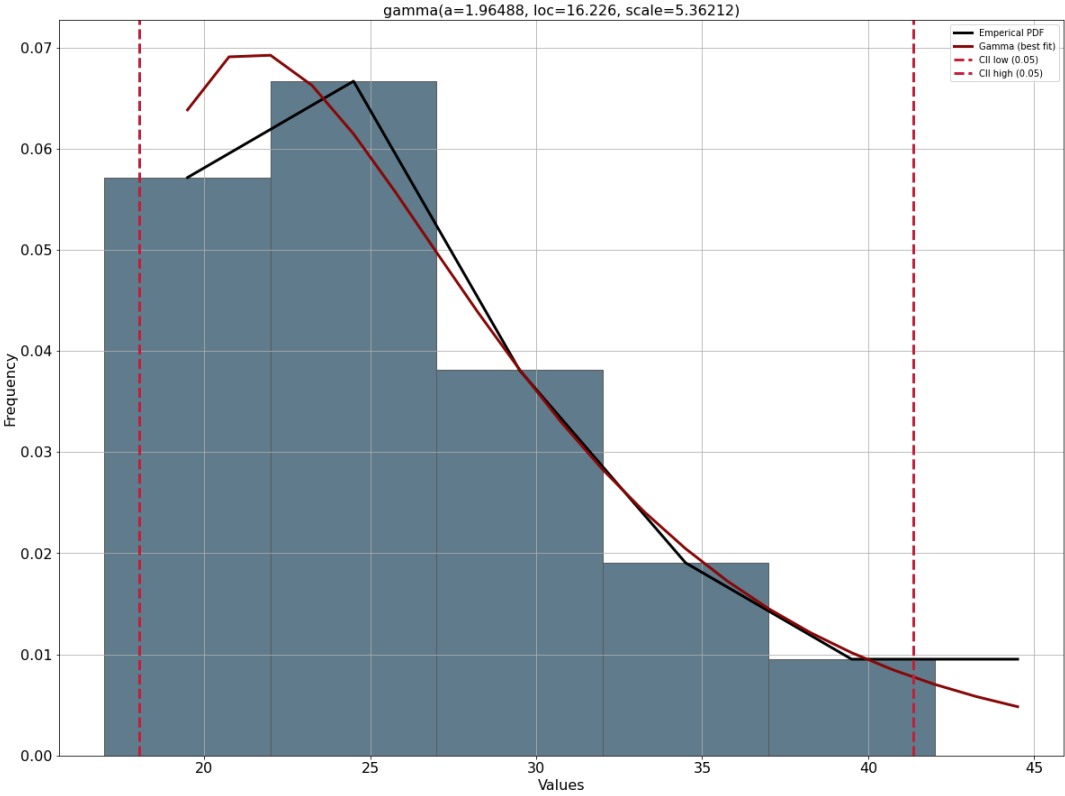**Figure 3.17:** CDT of nominal tests of the second test campaign: Gamma distribution fitted to the data
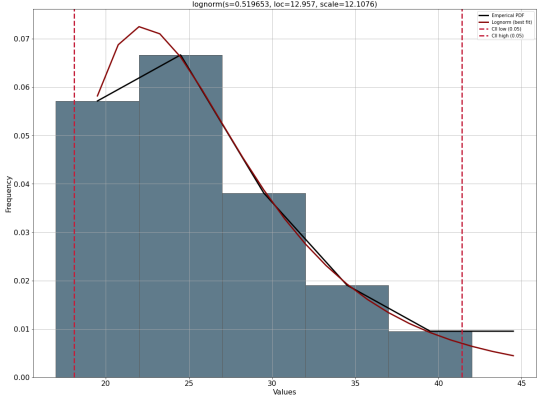

Figure 3.18: CDT of nominal tests of the second test campaign: Log-normal distribution fitted to the data
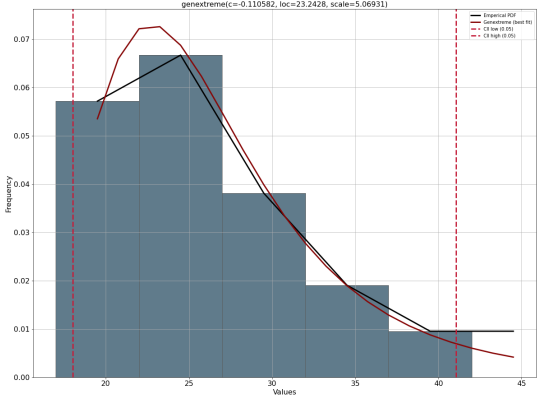
Figure 3.19: CDT of nominal tests of the second test campaign: Generalized extreme value distribution fitted to the data

<div style="text-align: right; font-size: 3em;">4</div>

Hermetic set-up

Developing a hermetic set-up was the next step in the process, which is described in this chapter. There were three iterations of the hermetic set-up, with the first one being sub-ambient hermetic and the other two being 0-40 bar hermetic. The reasoning behind this and other design choices will be explained in the three sections, each discussing a single iteration. The final set-up will be discussed in the greatest detail and will include two validation tests.

4.1. Sub-ambient hermetic set-up

The first iteration was a 0-1 bar set-up, which is lower than the preferred range which would allow for testing in operation conditions (up to ~10-~20 bar). The reason for this choice was as follows. Firstly, a sub-ambient set-up is easier to seal, is safer and requires less resources to manufacture than a high-pressure set-up. Furthermore, it was found that not a lot of extra resources were necessary to design an ambient set-up in such a way that it would be possible to upgrade to a sub-ambient set-up. This design plan was indeed executed as can be seen when comparing the ambient set-up and the initial version of the sub-ambient set-up in figures 4.1 and 4.2 respectively. It had the additional benefit of the sub-ambient set-up using multiple already-validated elements. These factors would greatly decrease the project risks associated with the development of the hermetic set-up.

Figure 4.1: Full view of ambient set-up

Figure 4.2: Full view of the sub-ambient hermetic set-up

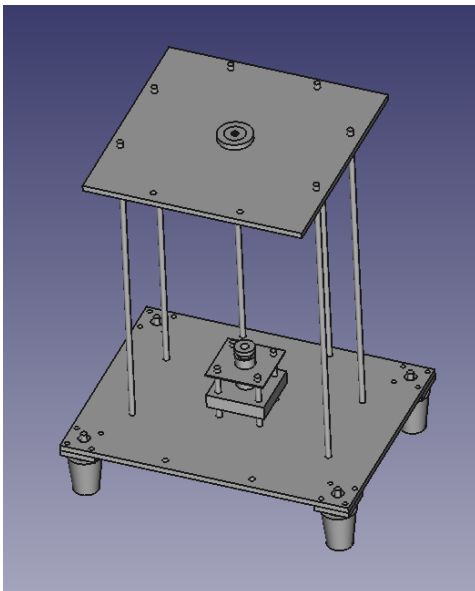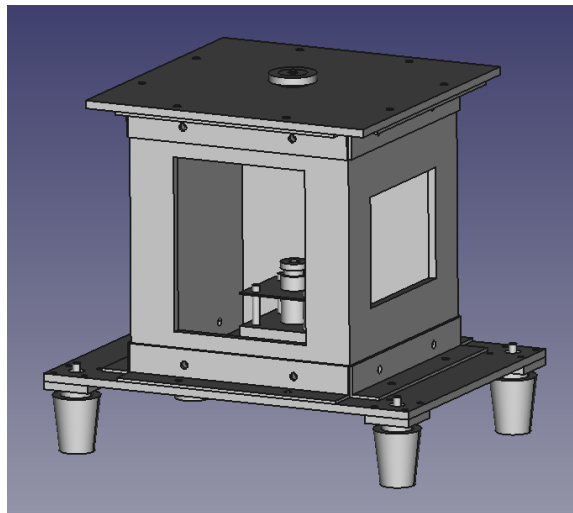Another reason for choosing a sub-ambient set-up was the fact that at this stage hypergolic propellant development it is more important to understand its behavior during ignition than during operation, as without successful ignition there is no successful operation. As stated, the former is tested in sub-ambient (space) conditions and the latter is tested in high-pressure (engine during operation) conditions. If one were to have to choose, having a sub-ambient set-up is thus more beneficial than having a set-up which can only test high pressures, although set-ups able to perform the latter almost certainly can also perform the former.
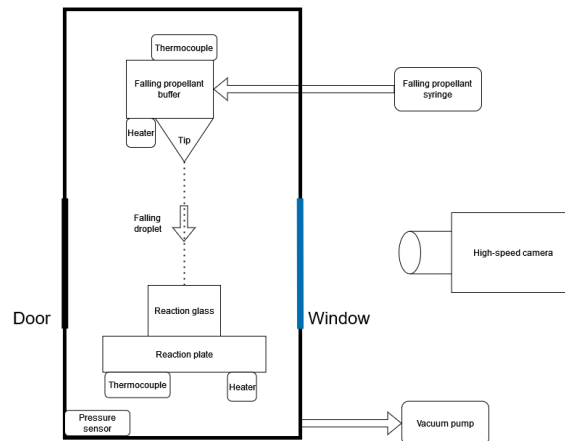

Figure 4.3: Conceptual full view of first hermetic set-up

As stated, the design itself can be summarized as the ambient set-up with additional walls to create a box-shaped chamber, very similar to the DLR set-up as seen in figure 1.13. A conceptual view of the set-up can be seen in figure 4.3. The design choices relating to this set-up are as follows.

- The square shape of the pressure chamber is due to the fact that this is the easiest shape with which a flat top plate, a flat bottom plate, a flat window or two (if spectroscopy capabilities are desired) and a flat door all can be attached and sealed
- As the pressure difference is 1 bar at most, a square shape was deemed an acceptable shape, even though round chambers are known to be better-suited as pressure chambers due to a lack of sharp angles which cause large stress concentrations
- The plates, windows and doors would be sealed using gaskets
- The top and bottom plates would be attached using L-brackets, as said brackets would not need to be load carrying due to the self-sealing nature of a sub-ambient set-up (the outside pressure pushes the plates against the gaskets)
- Any holes into the pressure chamber would be sealed using gaskets (for example, the initial screw-shaped buffer as well as any bolts would be sealed using dowty seals)
- A vacuum pump and a pressure sensor would be implemented
- The exact placement and attachment mechanism of the access door and the window(s) was undetermined when this set-up design was abandoned

4.2. Steel hermetic set-up

The first ambient test campaign showed that the only element of the ambient set-up which did not perform as expected at the end of said test campaign was the buffer. This was found to be a promising result from a project management perspective, as that meant that if one were to eliminate the buffer from the set-up then the rest of it had been validated. It was thus decided that the project risks were overestimated and a more ambitious high-pressure hermetic set-up could be developed. It was furthermore decided that the first version would exclude a heating buffer, although it could be implemented in later versions. As such, a novel high-pressure hermetic set-up was to be developed.

It was decided that a set-up based on (stainless) steel pipes was optimal. This was due to the fact that round shapes are preferred for pressure chambers. As a door and at least one window were to be included, pipes with flanges to accommodate them would be welded to the sides of the main pipe, which is easiest done using steel. This would result in a main structure as seen in figure 4.5 and an overall set-up as seen in figure 4.4. O-rings would be used to seal the bulkheads and door while a gasket would be used to seal the window.
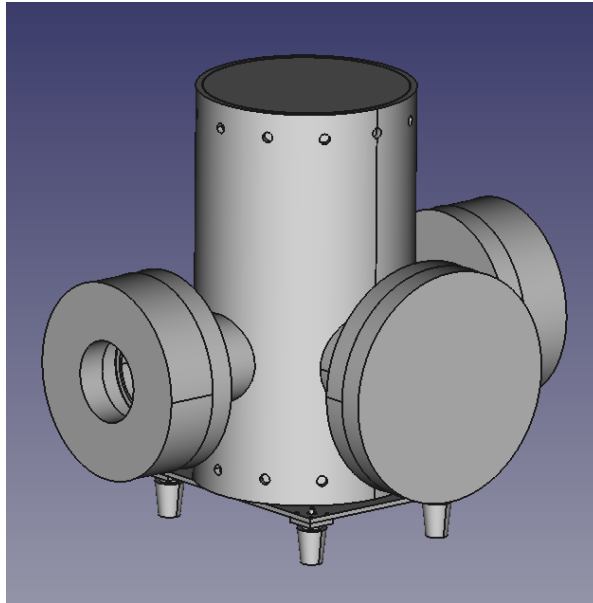
Figure 4.4: Full view of second hermetic set-up
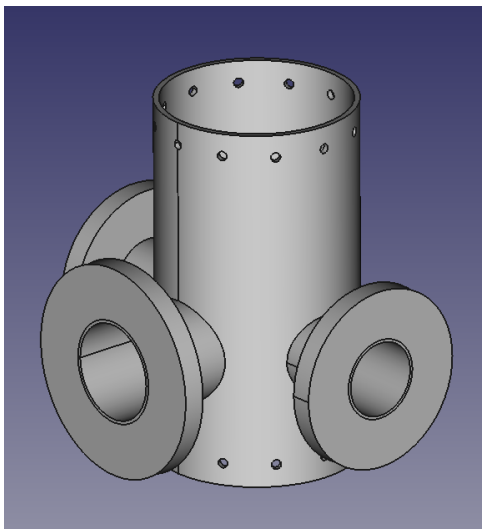
Figure 4.5: Main structural element of second hermetic set-up
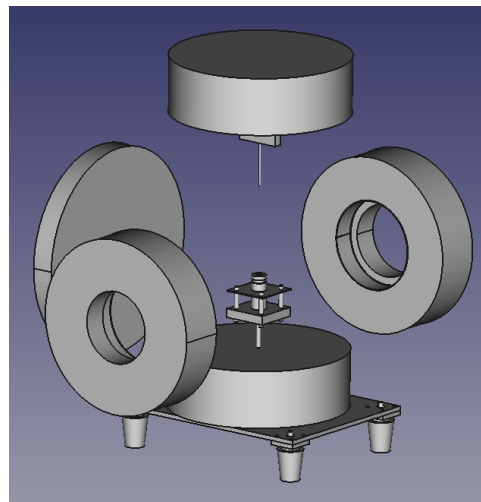
Figure 4.6: Inside view of second hermetic set-up

The choice for a set-up whose main pressure structure had the form of a pipe and was sealed using bulkheads with o-rings was also related to the manufacturing process. The author was the one to design and manufacture both the ambient set-up and the hermetic set-up. As the author had experience designing and manufacturing rocket engines in the shape of a tube attached to two bulkheads using radial bolts, choosing such a shape for a pressure chamber was thought to decrease the project risks. Furthermore, a party was found which ensured the pipes and flanges could be easily welded. It was thus decided that using this exact configuration carried the lowest overall project risk.

The final main design choice was the the pressure range of the set-up. As stated in chapter 1, ideally the set-up would be able to emulate conditions to ~20 bar. However, it would be useful to know how the propellant behaves beyond this point to expand the propulsion system design space for which the IDT is known (especially as ~20 bar implies a range of up to a few bar above 20 bar). Furthermore, as drop tests themselves slightly increase the pressure of the chamber, it was decided that 0-30 bar would be a good pressure range to strive for. However, when looking for COTS borosilicate glass solutions (the cheapest glass which meets the requirements for pressure, temperature and spectroscopy) it was found that the two pressure possibilities were 25 bar and 40 bar (for a diameter of 80 mm at the DIN 7080 standard). As a higher pressure was preferable and a high-pressure design could always be adapted for lower pressures, it was decided to design a 0-40 bar set-up. The further design choices were as follows.

- The main body would consist of a ~400 mm long stainless steel (304(L) or 316(L)) pipe with an inner diameter of 8" (219.1 mm) and a wall thickness of 8 mm, which would result in a yield failure at 150 bar as per the thin-walled assumption (d>~20t) hoop stress formula: $P_{yield} = \frac{2*t*\sigma}{d}$ using a stainless steel yield strength of 205 MPa, while a wall thickness of 6.35 mm would result a yield failure at 119 bar
- The top and bottom bulkheads would have a thickness of 65 mm each to accommodate two 10 mm wide o-ring grooves for redundancy and M10 bolts
- 10 M10 bolts would be used and they would have a distance of 19 mm from the edge, which would result in the following failure modes: for 6.35 mm main body thickness: bolt shear-out at 94 bar and a bolt tear-out at 89 bar (6.35 mm failure mode), for 8.00 mm main body thickness: bolt shear-out at 118 bar and a bolt tear-out at 112 bar, for both: bolt shear failure at 105 bar (8.00 mm failure mode) [56]
- The diameter of the door opening was set to ~100 mm as that was found to be the rough diameter which would allow practically all people to comfortably change the vial through said door
- DIN7080 borosilicate glass windows would be used with a viewing port diameter of 80 mm, a thickness of 25 mm, an outer diameter of 100 mm and a safety factor of 5, which was chosen as that was the largest COTS 40 bar rated window
- DIN EN 1092-1 PN-40 Typ 11 weld-neck flanges would be used for the door (DN100) and windows (DN80)
- Stainless steel pipes with a wall thickness matching that of the flanges (3.6 mm for the door and 3.2 mm for the windows) would be used for the connecting the flanges to the main body
- The door would be a DIN EN 1092-1 PN-40 Typ 05 blind flange made of aluminium with an appropriately increased thickness to reduce costs
- The door and window holders would be fastened using the appropriate bolts (8xM20 for the door, 8xM16 for the windows)
- Custom-made "window-holders" would be used to to hold the window in place
- 80 mm inner diameter and 102 mm outer diameter 2 mm thick PTFE seals would be used for the windows, as these were sold together with the window for a 40 bar use
- The outside of the window would be taped using PVC-tabe to increase its outer diameter to 102 mm thus preventing movement in the window holder

At this point in the design process the costs and mass (roughly 60 kg) were found to be too high. Although the mass could be reduced by lowering the pressure range requirement to 0-25 bar, the costs would still remain too high. As such, this design was abandoned in favor of the final hermetic design.

4.3. Aluminium hermetic set-up

The final version of the hermetic set-up was a design which was initially not chosen in favor of the steel hermetic set-up. This was partially due to the fact that the height of the pressurized volume is 17 cm which does not allow for a heated buffer to be easily included. This deficiency can be somewhat compensated by using the ambient set-up when measuring the effect of the falling droplet temperature, although no tests varying both the falling droplet temperature and the pressure and/or atmospheric composition can be performed. Nonetheless, this was deemed acceptable as a hermetic set-up would still provide useful data even without this capability.

The set-up can be seen in figures 4.7, 4.8 and 4.9, with the main structural element being a 200 mm wide, 200 mm long, 170 mm high aluminium cube as shown in figure 4.10. A detailed technical drawing of the main body can be found in appendix D, where the technical drawing of the window holders can be found as well.
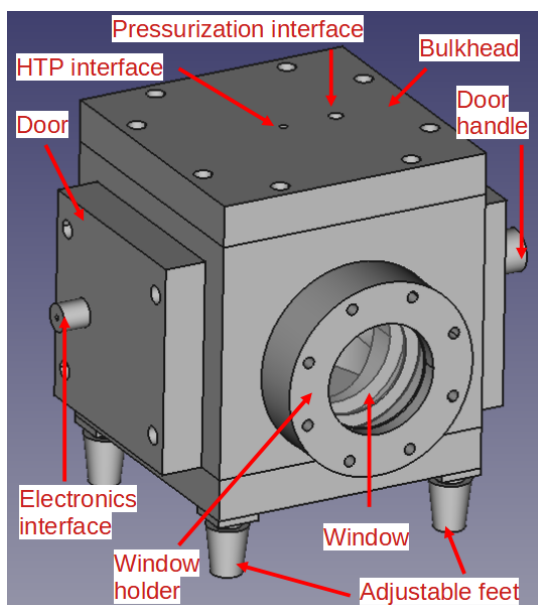

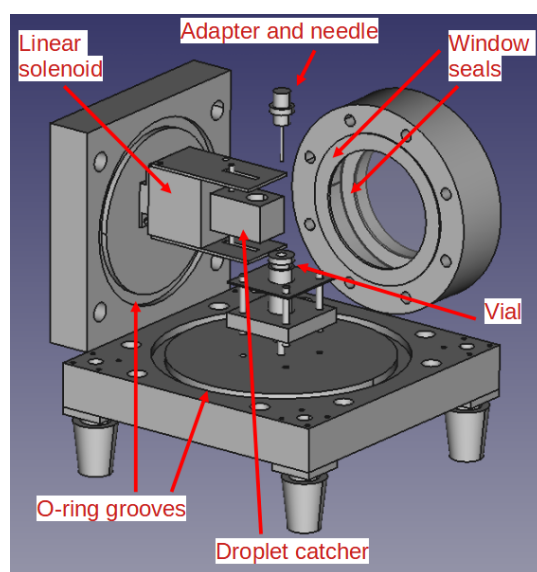**Figure 4.7:** Full view of final hermetic set-up
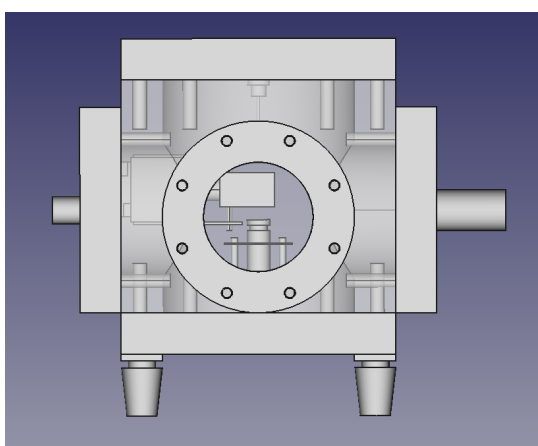

Figure 4.8: Inside view of final hermetic set-up

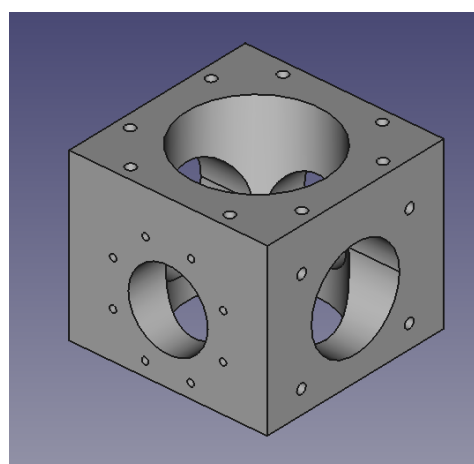**Figure 4.9:** Front view of final hermetic set-up

Figure 4.10: Main structural element of final hermetic set-up

4.3.1. Main structural elements

As the main body of this set-up was cube-shaped, its burst pressure cannot be easily calculated. However, its lower bounadry can be very roughly approximated if one ignores the corners resulting in a tubular shape. The thin-walled assumption (d>~20t) hoop stress formula can then be applied: $t = \frac{P_{yield} * d}{2 * \sigma}$ using a diameter of 200 mm, an aluminium 5083 yield strength of 165 MPa and a pressure of 40 bar which results in a thickness of 2.4 mm. As this relation is linear, a safety factor of 4 results in a thickness of 10 mm. During the design, a minimum thickness of roughly 30 mm was found to be necessary to ensure there would be enough material to accommodate the bolts. Although itself not meeting the thin-walled assumption criterion, it is over 12 times thicker than the 40 bar burst thickness. Furthermore the inner diameter has now decreased 140 mm resulting in a burst thickness of 1.7 mm and thus a safety factor of over 17. A thickness of 30 mm was thus assumed to be more than sufficient to prevent a failure of the main-body cube. This assumption would be tested during hydrostatic testing.

This same reasoning was applied to the thickness of both the bulkheads and doors, which were also set to 30 mm. This relatively high thickness furthermore increased stiffness in order to prevent outward deformation which could have resulted in a failure of the seals due to a decrease in compression. Since bulkheads were used to seal off the top and bottom of the main-body cube (resulting in a total height of 230 mm), their width and length were 200 mm by 200 mm. The door opening was 100 mm in diameter for the same reason as in the steel hermetic set-up. Furthermore, the choice was made to increase the number of door openings to two as this would increase the design flexibility of the set-up which was immediately utilized.

The borosilicate glass and seals were the same as the ones intended for the steel hermetic set-up. The window openings were 80 mm in diameter as that was what the borosilicate glass was designed for. Initially, a 102 mm wide and 20 mm deep hole would also be created resulting in one seal and most of the window being seated in said hole. The rest of the window along with the second seal would be located in the window holder which would accommodate a thickness of 8 mm, thus resulting in a gap of 1 mm between the window holder and the main body which could be used to compress and thus seal the seals. However, as the machine intended to create the 102 mm wide 20 mm deep hole turned out not to be capable of that, said hole was removed from the design. Instead, the window holder would now accommodate a thickness of 28 mm.

The problem was that the cylinder from which it would be machined was already delivered, thus requiring a redesign which would decrease the thickness of the part holding the window to 11 mm, as can be seen in the window holder drawing in appendix D. A FEM-analysis (seen in figure 4.11) was thus used to determine that the expected failure pressure at an aluminium yield strength of 165 MPa would be roughly 140 bar. This results in a safety factor of 3.5. This would be validated up to a safety factor of 2 during hydrostatic testing.
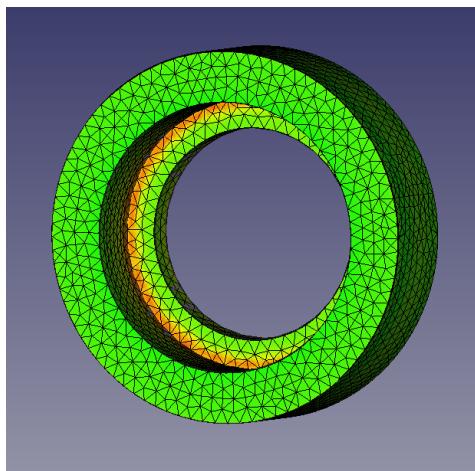
Figure 4.11: FEM analysis of the window holder with the maximum stress visible in orange

4.3.2. Feed system

As the set-up is hermetic, an additional challenge presented itself in the form of managing the pressure and atmospheric composition. The feed system used to accomplish this can be seen in figure 4.12. It consists of the following.

- The feed system is connected with a 1/4" SAE = 7/16"-20 UNF fitting to the chamber
- A digital pressure sensor accurately displays the chamber pressure
- An analog pressure sensor displays the chamber pressure in case the digital pressure sensor fails or the data is otherwise not easily readable, which increases the safety of the system
- A pressure relief valve set to the maximum operational pressure helps prevent overpressurization, which increases the safety of the system
- The chamber can be fully depressurized using a vacuum pump and a hand valve
- The chamber can be pressurized and/or filled with any gas using a gas cylinder (in this case an N2 gas cylinder), a compressed gas regulator and a hand valve
- The chamber pressure can be returned to ambient by opening the hand valve leading to a line stop
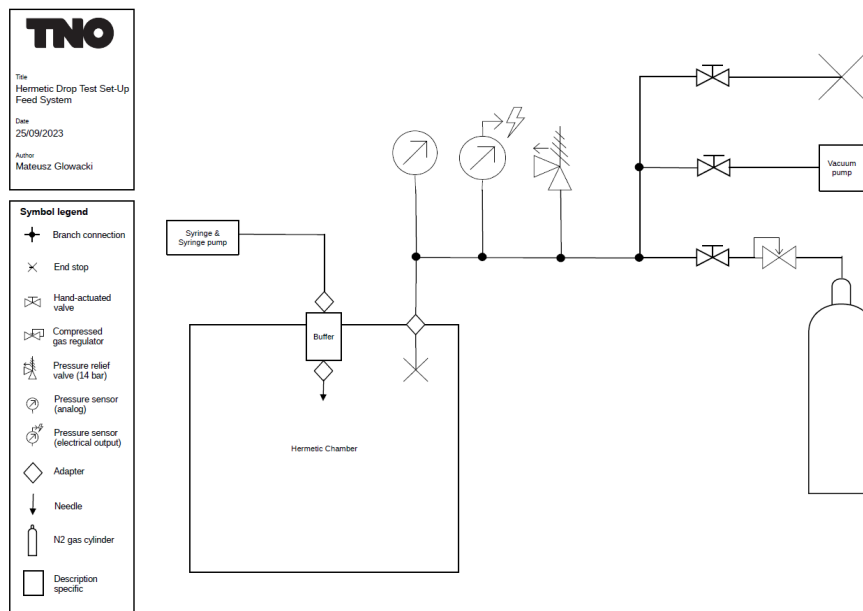
Figure 4.12: Feed system of hermetic set-up

The feed system also shows the droplet system, which including the syringe & syringe pump, adapters and the unheated buffer. This buffer consists of the same elements as the second ambient set-up buffer, with the exception that the aluminium part consists of the top bulkhead which cannot be easily heated. Another difference is an additional hole from the bottom of the top bulkhead to the empty space (which would be filled with water in the ambient set-up). The purpose of this is to ensure the pressure in said empty space is equal to that in the chamber, which in turn prevents the bottom adapter (connected to the needle) needing to withstand up to 40 bars of pressure.

It should be noted that for the Luer (Lock) syringe connection system which was used on the ambient set-up only components up to a pressure rating of 14 bar (200 psi) could be found. It was thus decided that 14 bar would be the maximum operating pressure for the first iteration of the hermetic set-up. This was done as it allowed for the use of the proven Luer (Lock) syringe connection system thus preventing the increase of the project risk. Furthermore, a pressure chamber of ~10 bar is a common figure for hypergolic thrusters, thus the scientific value of testing is high even when limited to a pressure range of up to 14 bar. Lastly, all of the ambient set-up components aside from the syringe turned out to be 14 bar rated, thus reducing the costs.

4.3.3. Other elements

A unique component is the droplet catcher, which can be seen in figures 4.8, 4.9 and 4.13. It consists of a linear solenoid attached (using an M4 threaded rod) to the droplet catcher part itself, both drawings of which can be found in appendix D (although the linear solenoid which was delivered deviated slightly from the drawing, which also necessitated a slight adjustment during the machining of the droplet catcher to match the moving part of the solenoid). In order to ensure the elements in the "open part" of the linear solenoid do not react with any accidentally spilled HTP, said part is to be non-hermetically closed off using a chemically compatible material like for example aluminium foil.

The droplet catcher has an extended and a retracted position. It is set to the extended position by hand after the vial with the resting propellant is placed (as seen in figures 4.8 and 4.13). This prevents any droplet from prematurely falling into the vial by catching the droplet in a 14 mm wide, 15 mm deep blind hole. Immediately before the test the solenoid is actuated which retracts the droplet catcher as can be seen in figure 4.8, which allows a droplet to fall into the vial. A simple validation test was performed consisting of retracting the droplet catcher while filled with multiple droplets of water and ensuring it would not spill. The water indeed did not spill both during and after retraction, which validates the design.

Figure 4.13: View of the droplet catcher

The structural elements of the set-up were fastened using bolts. The bulkheads were fastened using 8 M12 bolts, the doors using 4 M12 bolts and the window holders using 8 M8 bolts. Said bolts were initially intended to be made of aluminium to prevent corrosion. However, this was later found not to be a prevalent issue when fastening aluminium elements using stainless steel bolts, thus these were chosen due to their significantly lower costs. As this was done at a relatively late stage, the choice was made to keep the design of the fasteners the same thus greatly increasing their safety factor. The safety factors of the aluminium bolts were 4.7 for the bulkheads, 4.2 for the doors and 4.8 for the windows, which further increased when using steel bolts.

This also turned out to accommodate a manufacturing defect in the form of a thread tap breaking off and getting stuck in one of the 8 top bulkhead holes as can be seen in figure 4.15, with one bolt missing on the top right. Another problem turned out to be the length of the window bolts which were slightly too long and had to be relatively shortened by using two additional washers for a total of three per bolt.

The female threads in the cube were to be tapped to a depth of 30 mm for the M12 bolts and a depth of 20 mm for the M8 bolts in order to prevent the failure of said threads. This is based on a conservative approach of making the tapped depth 2.5 more than the major bolt diameter when the aluminium is involved. However, due to a defect of the depth dial on the milling machine some holes turned out deeper than that, although in the end this did not have any practical effects aside from one door bolt needing to be longer than the others. Aside from that, the bolts of the door which would be used to change the vial were substituted with a threaded rod and a nut, which allowed for a much faster opening of the door as only the nuts needed to be removed.

Other design choices can be described in less detail and have been summarized as follows.

- The bulkheads are sealed using FKM 75 151.77x6.99 mm o-rings and the doors are sealed using FKM 75 113.67x5.33 mm o-rings, which were chosen due to their chemical compatibility with HTP and the fact that larger o-rings result in better seals
- The bulkhead o-ring grooves (which can be seen in figure 4.8) have an inner diameter of 150 mm, an outer diameter of 168 mm and a depth of 5.4 mm resulting in a squeeze of 22% and a housing fill of 78%
- The door o-ring grooves (which can be seen in figure 4.8) have an inner diameter of 110 mm, an outer diameter of 125 mm and a depth of 4.1 mm for a squeeze of 23% and a housing fill of 72%
- One of the doors has a 1/2" G female thread which allows for an electronics interface to be inserted
- This union is kept sealed using a 1/2" dowty seal
- The electronics interface is a cylinder with a 1/2" G male thread and a hole through it, which allows for cables to be run through and sealed using epoxy resin, with the hole becoming smaller at the 5 mm farthest from the chamber thus holding the resin in place
- One of the doors has a 1/2" G 10 mm deep blind hole allowing for the attachment of a handle, which is used for easier handling of said door when changing vials or otherwise opening and closing the set-up
- The bottom bulkhead has 5 M5 10 mm deep blind holes allowing for the heating plate to be attached in multiple ways
- the linear solenoid is attached to the door with the electronics interface using a plate with two bolts connected to the linear solenoid and two bolts connected to the door
- A 12V LED strip installed in the main body itself ensures sufficient lighting for the high-speed camera
- An aluminium cylinder can be used as a window placeholder as it has identical dimensions, which can be seen in figure 4.15
- Adjustable feet connected to the bottom bulkhead allow for the chamber to be correctly leveled
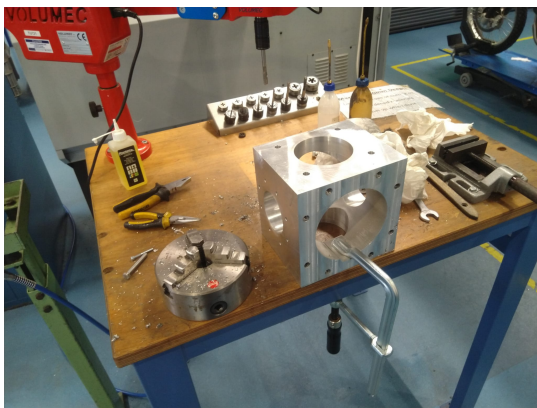
Figure 4.14: View of main structural element during tapping of threads
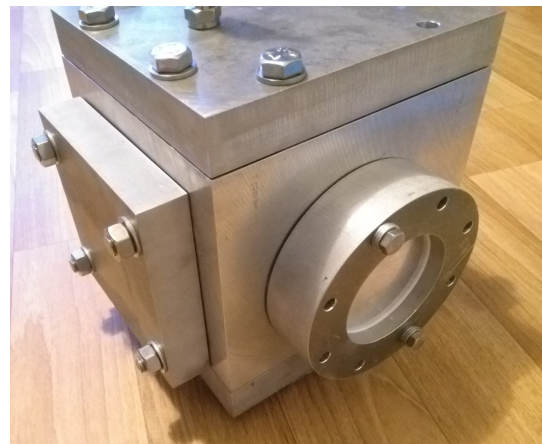
Figure 4.15: A back view of the set-up including the window placeholder

4.3.4. Hydrostatic test

Due to the novel nature of the set-up it was decided to hydrostatically test it to ensure safety at elevated pressures. Although the maximum testing pressure using the current feed system is 14 bar, it was decided that the set-up would be hydrostatically tested to 80 bar. This was done in order to validate that it is 40 bar capable and thus ensure that a future 40 bar upgrade of the feed system would be possible.

The hydrostatic test set-up can be seen in figure 4.16. The chamber was first filled with water while leaving the top valve open so air could escape. When water started flowing out of the tube connected

to said valve the valve was closed. The chamber was then pressurized twice, as can be seen in figures 4.17 and 4.18. The first time a maximum pressure of 80.14 bar was reached with no leaks in the set-up itself but rather in the connector to the chamber. The second time a maximum pressure of 81.20 bar was reached resulting in a leak of the COTS window seal, which was operating at 2 times its design pressure. As this is a favorable failure mode at a safety factor of 2 (as opposed to a structural failure), the hydrostatic test was considered a succes and the set-up was safe to be used.
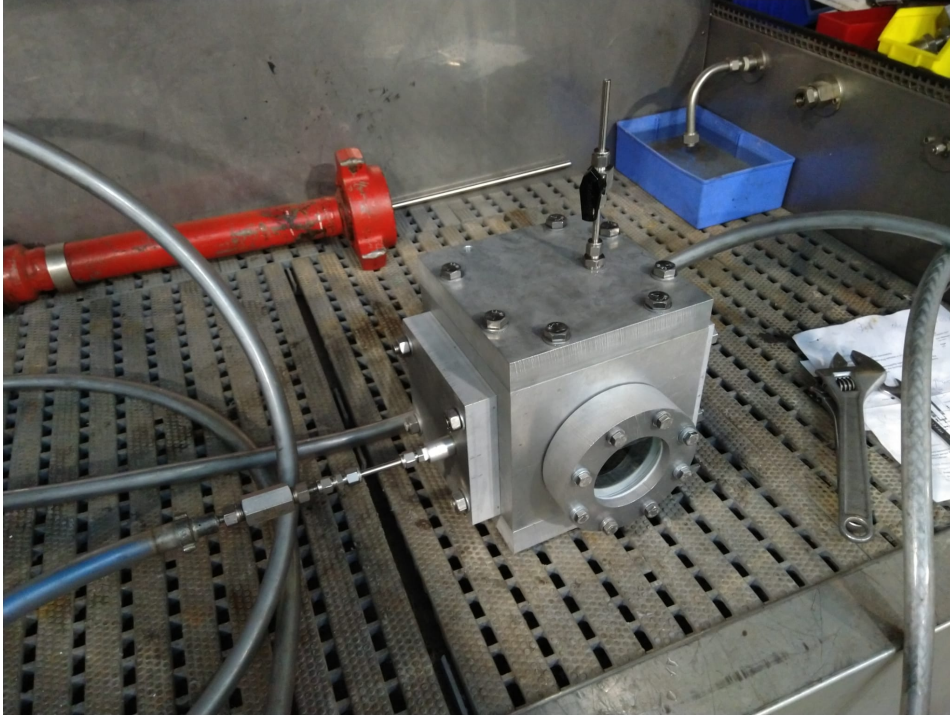
Figure 4.16: View of set-up during hydrostatic testing
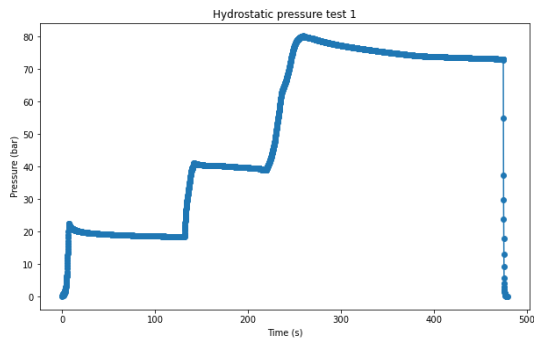
Figure 4.17: Pressure data of first hydrostatic test ($P_{max} = 80.14$bar)
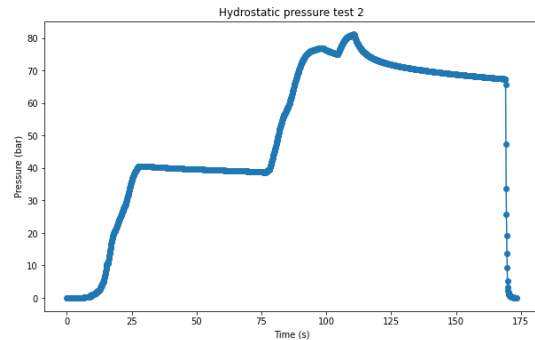
Figure 4.18: Pressure data of second hydrostatic test ($P_{max} = 81.20$bar)

5

Conclusion

The research objective and thus the main goal of this project was:

To design, build and calibrate a drop test set-up to be used to characterize the hypergolic performance of TNO's HTP/ethanol hypergolic propellant combinations.

In order to meet this objective, research questions and sub-questions were set up to guide this project in the right direction. These will be answered in a single section, as said answers are related to each other. Based on that, the conclusion concerning the research objective is stated.

Many test methods are available to perform characterization of hypergolic performance. The most notable ones are drop testing, impinging jet testing, small engine testing, force mixing testing, bomb testing and microreactor testing. Of these, the former three can be considered the standard order of hypergolic propellant characterization, while the latter three are less commonly used as they capture less critical aspects of hypergolic propellant performance.

Drop testing is used as a first step due to its relative simplicity and as it is a very good tool for initial screening of propellants. Furthermore, it can give insights into the effects of input parameters on the hypergolic performance parameters. The impinging jet test is an intermediate step, which is more complex than drop testing but less complex than small engine testing. It allows for the study of the phenomena present during injection of the hypergolic propellant combination into a combustion chamber. Although it can be quite similar to a small engine test, the latter involves the development of an actual small engine which is used to study the behavior of the propellant combination in conditions representative of commercial thruster operations.

As TNO's novel hypergolic propellant combination had not yet been tested using a drop test set-up which could measure the ignition delay time, that was the first step to take. It was decided to first develop an ambient drop test set-up which could both be used to determine the ignition delay time of TNO's propellant combination and to measure the hypergolic performance parameters as a function of the variable input parameters with the exception of pressure and atmospheric composition. The effect of the latter two would be measured using a hermetic drop test set-up which would be finished after the end of the thesis project and would incorporate the lessons learned during the two ambient drop test campaigns.

The ambient drop test set-up allowed for the variation of the propellant temperature, the drop height, the propellant volume, the reaction vessel and the propellant composition. Data was captured using a high-speed camera, which allowed for the ignition probability, the ignition delay time, the chemical delay time and the physical delay time to be measured. The main design philosophy of this set-up was maximum design flexibility, which allowed for the iteration of the "buffer" element which did not work as intended during the first test campaign.

The hermetic drop test set-up is basically the ambient drop test set-up in a hermetic structure with the exception that thermal control of the droplet was excluded due to spatial limitations. Its operational pressure range is 0-14 bar due to the pressure limitations of the droplet feed system. Upgrading said feed system would allow for the set-up to operate up to 40 bar. The design was created with a focus on safety, with design flexibility and ergonomics driving the design as well. This is reflected in both the design itself as well as the testing procedures.

The key performance parameters to quantify hypergolicity are the ignition probability, the ignition delay time, the chemical delay time and the physical delay time. The key variable input parameters are the propellant temperature, the fuel and oxidizer amount, the testing container geometry, the contact parameters and the pressure.

The most important one of these is the ignition probability, which determines how likely a hypergolic propellant combination is to ignite. Its importance is due to the fact that the very goal of a hypergolic propellant combination is to achieve ignition and it should thus be as high as possible. It is positively correlated with the propellant temperature, the oxidizer (droplet) volume and the fuel volume while being negatively correlated with the impact velocity. It was also found that the shape of the vessel in which the reaction occurs has an influence, although the exact relation is not understood.

The ignition delay time is the time between the hypergolic propellant combination making contact and the appearance of the ignition kernel. If this value is too large, a hard start can occur resulting in the destruction of the engine. It should thus be no more than 50 ms and preferably less than 10 ms. A very low value promotes the rapid stream separation combustion instability, although it does not guarantee it. It is negatively correlated with the propellant temperature. The ignition delay time can be divided into a physical delay time and the chemical delay time.

The physical delay time is the time from propellant contact until the first signs of a chemical reaction. It is negatively correlated with the propellant temperature. It also seemed to have a positive correlation with propellant volume when the total propellant volumes are relatively low (test series "LessOx" and "LessOF" compared to "BaseA" and "BaseB") and a very slight negative correlation with propellant volume when the total propellant volumes are relatively high (test series "BaseC" and "Vial"), although the latter could have been the result of stochastic error.

The chemical delay time is the time from the start of the chemical reaction until the appearance of the ignition kernel. It is sometimes seen as a more reliable value when comparing results of different drop test set-ups than the ignition delay time, as it omits the variable in the form of the physical delay time. It is negatively correlated with the propellant temperature.

Two relations which were found in literature but not observed were the negative correlation between the ignition delay time and both the pressure and the drop height. The former was not observed as the pressure could not be varied in the ambient set-up. The latter was not found as the "High" test series was characterized by a large variability in the results leading to a lack of clear conclusions. The Weber number of 250 was not exceeded, which according to literature could result in such a discontinuity of results. The oncly conclusion regarding the drop height is thus a positive relation between the drop height and the variability of the results.

Two things should be noted. Firstly, the number of tests with varying input parameters is relatively low, limiting the statistical significance of these results. Secondly, these conclusions are based on drop testing, which means they may not hold true for other testing methods and actual engine use. Nonetheless, they are very useful as an indicator of what can be expected in those conditions. As such, they are still a useful first step in hypergolic propellant research.

The performance of TNO's novel hypergolic propellant combination was determined to be promising. Firstly, an ignition probability of 100% was achieved when an HTP drop with a volume of 11 μL was dropped into a fuel pool with a volume of 200 μL or greater. The propellant combination furthermore had an average ignition delay time of 50 ms, which can already be seen as acceptable and which is a

good starting point for further testing. Moreover, as this propellant mixture has not yet been optimized for the minimization of the ignition delay time, it is likely that this value can be lowered by doing so.

Unfortunately, the varying of the fuel mixture has not been performed as priority was given to other aspects of this project. This means that the hypothesis:

"The ignition delay time can be divided into a mixing phase, an HTP decomposition phase and a propagator reaction phase."

was not sufficiently researched and thus it has neither peen proven nor disproven. Doing so would best be done by indeed varying the amounts of the catalyst and propagator in the fuel thus being able to study the effects of doing so, as well as using a high-speed infrared camera to observe the temperature of the mixture at different stages of the ignition process.

With the research questions answered, it can be determined that the research objective of designing, building and calibrating a drop test set-up to be used to characterize the hypergolic performance of TNO's HTP/ethanol hypergolic propellant combinations was performed successfully. The drop test set-up was indeed designed, built, calibrated and used for drop testing, although it does have room for improvement. Furthermore, the hermetic set-up should be finished to test the influence of pressure and atmospheric composition on the hypergolic performance parameters.

TNO's HTP/ethanol hypergolic propellant combination was characterized successfully as well, showing it is capable of a 100% ignition probability as well as having an acceptable IDT of 50 ms. Furthermore, as this mixture has not been optimized for IDT, a lower value can be expected to be reached by varying the mixture ratio in order to do so. As it stands, it is a viable candidate for becoming a hypergolic propellant combination which can be used in space missions.

<div align="right">

6

</div>

Recommendations

The recommendations chapter are divided in three sections: the ambient set-up, the hermetic set-up and testing.

6.1. Ambient set-up

The ambient drop test set-up works and can be used for the characterization of hypergolic propellants. Nonetheless, some improvements are possible. These are as follows.

The current vial is characterized by having a relatively small throat and a relatively large diameter compared to the resting propellant volume. The former results in the lining up of droplets needing to be very precise to avoid hitting the throat. Although it does have the benefit of ensuring the droplet is lined up very well with the center of the vial, it is not clear that this precision is necessary as long as the droplet impact is constant throughout a test campaign and does not bounce. Analysis of high-speed droplet impact footage could be done to ensure both of these. Decreasing the vial diameter results in the fuel level being higher, which could be beneficial in some way although this would need to be tested. A vial without a throat and a with smaller diameter could thus be used in future testing after being compared with the current vial.

The relation between the heating plate and the fuel in the vial should be characterized more accurately. Currently, for a given heating plate temperature the possible range of the fuel temperature is known. However, this range is relatively large and thus it would be beneficial to narrow it down. This could be done by repeating the heating plate temperature and fuel temperature relationship test while using a more powerful heating element and noting down more data points.

The effectiveness of the buffer in heating up HTP should be validated. Currently, an assumption is made that heating the buffer heats HTP to an equal temperature. It would be beneficial to test this assumption by for example screwing off the top adapter and putting a thermocouple into the buffer from that side and comparing the fluid (for example water) temperature with the buffer temperature. Furthermore, the temperature of a droplet for a given buffer temperature could be measured, although it is not clear what an optimal method to do so would be.

Lastly, the actual HTP droplet volume when using the blunt needle should be measured. This could be most easily done by performing the 10-drop test as described in chapter 2.

6.2. Hermetic set-up

At the time of writing the hermetic set-up is under development. The droplet catcher has been validated and the structure of the set-up has been hydrostatically tested to 81 bar. The next steps in the development of this set-up are as follows.

- Finish the manufacturing of the set-up to reach the design as described in chapter 4.

- Perform a dress rehearsal of a hermetic test campaign using water instead of the propellant combination and without actually changing the pressure when the procedures call for doing so.
- Ensure the set-up is leak-tight and functional at the maximum operational pressure of 14 bar.
- Perform a dress rehearsal of a hermetic test campaign using water instead of the propellant combination including changing the pressure when the procedures call for doing so.
- Clean the set-up to ensure no impurities remain which could result in combustion when reacting with accidentally spilled HTP.
- Perform a test campaign using the hermetic drop test set-up.

6.3. Testing

The two test campaigns performed during this thesis did not exhaust the testing potential of the ambient drop test set-up. More tests of scientific value are possible. These include the following.

- In order to optimize TNO's hypergolic propellant combination for a minimum ignition delay time tests could be performed where the fuel mixture is varied. These tests could furthermore be useful to better understand what phases the ignition delay time can be divided into and thus to test the related hypothesis which was not tested during this thesis.
- A high-speed thermal camera could be used to capture the thermal processes occurring during a drop tests. This would also be useful to better understand what phases the ignition delay time can be divided into.
- A spectrometer could be used, preferably in the hermetic set-up to ensure better control of the initial atmosphere, in order to detect what combustion products are produced by a given hypergolic propellant combination during a drop test.
- The test conditions of BaseA, BaseB and BaseC could be repeated to test the hypothesis that the an error in the preparation of one of the two fuel mixture resulted in the discrepancy of the results of BaseA+BaseB and BaseC. If the results of such a test series would match one of these two, then that would support the hypothesis that the fuel mixture of the other one was different from what was intended.
- More tests could be performed at the test conditions chosen during the first test campaign in order to increase the statistical significance of certain test series. This would allow for a much better characterization of the effects of variable input parameters on the hypergolic performance parameters. Said tests could also be performed using at least 200 µL of fuel in order to increase the ignition probability, as tests which do not result in ignition do not give data on the CDT and IDT.
- Tests could be performed in which one or multiple variable input parameters are varied to values different than the ones seen in the two test campaigns. That would provide more data points which could be used to establish clearer relations between the the variable input parameters and the hypergolic performance parameters.
- The HTP concentration could be varied in order to study the effects of doing so on the ignition probability and the delay times. This would be useful in order to understand what minimum HTP concentration is necessary to achieve sufficient hypergolic performance of the propellant combination.
- Propellant combinations from literature could be tested in order to be able to better compare the performance of TNO's novel hypergolic propellant combination with state-of-the-art hypergolic propellant combinations. This would give a better understanding of the viability of TNO's propellant combination as an alternative to the state-of-the-art propellant combinations.
- An impinging jet test set-up could be designed, built and tested in order to move the development of TNO's novel propellant combination forward. However, it is advisable to first perform further testing using the hermetic drop test set-up and to optimize the fuel mixture to minimize the IDT.

References

[1] A.R. Tummala; A.Dutta. "An Overview of Cube-Satellite Propulsion Technologies and Trends". In: *Aerospace* (2017).

[2] C.S. Hampton; K.K. Ramesh; et. al. "Atmospheric Effects on the Chemical Delay Time for Hypergolic Bipropellants". In: *AIAA* (2004).

[3] B.V.S. Jyoti; M.S. Naseem; et al. "Hypergolicity and ignition delay study of gelled ethanolamine fuel". In: *Combustion and Flame* (2017).

[4] D. Zhang; P. Zhang; et al. "Hypergolic ignition by head-on collision of N,N,N,N−tetramethylethylenediamine and white fuming nitric acid droplets". In: *Combustion and Flame* (2016).

[5] F. Lauck ; J. Balkenhohl; et al. "Green bipropellant development – A study on the hypergolicity of imidazole thiocyanate ionic liquids with hydrogen peroxide in an automated drop test setup". In: *Combustion and Flame* (2021).

[6] F. Lauck ; J. Balkenhohl; et al. "Ignition Investigations of a Novel Hypergolic Ionic Liquid with Hydrogen Peroxide in Drop Tests". In: *Space Propulsion Conference* (2020).

[7] F.A.S. Mota; L. Fei; et al. "Hypergolic ignition behaviors of green propellants with 2 hydrogen peroxide: The TMEDA/DMEA system". In: *SSRN Electronic Journal* (2022).

[8] H. Sheng; X. Huang; et al. "Low-Temperature Hypergolic Ignition of 1□Octene with Low Ignition Delay Time". In: *The Journal of Physal Chemistry* (2021).

[9] H. Xiao; Y.Y. Shi; et al. "Atomization Characteristics of Gelled Hypergolic Propellant Simulants". In: *International Journal of Precision Engineering and Manufacturing* (2015).

[10] J. John; P. Nandagopalan; et al. "Hypergolic ignition delay studies of solidified ethanol fuel with hydrogen peroxide for hybrid rockets". In: *Combustion and Flame* (2020).

[11] J. Li; X. Weng; et al. "The ignition process measurements and performance evaluations for hypergolic ionic liquid fuels: [EMIm][DCA] and [BMIm][DCA]". In: *Fuel* (2017).

[12] M.J. Farmer; L.O. Mays; et al. "Reaction Rates for Hypergolic Propellants Using Chemical Delay Times". In: *Propulsion* (2003).

[13] O. Jobin; B. Dumas; et al. "Hypergolic ignition of paraffin-based hybrid rocket fuels by sprays of liquid oxidizer". In: *Proceedings of the Combustion Institute* (2022).

[14] S. Nath; I. Laso; et al. "Comprehensive ignition characterization of a non-toxic hypergolic hybrid rocket propellant". In: *Proceedings of the Combustion Institute* (2022).

[15] S. Park; K. Lee; et al. "Effects of oxidizing additives on the physical properties and ignition performance of hydrogen peroxide-based hypergolic propellants". In: *Acta Astronautica* (2022).

[16] S. Ricker; M. Kurilov; et al. "Novel gelled fuels containing nanoparticles as hypergolic bipropellants with HTP". In: *European Conference for Aeronautics and Space Studies (EUCASS)* (2019).

[17] T.D. Kubal; E.M. Dambach; et al. "Aspects of Monomethylhydrazine and Red Fuming Nitric Acid Ignition". In: *AIAA/ASME/SAE/ASEE Joint Propulsion Conference & Exhibit* (2010).

[18] V.K. Bhosale; J. Gwak; et al. "Rapid ignition of "green" bipropellants enlisting hypergolic copper (II) promoter-in-fuel". In: *Fuel* (2021).

[19] Y. Liu; Y. Guo; et al. "Experimental study on hypergolic ignition and non-ignition for dicyanamide-based ionic liquids at low impact velocity conditions". In: *Energetic Materials Frontiers* (2021).

[20] S.A. Frolik; B.L. Austin. "Development of Hypergolic Liquid Fuels for use with Hydrogen Peroxide". In: *AIAA* (2001).

[21] C. Indiana; B. Boust; N. Azuma. "Combustion of sprays from triplet injector with green propellants: ethyl alcohol and hydrogen peroxide". In: *EEUCASS* (2017).

[22] B.V.S. Jyoti; M.S. Naseem; S.W. Baek. "Hypergolicity and ignition delay study of pure and energized ethanol gel fuel with hydrogen peroxide". In: *Combustion and Flame* (2017).

[23] J. Balkenhohl. "Design, Construction and Comissioning of a Reaction Chamber for Hypergolic Fuels as well as first Optical Measurements of the Flame Emission". In: *Institut für Raumfahrtsysteme, Universität Stuttgart* (2019).

[24] B. Bicer. "Numerical Simulation of Cavitation Phenomena inside Fuel Injector Nozzles". In: *Kobe University* (2015).

[25] A. Braeuer. "Shadowgraph and Schlieren Techniques". In: *Supercritical Fluid Science and Technology* (2015).

[26] B.R. Lawver; B.P. Breen. "Hypergolic Stream Impingement Phenomena - Nitrogen Tetroxide/Hydrazine". In: *NASA* (1968).

[27] J.D. Clark. *Ignition!: An Informal History of Liquid Rocket Propellants*. 6th ed. Rugers University Press, 1972.

[28] J.D. Dennis. "Investigation of condensed and early stage gas phase hypergolic reactions". In: *Purdue e-Pubs* (2014).

[29] Modern Engineering for Design of Liquid-Propellant Rocket Engines. *D.K. Huzel; D.H. Huang*. AIAA, 1992.

[30] P.A.W. Dommelen. "Novel and Green Hypergolic BiPropellant System for Propulsion Application". In: *TU Delft* (2021).

[31] G. Rarata; W. Florczuk. "Novel Liquid Compounds as Hypergolic Propellants with HTP". In: *Journal of KONES Powertrain and Transport* (2016).

[32] M. Glowacki. *Literature Study Final Report*. 2022.

[33] J.Q. Manas; B.V.S. Jyoti; P. Gurumallapa. "Hypergolicity and ignition delay study of green bipropellant system without catalyst (PPT)". In: *Aerospace Europe Conference* (2020).

[34] J.M. Forness; T.L. Pourpoint; S.D. Heister. "Experimental Study of Impingement and Reaction of Hypergolic Droplets". In: *AIAA/ASME/SAE/ASEE Joint Propulsion Conference* (2013).

[35] S.F. Son; T.L. Poupoint J.D. Dennis. "Critical Ignition Criteria for Monomethylhydrazine and Red Fuming Nitric Acid". In: *Journal of Propulsion and Power* (2015).

[36] C.S. Hampton; K.K. Ramesh; J.E. Smith Jr. "Importance of Chemical Delay Time in Understanding Hypergolic Ignition Behaviors". In: *Aerospace Sciences Meeting and Exhibit* (2003).

[37] H. Kang; E. Lee; S. Kwon. "Suppression of Hard Start for Nontoxic Hypergolic Thruster Using H2O2 Oxidizer". In: *Journal of Propulsion and Power* (2017).

[38] H. Kang; J. Huh; S. Kwon. "Experiment and Speculations on Nontoxic Hypergolic Propulsion with Hydrogen Peroxide". In: *Journal of Spacecraft and Rockets* (2018).

[39] H. Kang; J. Huh; S. Kwon. "Measuring the Reaction Rate of Hypergolic Propellants with a Microelectromechanical Systems Reactor". In: *Journal of Spacecraft and Rockets* (2017).

[40] K.S. Kim; V.K. Bhosale; S. Kwon. "Synergistic effect of a hybrid additive for hydrogen peroxide-based low toxicity hypergolic propellants". In: *Combustion and Flame* (2021).

[41] V.K. Bhosale; K.S. Kim; S. Kwon. "Sodium iodide: a Trigger for Hypergolic Ignition of Non-Toxic Fuels with Hydrogen Peroxide". In: *AIAA Propulsion and Energy Forum* (2020).

[42] M. Negri; F. Lauck. "Hot Firing Tests of a Novel Green Hypergolic Propellant in a Thruster". In: *JOURNAL OF PROPULSION AND POWER* (2022).

[43] B.R. Lawver. "High Performance N2O4 /Amine Elements – "Blowapart"". In: *NASA* (1977).

[44] B.R. Lawyer. "A Model of the Hypergolic Propellant Pop Phenomena". In: *Journal of Spacecraft and Rockets* (1972).

[45] et al. M. Kurilov; C. Kirchberger. "A Method for Screening and Identification of Green Hypergolic Bipropellants". In: *International Journal of Energetic Materials and Chemical Propulsion,* (2018).

[46] S. Carlotti; F. Maggi. "Evaluating New Liquid Storable Bipropellants: Safety and Performance Assessments". In: *Aerospace* (2021).

[47] J. Malm. "Inclusion of Substances of Very High Concern in the Candidate List". In: *European Chemicals Agency (EACH)* (2011).

[48] H. Tani; Y. Daimon; M. Sasaki; Y. Matsuura. "Atomization and hypergolic reactions of impinging streams of monomethylhydrazine and dinitrogen tetroxide". In: *Combustion and Flame* (2017).

[49] K. Hatai; T. Nagata. "Quantitative Clarification of Stable Ignition Region for HKP110 Green Hypergolic Bipropellant". In: *Aerospace* (2022).

[50] N. Zarbo; H. Belal; T. Pourpoint. "Effect of Water and Humidity on Hypergolic Propellant Ignition and Combustion". In: *51st AIAA/SAE/ASEE Joint Propulsion Conference* (2015).

[51] D. Wu; X. Qian. "Experimental study on the thermal runaway of hydrogen peroxide with in-/organic impurities by a batch reactor". In: *Journal of Loss Prevention in the Process Industries* (2018).

[52] W. Florczuk; G. Rarata. "Assessment of Various Fuel Additives for Reliable Hypergolic Ignition with 98% HTP". In: *66th International Astronautical Congress* (2015).

[53] W. Florczuk; G. Rarata. "Performance evaluation of hypergolic green propellants based on HTP for future next-generation spacecraft". In: *53rd AIAA/SAE/ASEE Joint Propulsion Conference* (2017).

[54] *REACH - Dinitrogen tetraoxide*. URL: `https://echa.europa.eu/substance-information/-/substanceinfo/100.031.012` (visited on 09/23/2023).

[55] *REACH - Methylhydrazine*. URL: `https://echa.europa.eu/substance-information/-/substanceinfo/100.000.429` (visited on 09/23/2023).

[56] Offices of Research Development Structures and Applied Mechanics Division. "An Experimental Study of Bolted Shear Connections". In: *U.S. Department of Transportation* (1981), 208210.

[57] P. Saksena. "Study Of Condensed Phase Reactions Between Hypergolic Propellants Using Microreactors". In: *The Pennsylvania State University* (2014).

[58] F.W. Hoehn; J.H. Rupe; J.G. Sotter. "Liquid-Phase Mixing of Bipropellant Doublets". In: *NASA* (1972).

[59] M.H. Straathof. "Test plan hypergolic fuel experiment". In: *TNO internal* (2012).

[60] *Thumbnail of video: Impinging Jet Dynamics*. URL: `https://www.youtube.com/watch?v=4HEbIRAcwuA` (visited on 10/02/2023).

[61] A. Chowdhury; C. Bapat; S.T. Thynell. "Apparatus for probing preignition behavior of hypergolic materials". In: *Review of Scientific Instruments* (2009).

[62] Z. Slocum-Wang; L. D. Felton; T. W. Turner. "Ignition Delay Screening Techniques: Drop Testing vs. Engine Testing". In: *AIAA/ASME/SAE/ASEE Joint Propulsion Conference & Exhibit* (2006).

[63] M.C. Ventura. "Long Term Storability of Hydrogen Peroxide". In: *41st AIAA/ASME/SAE/ASEE Joint Propulsion Conference & Exhibit* (2005).

[64] *Weber Number*. URL: `https://www.engineeringtoolbox.com/weber-number-d_583.html` (visited on 09/23/2023).

[65] L.B. Zung;J.R. White. "Combustion Process of Impinging Hypergolic Propellants". In: *NASA* (1971).

[66] A. Mayer; W. Wieling. "Green Propulsion Research at TNO The Netherlands". In: *Transactions on Aerospace Research* (2018).

[67] S.M. Davis; N. Yilmaz. "Advances in Hypergolic Propellants: Ignition, Hydrazine, and Hydrogen Peroxide Research". In: *Advances in Aerospace Engineering* (2014).

[68] B.T.C. Zandbergen. "Thermal Rocket Propulsion reader". In: *TU Delft course reader* (2018).

[69] D. Zhang. "Experimental Study of Hypergolic Ignition by Droplet Collisions". In: *The Hong Kong Polytechnic University PhD Thesis* (2017).

A
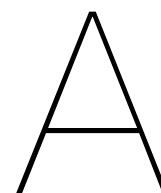
Detailed test results

Table A.1: Test results of the first test campaign

Date	Time	Test ID	Impact [ms]	PDT	Reaction start [ms]	CDT	Ignition [ms]	IDT	Comment
11-apr	14:01	Prep1	-	-	-	-	-	-	100 µL, no ignition, no recording
11-apr	14:05	Prep2	-	-	-	-	-	-	150 µL, ignition, no recording
11-apr	15:25	Prep3	-	-	-	-	-	-	150 µL, no ignition, no recording
11-apr	15:27	Prep4	-	-	-	-	-	-	150 µL, no ignition, no recording
11-apr	15:29	Prep5	2123	25	2148	26	2174	51	150 µL
11-apr	16:01	Prep6	-439	22	-417	39	-378	61	50 µL
11-apr	16:21	Prep7	-502	26	-476	46	-430	72	200 µL
11-apr	16:28	Prep8	-828	22	-806	-	-	-	25 µL, no ignition
11-apr	16:35	Prep9	-448	24	-424	22	-402	46	100 µL
11-apr	17:07	BaseA1	-645	22	-623	33	-590	55	
11-apr	17:14	BaseA2	-465	23	-442	30	-412	53	
11-apr	17:22	BaseA3	-762	23	-739	-	-	-	Ignition kernel at -699 (IDT: 63, CDT: 40)
11-apr	17:27	BaseA4	-495	21	-474	21	-453	42	
11-apr	17:29	BaseA5	-705	21	-684	67	-614	91	
12-apr	12:16	LessOx1	-865	25	-840	-	-	-	Ignition kernel at -827 (IDT: 38, CDT: 12)
12-apr	12:20	LessOx2	-979	22	-957	-	-	-	Ignition kernel at -944 (IDT: 35, CDT: 13)
12-apr	12:23	LessOx3	-805	25	-780	-	-	-	No ignition
12-apr	12:26	LessOx4	-	-	-	-	-	-	No ignition, no recording
12-apr	12:29	LessOx5	-968	23	-945	-	-	-	No ignition
12-apr	12:33	LessOF1	-868	26	-842	-	-	-	No ignition, weak decomposition
12-apr	12:43	LessOF2	-846	30	816	-	-	-	No ignition, weak decomposition
12-apr	12:46	LessOF3	-866	26	-840	-	-	-	No ignition, weak decomposition
12-apr	12:49	LessOF4	-	-	-	-	-	-	No ignition, no recording
12-apr	12:51	LessOF5	-685	24	-661	-	-	-	No ignition, weak decomposition
12-apr	14:12	High1	-863	22	-841	-	-	-	No ignition
12-apr	14:16	High2	-785	19	-766	-	-	-	No ignition
12-apr	14:26	High3	-507	22	-485	43	-442	65	
12-apr	14:30	High4	-555	20	-535	-	-	-	Ignition kernel at -509 (IDT: 46, CDT: 26)
12-apr	14:34	High5	-532	20	-512	22	-490	42	
12-apr	14:40	High6	-708	23	-685	-	-	-	No ignition
12-apr	14:43	High7	-649	20	-629	72	-537	92	First kernel at -617 (IDT: 32, CDT: 12)
12-apr	14:51	High8	-819	23	-796	-	-	-	No ignition
14-apr	12:38	HTPHeat1	-567	22	-545	25	-520	47	
14-apr	12:42	HTPHeat2	-828	21	-807	35	-772	56	
14-apr	12:46	HTPHeat3	-1027	22	-1005	-	-	-	No ignition
14-apr	12:50	HTPHeat4	-790	21	-769	-	-	-	No ignition
14-apr	12:53	HTPHeat5	-	-	-	-	-	-	No ignition, no recording
14-apr	12:55	HTPHeat6	-595	22	-573	33	-540	55	
14-apr	15:46	FuelHeat1	-499	16	-483	24	-459	40	T=0:00 27.73C, T=11:30 28.12C
14-apr	16:03	FuelHeat2	-384	15	-369	32	-337	47	T=0:00 28.12C, T=16:30 28.34C
14-apr	16:16	FuelHeat3	-550	14	-536	27	-509	41	T=0:00 28.34C, T=12:00 28.40C
14-apr	14:21	BaseB1	-596	20	-576	33	-543	53	
14-apr	14:24	BaseB2	-628	21	-607	-	-	-	No ignition
14-apr	14:28	BaseB3	-654	20	-634	33	-601	53	
14-apr	14:31	BaseB4	-502	21	-481	28	-453	49	
14-apr	14:33	BaseB5	-579	20	-559	76	-475	96	

Table A.2: Test results of the second test campaign

Date	Time	Test ID	Impact [ms]	PDT	Reaction start [ms]	CDT	Ignition [ms]	IDT	Comment
10-jul	16:48	Blunt110_1	204	26	230	14	271	67	
10-jul	16:53	Blunt110_2	-	-	-	-	-	-	No ignition, recording started late
10-jul	16:57	Blunt110_3	137	25	162	-	-	-	No ignition
10-jul	16:59	Blunt110_4	44	23	67	-	-	-	No ignition
10-jul	17:01	Blunt110_5	147	25	172	22	194	46	
13-jul	16:26	BaseC110_1	113	30	142	-	-	-	No ignition, via side
13-jul	16:29	BaseC110_2	-	-	-	-	-	-	No ignition, via side, recording started late
13-jul	16:36	BaseC110_3	126	21	147	-	-	-	No ignition
13-jul	16:40	BaseC110_4	140	21	161	-	-	-	No ignition
13-jul	16:44	BaseC110_5	130	22	152	-	-	-	No ignition
13-jul	16:48	BaseC150_1	163	22	185	26	211	48	
13-jul	16:54	BaseC150_2	156	21	177	-	-	-	No ignition
13-jul	16:56	BaseC150_3	178	23	201	-	-	-	No ignition
14-jul	14:30	BaseC150_4	150	21	171	31	202	53	
14-jul	14:34	BaseC150_5	159	18	177	33	211	51	
13-jul	17:01	BaseC200_1	153	23	176	31	208	55	
13-jul	17:03	BaseC200_2	164	21	185	24	209	45	
13-jul	17:04	BaseC200_3	168	24	193	22	215	47	
14-jul	11:29	BaseC200_4	117	27	144	17	161	44	
14-jul	11:32	BaseC200_5	133	25	158	47	205	72	
14-jul	14:44	BaseC250_1	173	25	198	31	229	55	
14-jul	14:47	BaseC250_2	193	23	216	20	236	43	
14-jul	14:50	BaseC250_3	156	20	176	21	197	41	
14-jul	14:53	BaseC250_4	151	24	175	24	199	48	
14-jul	14:55	BaseC250_5	144	23	167	21	188	44	
14-jul	15:05	BaseC350_1	147	27	173	19	192	45	
14-jul	15:08	BaseC350_2	189	25	214	19	233	44	
14-jul	15:11	BaseC350_3	165	25	190	39	229	64	
14-jul	13:30	Vial110_1	150	22	172	26	198	47	
14-jul	13:33	Vial110_2	186	24	210	26	236	50	
14-jul	13:36	Vial110_3	64	22	86	-	-	-	No ignition
14-jul	13:40	Vial110_4	199	24	223	-	-	-	No ignition
14-jul	13:43	Vial110_5	147	23	170	-	-	-	No ignition
14-jul	13:52	Vial150_1	225	24	249	29	278	53	
14-jul	13:54	Vial150_2	194	22	216	-	-	-	No ignition
14-jul	13:59	Vial150_3	260	21	282	23	305	45	
14-jul	14:02	Vial150_4	164	24	188	-	-	-	No ignition
14-jul	14:05	Vial150_5	193	24	217	-	-	-	No ignition
14-jul	12:01	Vial200_1	180	29	210	27	236	56	Via side
14-jul	13:11	Vial200_2	133	25	158	-	-	-	No ignition
14-jul	13:14	Vial200_3	138	28	166	-	-	-	No ignition, via side
14-jul	13:17	Vial200_4	136	23	159	-	-	-	No ignition
14-jul	13:20	Vial200_5	145	25	169	33	202	58	

B

Ignition delay times of different studies

The following list shows all the information necessary for understanding the composition of the propellants of the figures in question.

- Figure B.1 [53]

    - -

- Figure B.2 [30]

    - Oxidizer: 97% HTP
    - Fuel: Liquid ethanol for experiments #9, #10, #11
    - MCAT: Manganese (III) acetylacetonate
    - HSC: High-speed camera
    - PD: Photodiodes
    - The results of the high-speed camera were determined to be more reliable than those of photodiodes
    - Drop height: 23 cm

- Figure B.3 [22]

    - Oxidizer: 90% HTP
    - Fuel: Ethanol
    - Gelling agent: propyl cellulose
    - S_P: 6% Gelling agent
    - S_{Al}: 4% Gelling agent 4% Aluminum
    - S_B: 4% Gelling agent 4% Boron
    - S_C: 4% Gelling agent 4% Carbon
    - CCAT: 1% copper chloride hydrous
    - MCAT: 1% Manganese (II) acetylacetonate

- Figure B.4 [3]

    - Oxidizer: 90% HTP
    - Fuel: Ethanolamine
    - Gelling agent: 50% Polyvinylpyrrolidone 50% Fumed Silica
    - Liquid: no gelling agent
    - Pure: 12% Gelling agent
    - Al: 11% Gelling agent 2% Aluminum
    - B: 11% Gelling agent 2% Boron
    - C: 11% Gelling agent 2% Carbon
    - CCAT: copper chloride hydrous
    - MCAT: Manganese (II) acetylacetonate

- Figure B.5 [52]

  – -

- Figure B.6 [10]

  – Fuels are different combinations of ethanol, water, manganese (III) acetylacetonate and methylcellulose or hydroxpropyl methylcellulose
  – Oxidizer: 90% HTP

- Figure B.7 [15]

  – EMIM SCN: 1-ethyl-3-methyl-imidazolium- thiocyanate
  – BMIM SCN: 1-butyl-3-methyl-imidazolium-thiocyanate

- Figure B.8 [18]

  – IL: $[EMIM][BH_3CN]$
  – TG: tetraglyme
  – ILTG: 1:1 of IL & TG
  – CU-P1: $[Cu^{II}(1-H-imidazole)_4(BH_3CN)][BH_3CN]$
  – CU-P2: $[Cu^{II}(1-methylimidazole)_4(BH_3CN)_2]$

- Figure B.9 [41]

  – Oxidizer: 95% HTP

- Figure B.10 [49]

  – Oxidizer: 98% HTP
  – Fuel: HKP111 (3-methylaminopropylamine (MAPA) with 10 wt% of sodium borohydride)

- Figure B.11 [17]

  – Oxidizer: 91.2% HTP
  – Fuel A: Hydrocarbon-based mixture with sensitizing agent

- Figure B.12 [34]

  – -

- Figure B.13 [20]

  – Block 0: methanol with the manganese based catalyst in solution
  – SSR: Soluble Strained Ring compound from Organic Technologies

- Figures B.14, B.15, B.16, B.17, B.18 and B.19 [16]

  – Oxidizer: 96% HTP
  – Fuel: amine TMEDA (N,N,N',N'- tetramethylethylenediamine)

- Figure B.20 [6]

  – Oxidizer: 96.1% HTP
  – Fuel: EMIM SCN (1-ethyl-3-methylimidazole thiocyanate)

- Figure B.21 [7]

  – TMEDA: N,N,N',N'- tetramethylethylenediamine
  – DMEA: dimethylaminoethanol

- Figure B.22 [5]

  – Oxidizer: 98% HTP
  – Fuel: EMIM SCN (1-ethyl-3-methylimidazolium thiocyanate)

- Figure B.23 [38]

  - -

- Figure B.24 [69]

  - Oxidizer: 92% HTP
  - Fuel: 91.4% Ethanolamine 8.6% Sodium borohydride

- Figure B.25 [31]

  - -

Table 3. Results of IDT for catalytically promoted fuels at highest content of additives with 98% HTP.

Fuel	Additive/ Content	Lowest IDT, [ms]	Averaged IDT, [ms]	Highest IDT, [ms]
Benzaldehyde	20% $FeCl_3 \cdot 6H_2O$	47	50,1	53,7
Ethanolamine (MEA)	4% $CuCl_2 \cdot 2H_2O$	32,1	37	44
Ethanol	15% 2-ethylohexanoate cobalt (II)	53,1	63,2	82,7
Izoamyl Alcohol	20% 2-ethylohexanoate cobalt (II)	38,8	48,5	54,7
Jet-A/TMPDA (80/20)	20% (II) cobalt neodecanoate	21,2	22,5	24,6
TMPDA	20% 2-ethylohexanoate cobalt (II)]	5,4	6,6	7,8

Figure B.1: Ignition delay times [53]

Table 6.5: Average physical, chemical, and total ignition delay times measured using PDs and HSC for all samples presented in Table 6.4. All values are given in ms.

#	Variant	Physical delay		Chemical delay		Total ignition delay	
		PD	HSC	PD	HSC	PD	HSC
1	5% MCAT	43±12.3	51.6±9.8	45.5±9.8	23.8±4.2	89.5±3	75.4±5.6
2	3% MCAT	65.3±8.4	68.8±8.9	57.2±3.3	27.2±12.9	122.4±9.6	96.1±17.6
3	2% MCAT	82.1±2.4	84.6±4.1	62.7±27.7	46±17.3	144.8±26.4	130.6±13.5
4	1% MCAT	155.2±5.7	158.9±18.6	228.7±9.9	224.7±13.6	383.9±14.4	383.5±13.2
5	0.5% MCAT	430±41.8	445±26.3	627.2*	567*	1086.7*	1038.3*
6	95% HTP	74±1.8	78.3±4.7	77.3±4.7	45.2±6.7	151.4±4.7	123.4±3.9
7	90% HTP	86±9.7	87.9±12.2	83.1±12.3	67.6±7.5	169.1±3.6	155.5±5
8	87.5% HTP	112±8.1	118.5±4.7	**	**	**	**
9	Liq. 10% MCAT	13.9±3.6	16.8±3.9	40.3±5.3	35.5±4.4	54.2±21	52.3±1
10	Liq. 5% MCAT	14.7±4.1	14.9±4.6	46.2±20.6	35.7±17.7	60.9±16.6	50.6±13.1
11	Liq. 3% MCAT	22.2±1.3	23.6±1	**	**	**	**
12	But. 5% MCAT	42.4±4.1	43.3±3.5	38.9±7	20±1.7	81.4±9.7	63.3±5
13	But. 3% MCAT	61.5±4.9	62.8±4.1	77.6±23	29.5±2.7	141.9±19.4	94.8±0.2
14	5% FCAT	2161.2±970.8	1513.2±90.8	145±65.7	115±32.4	2306.2±91.4	1628.4±58.4
15	3% FCAT	3341.2±158.3	3374.1±163.3	153.4±19.5	92.8±38.6	3494.6±140.9	3466.9±137.3
16	0.3 ml fuel	48.2±17.5	53.7±15.2	84.3±18.8	36.4±4.8	132.6±2.4	90.1±10.7
17	0.2 ml fuel	50.7±8.8	55.6±7.9	58.5±9.3	29.4±3.8	109.2±2.7	85±9.6
18	0.05 ml fuel	65.3±5.5	68.6±6.5	53.5±6.2	19.7±3.4	118.8±3	88.2±4.1
19	4 weeks old	202.3±16.9	219.9±15.2	271.2±17.7	230.3±28.1	473.5±33.5	450.2±40.3
20	18 cm drop height	65.8±4.7	67±7	53.4±6.4	22.6±7	119.2±11	89.6±13.8
21	28 cm drop height	52.7±0.4	55.6±2.4	48.5±3.6	33.1±2.2	101.1±3.7	88.7±3.6

*Ignition was achieved only one out of three times. Therefore no standard deviation could be calculated.

**Ignition was not achieved in any case.

Figure B.2: Ignition delay times [30]

Table 2
Ignition delay of pure and metalized gelled ethanol fuel with hydrogen peroxide.

Gelled fuel	Oxidizer quantity	Ignition delay (ms)
S_P CCAT	Single drop	Rapid decomposition, No ignition
S_P CCAT	Multi drop	50
S_P MCAT	Single drop	13.46
S_P MCAT	Multi drop	19.8
S_{Al} CCAT	Single drop	4.15
S_{Al} CCAT	Multi drop	28.7
S_{Al} MCAT	Single drop	47.7
S_{Al} MCAT	Multi drop	7.0
S_B CCAT	Single drop	115.0
S_B CCAT	Multi drop	90.0
S_B MCAT	Single drop	37.0
S_B MCAT	Multi drop	1.33
S_C CCAT	Single drop	24
S_C CCAT	Multi drop	14.35
S_C MCAT	Single drop	19.2
S_C MCAT	Multi drop	18.6

Figure B.3: Ignition delay times [22]

Table 3
Ignition delay of pure and metalized gelled ethanolamine fuels with hydrogen peroxide.

Gelled fuel	Oxidizer quantity (µl)	Ignition delay (ms)	Critical catalyst concentration (wt%)	Flame length (mm)
CNO.Liquid.CCAT	50	N/A	0.1–1.0	N/A
CNO.Liquid.MCAT	50	N/A	0.1–1.0	N/A
CNO.Pure.CCAT	50	1.88	0.63	96
CNO.Pure.MCAT	50	20.42	0.50	101
CNO.Al.CCAT	50	3.90	0.35	113
CNO.Al.MCAT	50	5.6	0.31	186
CNO.B.CCAT	50	2.62	0.97	61
CNO.B.MCAT	50	4.06	0.38	116
CNO.C.CCAT	50	2.84	0.57	81
CNO.C.MCAT	50	5.02	0.40	10 approx.

Figure B.4: Ignition delay times [3]

Fuel	Additive	H_2O_2	IDT	Experiment Method
Methanol	10% MAT	98%	30ms[14]	Drop Test
Methanol	30% MAT	98%	10ms[14]	Drop Test
Ethanolamine	5% $CuCl_2$	85%	200ms[14]	Drop Test
Ethanolamine	10%$CuCl_2$	85%	30ms[14]	Drop Test
Ethanolamine	10%$CuCl_2$	85%	190ms[14]	Impinging Test
Ethanolamine[40degC]	10%$CuCl_2$	85%	130ms[14]	Impinging Test
Kerosene	Metal Salts	98%	19ms[15]	Drop Test
dimethylhexolamine	$C_{16}H_{30}CoO_4$	98%	12.7ms[10]	Drop Test
dimethylbutylamine	$C_{16}H_{30}CoO_4$	98%	9.8ms[10]	Drop Test
Triglyme	8% H_4BNa	88.5%	10.6ms[13]	Drop Test
Tetraglyme	10% H_4BNa	88.5%	12ms[13]	Drop Test
Dimethyl Formamide	12% H_4BNa	88.5%	9.12ms[13]	Drop Test
Dimethyl Sulfoxide	10% H_4BNa	88.5%	14ms[13]	Drop Test
Triglyme	8% H_4BNa	88.5%	9ms[13]	Impinging Test
Dimethyl Formamide	12% H_4BNa	88.5%	7ms[13]	Impinging Test
Dimethyl Sulfoxide	10% H_4BNa	88.5%	7ms[13]	Impinging Test

Table I. Fuel compositions that are hypergolic with concentrated hydrogen peroxide.

Figure B.5: Ignition delay times [52]

Table 5

Ignition delay times of solidified ethanol fuel containing a various concentration of gellant and catalyst loading.

Sample	Ignition delay (ms)
M13MAC1	No ignition
M13MAC2	No ignition
M13MAC3	242.33 ± 33
M13MAC4	129.20 ± 15
M13MAC5	89.50 ± 10
M13MAC6	150.0 ± 15
M13MAC7	207.67 ± 12
M14MAC5	72.20 ± 10
H13MAC1	307.00 ± 10
H13MAC2	218.00 ± 33
H13MAC3	49.00 ± 09
H13MAC4	88.25 ± 07
H12MAC3	66.67 ± 18
H10MAC3	163.33 ± 10

Figure B.6: Ignition delay times [10]

Table 2
Ignition delay of EMIM SCN with the oxidizer mixtures.

Oxidizer additives	H_2O_2 95 wt%	H_2O_2 90 wt%	H_2O_2 80 wt%	H_2O_2 70 wt%	H_2O_2 60 wt%
Pure	23.0 (2.3)	32.3 (1.2)	127.9 (5.8)	189.6 (11.2)	–
$LiNO_3$					
0.5 wt%	22.9 (1.2)	32.4 (2.3)	68.8 (2.1)	146.1 (13.0)	–
1.0 wt%	21.5 (0.6)	32.0 (4.0)	73.3 (5.0)	146.4 (13.5)	–
5.0 wt%	19.3 (1.4)	28.6 (2.6)	61.1 (5.1)	128.8 (13.0)	–
20.0 wt%	15.0 (1.0)	26.0 (2.4)	46.4 (3.8)	100.5 (5.8)	–
NH_4NO_3					
0.5 wt%	21.6 (1.8)	34.5 (2.7)	72.0 (9.3)	180.6 (15.4)	–
1.0 wt%	21.9 (1.5)	26.1 (3.4)	77.2 (2.9)	134.9 (24.1)	–
5.0 wt%	23.0 (2.1)	33.1 (1.0)	100.9 (2.8)	150.8 (8.3)	–
20.0 wt%	27.8 (1.9)	49.5 (4.5)	104.4 (7.4)	146.7 (11.3)	–

(): Standard deviation.
Four repetitions per case.

Table 3
Ignition delay of BMIM SCN with the oxidizer mixtures.

Oxidizer additives	H_2O_2 95 wt%	H_2O_2 90 wt%	H_2O_2 80 wt%	H_2O_2 70 wt%	H_2O_2 60 wt%
Pure	35.1 (3.8)	43.4 (1.5)	99.5 (2.1)	197.5 (14.9)	–
$LiNO_3$					
0.5 wt%	33.1 (2.9)	44.0 (2.7)	97.1 (6.1)	190.0 (16.8)	–
1.0 wt%	32.2 (3.0)	45.0 (3.0)	98.6 (5.0)	193.0 (20.6)	–
5.0 wt%	30.1 (3.1)	43.1 (4.1)	87.6 (4.9)	164.2 (16.0)	370.6
20.0 wt%	23.7 (1.1)	32.1 (2.1)	75.4 (1.7)	115.1 (12.8)	230.8 (18.2)
NH_4NO_3					
0.5 wt%	34.6 (2.6)	48.8 (3.0)	94.4 (7.0)	199.7 (9.0)	–
1.0 wt%	32.7 (1.5)	47.2 (1.6)	94.1 (3.7)	199.8 (14.2)	–
5.0 wt%	31.6 (1.4)	47.4 (3.6)	93.3 (3.0)	199.9 (11.7)	–
20.0 wt%	36.7 (1.1)	48.9 (3.4)	93.6 (8.3)	163.3 (3.9)	–

(): Standard deviation.
Four repetitions per case.
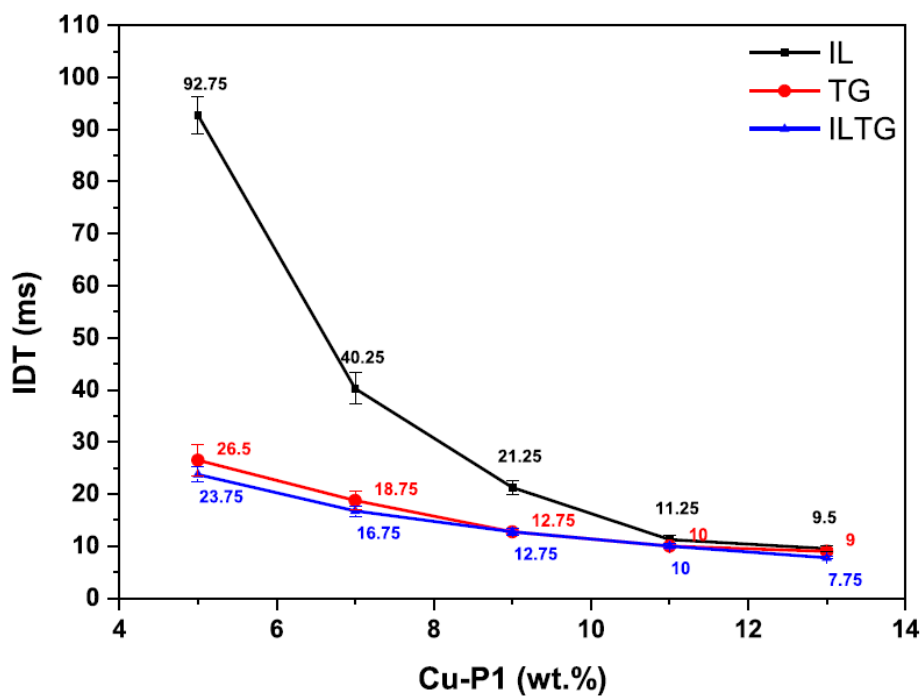
Figure B.7: Ignition delay times [15]

Fig. 4. IDT of fuels *vs* additive (**Cu-P1**) concentration in the fuel (**IL**: [EMIM][BH$_3$CN]; **TG**: tetraglyme; **ILTG**: 1:1 of IL & TG (wt/wt%)).

Figure B.8: Ignition delay times [18]

Table 2: Hypergolic ignition delay time of hypergolic fuels

Fuels	[EMIM][BH$_3$CN] (wt.%)	MIMBH$_3$ (wt.%)	Furfuryl alcohol (wt.%)	NaBH$_3$CN (wt.%)	NaI (wt.%)	Ignition delay time (ms)
HF1	100	0	0	0	0	>1000
HF2	95	0	0	0	5	95.50
HF3	93	0	0	0	7	93.57
HF4	91	0	0	0	<9	75.50
HF5	47.5	0	47.5	0	5	80.25
HF6	46.5	0	46.5	0	7	64.50
HF7	45.5	0	45.5	0	9	56.00
HF8	44.5	0	44.5	0	<11	44.50
HF9	0	100	0	0	0	392.5
HF10	0	97	0	0	<3	25.25
HF11	0	54	46	0	10	44.00
HF12	0	76	19	0	5	82.75
HF13	0	0	100	0	0	Non hypergolic
HF14	0	0	85	10	5	48.75
HF15	0	0	83	10	7	34.00
HF16	0	0	81	10	9	30.00
HF17	0	0	79	10	<11	29.00

Figure B.9: Ignition delay times [41]
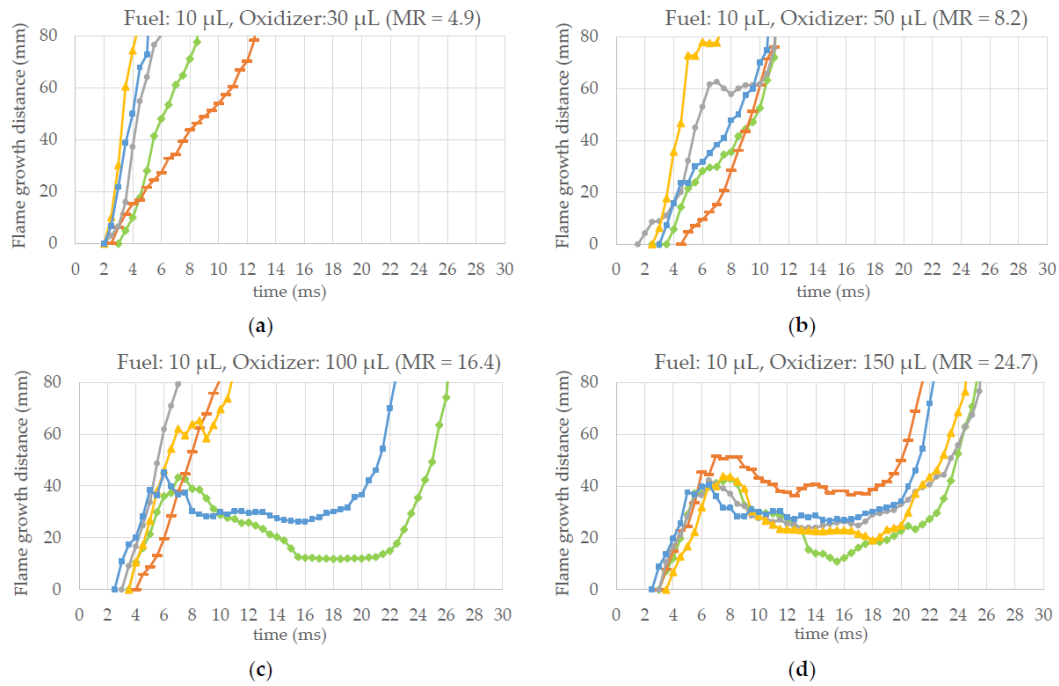
Figure 6. Time history of flame growth in the test tube ((**a**) *MR* = 1.6, (**b**) *MR* = 8.2, (**c**) *MR* = 16.4, (**d**) *MR* = 24.7, five test results for each test condition are plotted per graph).

Figure B.10: Ignition delay times [49]

Table 15. Fuel A/H_2O_2 test series ignition delay results.

Test	O/F	R_m	Propellant	Re [-]	Velocity [ft/s]	ID [ms]	ID dev. [ms]
1	2.00	2.87	H_2O_2	10000	69	8.6	0.2
			Fuel A	-	48		
2	2.00	2.87	H_2O_2	14242	98	8.3	0.3
			Fuel A	-	69		
3	2.00	2.87	H_2O_2	20000	138	6.5	0.1
			Fuel A	-	96		

Figure B.11: Ignition delay times [17]

Table 1. Summary of test conditions.

Table 4.1 Summary of test conditions. Simulant tests*

Fuel Type	Oxidizer Type	Number of Tests	Impact Velocity	Oxidizer Temp.	Ign. Prob.	Average Ign. Delay	Explosion Prob.	Average Explosion Delay
			$\pm$ 0.1 m/s	$\pm$ 1°C		ms		ms
Fuel A	95% H_2O_2	10	2.9	10	90%	15	0%	—
Fuel A	95% H_2O_2	6	1.2	10	100%	25	0%	—
MMH	RFNA	25	2.9	10	32%	26	44%	2
MMH	RFNA	21	1.3	10	9%	16	43%	2
MMH	WFNA	9	2.9	20	0%	—	0%	—
MMH	WFNA	7	2.3	20	0%	—	0%	—
MMH	WFNA	5	1.6	20	0%	—	40%	7
MMH	WFNA	5	1.3	10	0%	—	40%	22
MMH	WFNA	10	1.3	20	0%	—	30%	6
MMH	WFNA	5	1.3	30	0%	—	0%	—
TEDMAZ	RFNA	9	2.9	10	78%	27	0%	—
TEDMAZ	RFNA	7	2.2	10	100%	25	0%	—
TEDMAZ	RFNA	5	1.2	10	80%	41	0%	—
Methanol*	70% HNO_3	18	1.2	20	0%	—	0%	—

Figure B.12: Ignition delay times [34]

Oxidizer	Fuel	Average Ignition Delay (msec)	Optimum Mixture Ratio	Isp_v (sec)	Chamber Temp. (K)
NTO	MMH	To be determined	2.10	313.6	3314
98.3% H2O2	Block 0	15.54	2.77	283.5	2876
98.2% H2O2	75% Methanol 25% Mn( )4H2O	12.17	2.71	282.3	2666
98.2% H2O2	45% Methanol 40% SSR 15% Mn( )4H2O	14.06	4.13	296.9	2903
98.2% H2O2	37.5% Methanol 50% SSR 12.5% Mn( )4H2O	10.33	4.43	299.1	2940

Table 5: Ignition delays and vacuum Isp's for several different fuels. (Chamber pressure 500 psia, expansion ratio of 10).

Figure B.13: Ignition delay times [20]

Table 2: Parameters of test series 1 with average IDTs and respective standard deviations.

Catalyst	Average particle size (DLS) [nm]	Amount of catalyst [wt%]	Condition of the nanoparticles	Number of tests	Average IDT [ms]	Standard deviation [ms]
Pt_{nano}	73.5	1	dried	3	79.2	4.4
Ag^G_{nano}	78.6	1	dried	3	55.8	3.7
$MnO_{2(nano)}$	67.7	1	dried	3	148.3	6.4

Figure B.14: Ignition delay times [16]

Table 3: Parameters of test series 2 with average IDTs and respective standard deviations.

Catalyst	Average particle size (DLS) [nm]	Amount of catalyst [wt%]	Condition of the nanoparticles	Number of tests	Average IDT [ms]	Standard deviation [ms]
Ag^P_{nano}	37.4	1	dried	3	47.8	2.3
Ag^C_{nano}	60.2	1	dried	3	46.3	7.1
Ag^G_{nano}	78.6	1	dried	3	55.8	3.7

Figure B.15: Ignition delay times [16]

Table 4: Parameters of test series 3 with average IDTs and respective standard deviations.

Catalyst	Average particle size (DLS) [nm]	Amount of catalyst [wt%]	Condition of the nanoparticles	Number of tests	Average IDT [ms]	Standard deviation [ms]
Ag^P_{nano}	37.4	5	dried	3	24.7	2.3
Ag^C_{nano}	60.2	5	dried	3	17.3	0.5
Ag^G_{nano}	78.6	5	dried	3	51.8	1.4

Figure B.16: Ignition delay times [16]

Table 5: Parameters of test series 4 with average IDTs and respective standard deviations.

Catalyst	Amount of catalyst [wt%]	Condition of the nanoparticles	Number of tests	Average IDT [ms]	Standard deviation [ms]
Ag^P_{nano} (10 wt% PVP)	5	dried	2	51.1	4.3
Ag^P_{nano} (30 wt% PVP)	5	dried	2	55.3	8.0
Ag^P_{nano} (10 wt% citrate)	5	dried	2	23.4	0.4
Ag^P_{nano} (30 wt% citrate)	5	dried	2	24.0	0.3

Figure B.17: Ignition delay times [16]

Table 6: Parameters of test series 5a with average IDTs and respective standard deviations.

Catalyst	Average particle size (DLS) [nm]	Amount of catalyst [wt%]	Condition of the nanoparticles	Number of tests	Average IDT [ms]	Standard deviation [ms]
Ag^P_{nano}	37.4	1	Dispersion (EtOH)	3	31.7	1.7
Ag^C_{nano}	60.2	1	Dispersion (EtOH)	3	18.0	0.8
Ag^G_{nano}	78.6	1	Dispersion (EtOH)	3	51.2	15.8

Figure B.18: Ignition delay times [16]

Table 8: Parameters of test series 5b with average IDTs and respective standard deviations.

Catalyst	Amount of catalyst [wt%]	Condition of the nanoparticles	Number of tests	Average IDT [ms]	Standard deviation [ms]
Ag^P_{nano} (10 wt% PVP)	5	Dispersion (EtOH)	2	45.7	1.3
Ag^P_{nano} (30 wt% PVP)	5	Dispersion (EtOH)	2	51.4	0.7
Ag^P_{nano} (10 wt% citrate)	5	Dispersion (EtOH)	3	8.8	1.0
Ag^P_{nano} (30 wt% citrate)	5	Dispersion (EtOH)	2	18.9	2.2

Figure B.19: Ignition delay times [16]

Table 2 TVG and IDT

CONFIG	#	IDT	SD	TVG	SD	IDT-TVG
0	20	31.3	3.7	28.1	3.6	3.2
1	20	30.9	6.1	26.9	5.5	4.0
2	17	29.5	2.5	25.8	2.5	3.7
3	8	30.4	2.3	27.0	1.9	3.4
4	9	65.3	6.6	61.9	5.8	3.5

Figure B.20: Ignition delay times [6]
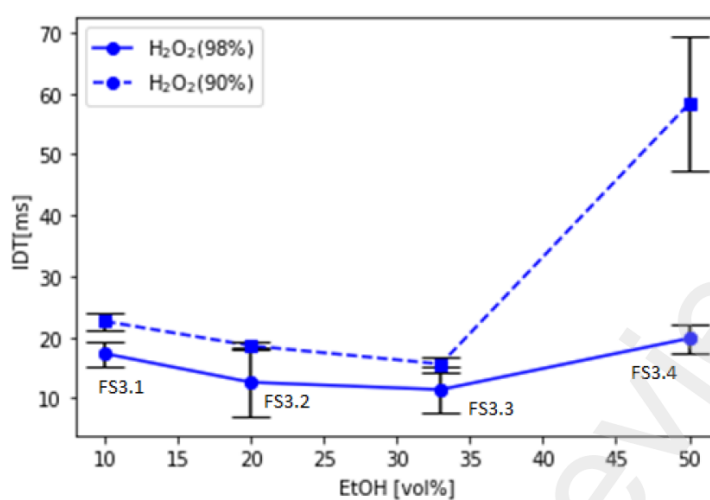
Fig. 11. Ignition delay time for different proportions of EtOH in TMEDA/DMEA(sample FS1.5) using 1wt% $CuCl_2$ with 90% and 98% hydrogen peroxide.

Figure B.21: Ignition delay times [7]

Table 3
Influence of copper additive on time to vapor generation and ignition delay time.

Additive content[wt%]	Time to vapor generation[ms]	SD TVG[ms]	Ignition delay time[ms]	SD IDT[ms]	Difference between IDT and TVG[ms]	# of tests
0	28.3	4.2	31.7	4.2	3.4	30
0.5	17.0	0.8	19.3	0.6	2.3	6
1	14.9	1.8	16.2	2.0	1.4	23
2	14.3	1.8	15.7	1.9	1.4	8
3	14.5	1.7	15.6	1.7	1.1	7
5	13.1	1.7	13.9	1.8	0.8	24
7	15.5	1.5	16.4	1.2	0.9	7
10	16.3	1.2	16.9	1.0	0.6	6

Figure B.22: Ignition delay times [5]
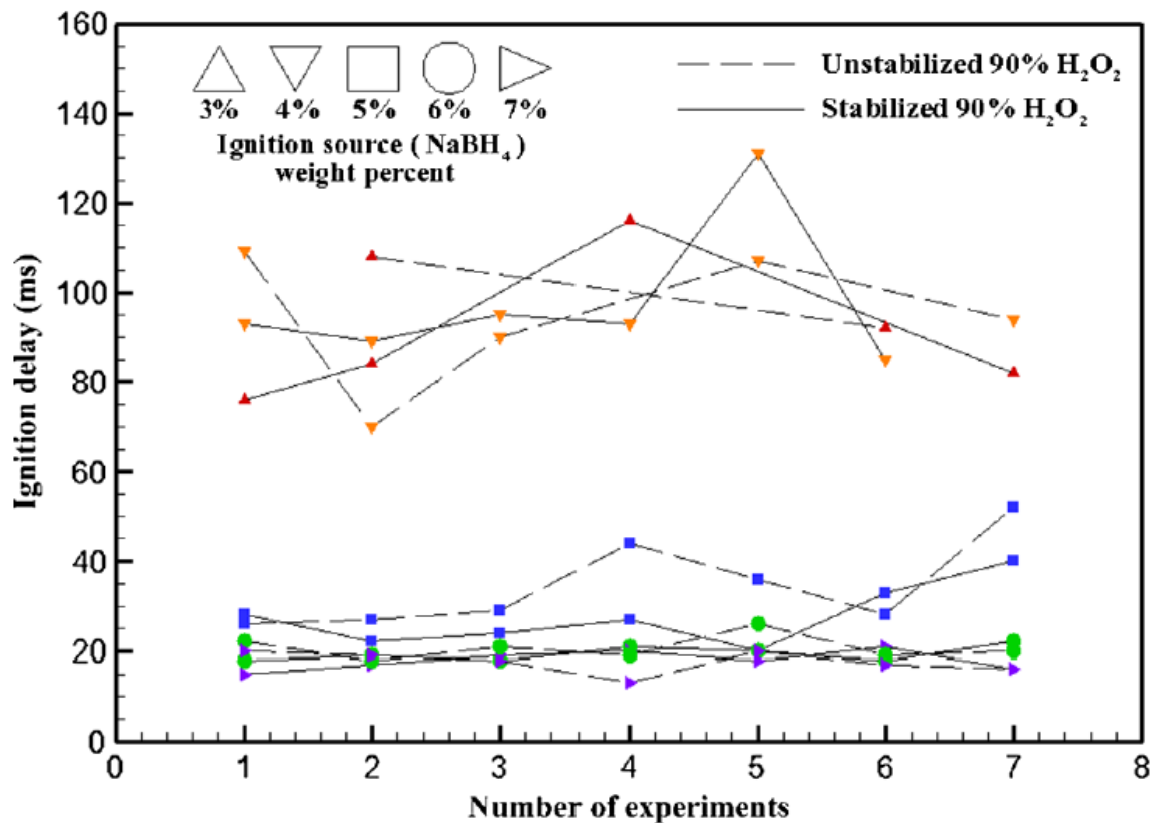
Fig. 4   The relation between the ignition delay and the content of the ignition source in nontoxic hypergolic fuel (stock 3) depending on the two different types of hydrogen peroxide.

Figure B.23: Ignition delay times [38]
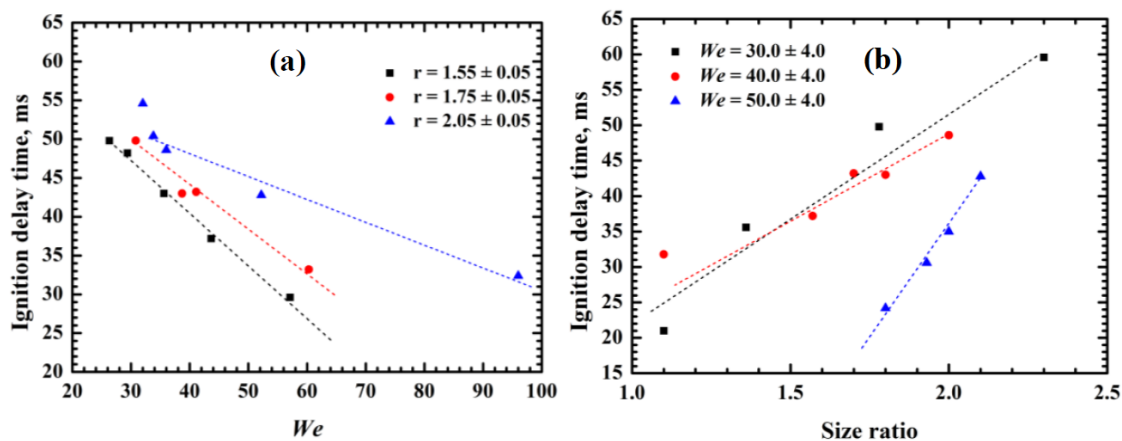
Figure 5.6 Dependence of IDT on (a) We with $\Delta = 1.5, 1.75$ and 2.1, and (b) Δ with $We = 31, 41$ and 61.

Figure B.24: Ignition delay times [69]

Fig. 2. The droplet test performed on catalytically promoted fuel with 98% hydrogen peroxide – the IDT=16 ms (IoA)

Tab. 1. Mixtures of fuels and additives being hypergolic with hydrogen peroxide

Fuel	Additives	HTP	IDT	Method of Experiment
Methanol	10% MAT	98%	30 ms	Drop Test
Methanol	30% MAT	98%	10 ms	Drop Test
Ethanolamine	5% CuCl$_2$	85%	200 ms	Drop Test
Ethanolamine	10%CuCl$_2$	85%	30 ms	Drop Test
Ethanolamine	10%CuCl$_2$	85%	190 ms	Impinging Test
Ethanolamine[40degC]	10%CuCl$_2$	85%	130 ms	Impinging Test
Kerosene	Metal Salts	98%	19 ms	Drop Test
dimethylhexolamine	C$_{16}$H$_{30}$CoO$_4$	98%	12.7 ms	Drop Test
dimethylbutylamine	C$_{16}$H$_{30}$CoO$_4$	98%	9.8 ms	Drop Test
Triglyme	8% H$_4$BNa	88.5%	10.6 ms	Drop Test
Tetraglyme	10% H$_4$BNa	88.5%	12 ms	Drop Test
Dimethyl Formamide	12% H$_4$BNa	88.5%	9.12 ms	Drop Test
Dimethyl Sulfoxide	10% H$_4$BNa	88.5%	14 ms	Drop Test
Triglyme	8% H$_4$BNa	88.5%	9 ms	Impinging Test
Dimethyl Formamide	12% H$_4$BNa	88.5%	7 ms	Impinging Test
Dimethyl Sulfoxide	10% H$_4$BNa	88.5%	7 ms	Impinging Test

Figure B.25: Ignition delay times [31]

$$C$$
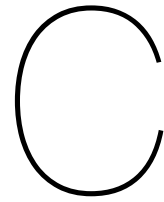
Test procedures

These are the test procedures for the hermetic test set-up. The ambient test procedures are virtually identical with the omission of steps relating to pressurization. The procedures are divided in seven different parts, which are:

- Preparation of test campaign
- Preperation of test day
- Preparation of test series
- Execution of one test
- End of test day
- End of test campaign
- Contingency checklist (in order of severity)

Preparation of test campaign
Materials

- Hermetic set-up
- Laptop
- NI compact DAQ
- High-speed camera
- Syringe pump unit
- Distilled water
- Syringe needles
- 2 spill trays
- Paper towels

Steps

1. Wear appropriate PPE (safety shoes, safety glasses, lab coat)
2. Put hermetic set-up in fume hood
3. Place NI compact DAQ in appropriate place
4. Put syringe pump in fume hood
5. Put 2 spill trays in fume hood
6. Set up laptop
7. Set up NI compact DAQ
8. Connect hermetic set-up to laptop
9. Set up high-speed camera
10. Turn on and set up FlexLogger

11. Ensure LED-lights work
12. Ensure the pressurization system and syringe system work and do not leak by using the low pressure connectors in the fume hood
13. Calibrate falling droplet thermal system
14. Calibrate resting droplet thermal system
15. Calibrate high-speed camera
16. Calibrate the syringe pump unit using an ethanol needle and distilled water (write down droplet volume)
17. Calibrate falling droplet feed system using distilled water (write down droplet volume)
18. Dry the falling droplet feed system

Preperation of test day

Materials

- Safety glasses
- Lab coat
- Safety gloves
- Safety shoes
- 1 bucket with water
- 1 cup with water
- Paper towels

Steps

1. Set up laptop
2. Connect hermetic set-up to laptop
3. Set up high-speed camera
4. Turn on and set up FlexLogger
5. Ensure proper calibration of set-up
6. Set up bucket with water on the floor next to fume hood
7. Set up cup with water outside of fume hood
8. Have paper towels outside of fume hood

Preparation of test series

Materials

- Borosilicate vials
- Hydrogen peroxide
- Ethanol
- Catalyst(s)
- Propagator(s)

Steps

1. Wear proper PPE (safety glasses, lab coat)
2. Prepare ethanol and alternative fuel mixtures and put them in borosilicate vials storage containers

    (a) Use a syringe pump unit, syringe and needle
    (b) Label the borosilicate vials containers
    (c) Put the appropriate mixtures in the appropriate vials containers
    (d) Close the borosilicate vials containers

3. Put the prepared borosilicate vials containers in the appropriate spill tray
4. Put the hydrogen peroxide bottle in the other spill tray

5. Put empty hydrogen peroxide borosilicate glass in test stand

6. Put hydrogen peroxide in the falling droplet feed system syringe

7. Connect falling droplet feed system syringe to falling droplet feed system tube

8. Put falling droplet feed system syringe in syringe pump unit

9. Actuate syringe pump unit until a droplet falls

10. Ensure no further droplet is about to fall

11. Remove hydrogen peroxide borosilicate glass, empty it in bucket with water, put it in hydrogen peroxide spill tray

Execution of one test

1. Wear proper PPE (safety glasses, lab coat, safety gloves, hearing protection)

2. Note down vial label fuel mixture to be tested in laptop as well as other relevant information

3. If necessary: open hermetic set-up door

4. Put a pre-determined amount of fuel mixture in a borosilicate vial using a syringe and syringe pump

5. Ensure no droplet is forming under falling droplet buffer the droplet stopper is extended

6. Put closed borosilicate vial in test stand

7. If testing atmosphere deviates from standard: close hermetic set-up door

8. Ensure readiness of the system

   (a) Droplet stopper
   (b) High-speed camera and LED-lights
   (c) Falling droplet thermal system
   (d) Resting droplet thermal system
   (e) Syringe pump unit
   (f) Pressurization system

9. Ensure test is about to be conducted safely

10. If required: pressurize system to the desired pressure and ensure the system does not leak

11. Open borosilicate vial

12. Actuate syringe pump unit and ensure high-speed camera is active

13. After test:

   (a) De-pressurize system
   (b) Ensure data is saved
   (c) Open hermetic set-up door
   (d) Ensure the droplet stopper is extended

14. Throw used borosilicate glass into bucket with water

End of test day

1. Empty cup with water

2. Put cup without water in test stand

3. Fully actuate HTP syringe

4. Flush falling droplet feed system with distilled water

5. Empty cup with HTP/water mixture in bucket

6. Throw away cup

7. Dry falling droplet feed system

8. Empty bucket with water

9. Pack up high-speed camera

10. Pack up laptop

11. Return chemicals to correct location(s)

End of test campaign

1. Clean hermetic set-up
2. Clean spill trays
3. Clean fume hood
4. Return high-speed camera
5. Return NI compact DAQ
6. Return syringe pump unit
7. Return spill trays
8. Store hermetic set-up and other materials in appropriate places

# Contingency checklist (in order of severity)

1. Major injury?

   (a) Eye: Rinse with eye rinse unit
   (b) Burn: Rinse with large amount of cool (not cold) water
   (c) Call 088 866 2222

2. Large fire?

   (a) Optional: extinguish using 1 fire extinguisher
   (b) Evacuate area
   (c) Call 088 866 2222

3. Small fire?

   (a) Extinguish using cup with water

      i. Didn't work:
   (b) Extinguish using bucket with water

      i. Didn't work:
   (c) Extinguish using 1 fire extinguisher

      i. Didn't work:
   (d) Evacuate area
   (e) Call 088 866 2222

4. Minor injury?

   (a) Go to a First Aid station

D
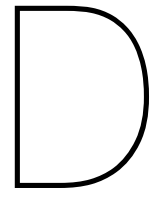
Hermetic set-up drawings
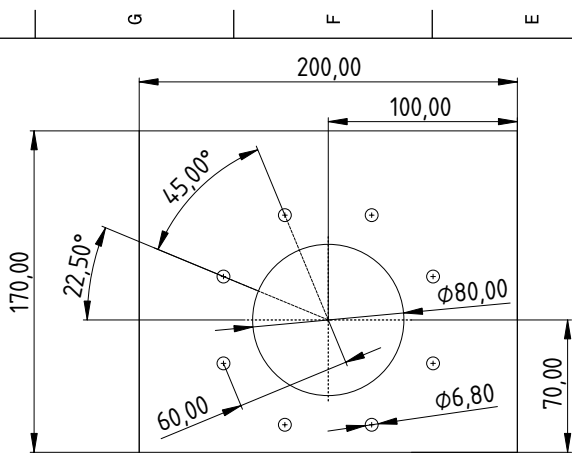
Front and Back
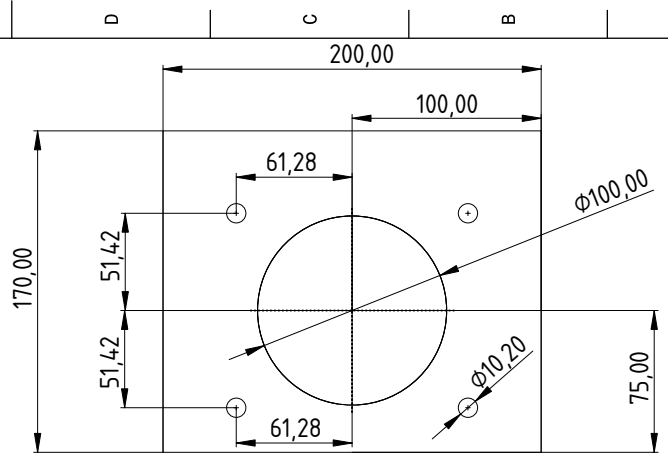
Left and Right

Top and Bottom
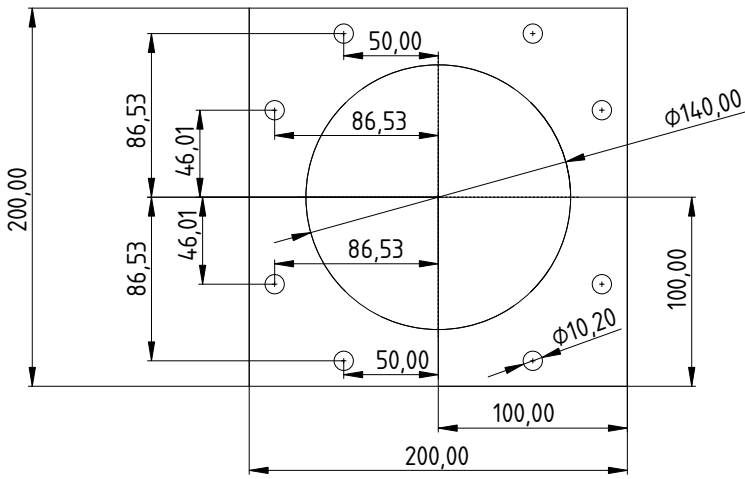
View of the front, top and right sides
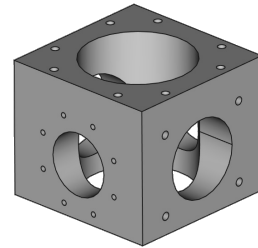
DESIGNED BY: Mateusz Glowacki		**Main body**			I	–
DATE: 28/09/2023		Of The Hermetic Set-Up			H	–
CHECKED BY: –					G	–
DATE: –					F	–
SIZE A3					E	–
					D	–
SCALE 1:2	WEIGHT (kg) 8	DRAWING NUMBER –		SHEET –	C	–
					B	–
					A	–

Front View

Ø140,00
Ø80,00
45,00°
22,50°
60,00
Ø8,00

Section View

39,00
140,00
80,00
102,00
28,00
11,00

Window Holder
Of The Hermetic Set-Up

SIZE A3		
SCALE 1:1	WEIGHT (kg) 0,8	DRAWING NUMBER –
		SHEET –

I	–
H	–
G	–
F	–
E	–
D	–
C	–
B	–
A	–

Top View

Side View

Section A-A

1:1 view

Datasheet

RS Article: 177 - 0135
DC – D Frame Solenoid 12V

Dimensions in millimetres
Total Solenoid Weight : 400g
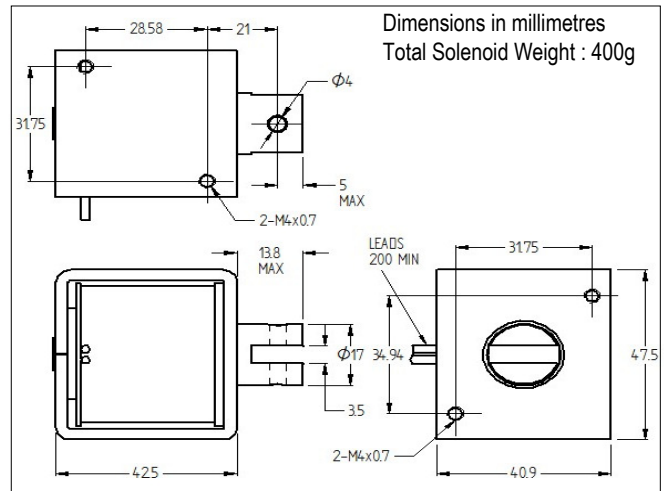
Specifications:

Force/Stroke Characteristics

Legend:
- AC 5% 500VA
- DC 5% 250W
- AC 25% 150VA
- DC 25% 56W
- AC 100% 50VA
- DC 100% 14W

Y-axis: Force (gf)
X-axis: Stroke (mm)

Features:
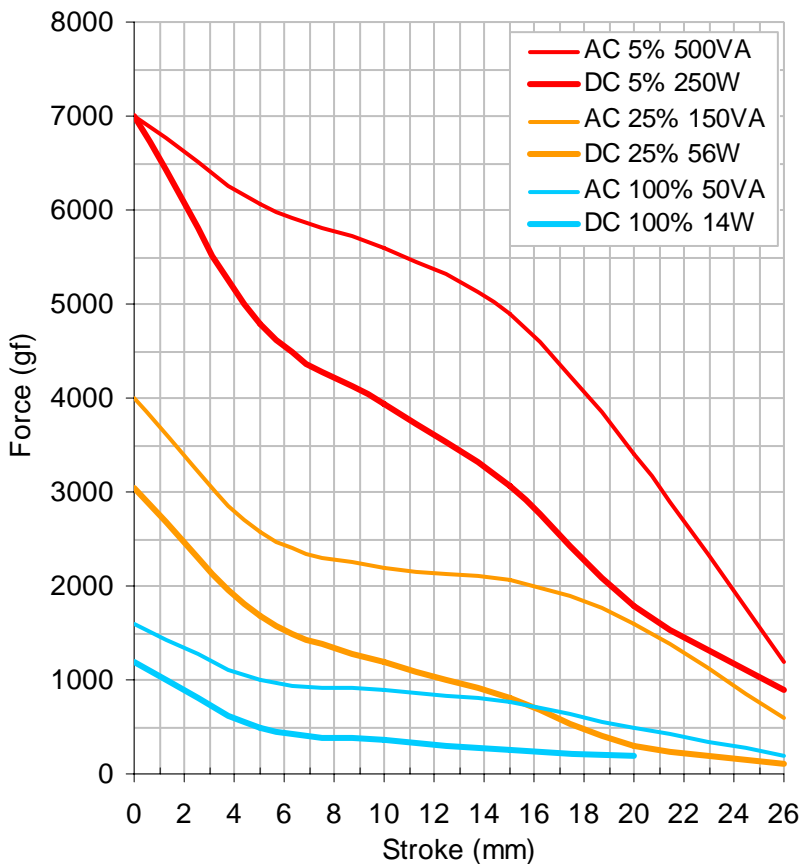
- Pull type
- Flying leads
- Corrosion resistant